2013

SOLID STATE GAS SENSORS FOR DETECTION OF EXPLOSIVES AND EXPLOSIVE PRECURSORS

Yun Chu
University of Rhode Island, yun.z.chu@gmail.com

SOLID STATE GAS SENSORS FOR DETECTION OF EXPLOSIVES AND EXPLOSIVE PRECURSORS

BY

YUN CHU

A DISSERTATION SUBMITTED IN PARTIAL FULFILLMENT OF THE REQUIREMENTS FOR THE DEGREE OF

DOCTOR OF PHILOSOPHY

IN

CHEMICAL ENGINEERING

UNIVERSITY OF RHODE ISLAND

2013

DOCTOR OF PHILOSOPHY OF CHEMICAL EGINEERING

OF

YUN CHU

Thesis Committee:

Major Professor

Otto J. Gregory

Hamouda Ghonem

Donald J. Grey

Nasser H. Zawia

DEAN OF GRADUATE SCHOOL

UNIVERSITY OF RHODE ISLAND
2013

ABSTRACT

The increased number of terrorist attacks using improvised explosive devices (IEDs) over the past few years has made the trace detection of explosives a priority for the Department of Homeland Security. Considerable advances in early detection of trace explosives employing spectroscopic detection systems and other sensing devices have been made and have demonstrated outstanding performance. However, modern IEDs are not easily detectable by conventional methods and terrorists have adapted to avoid using metallic or nitro groups in the manufacturing of IEDs. Instead, more powerful but smaller compounds, such as TATP are being more frequently used. In addition, conventional detection techniques usually require large capital investment, labor costs and energy input and are incapable of real-time identification, limiting their application. Thus, a low cost detection system which is capable of continuous online monitoring in a passive mode is needed for explosive detection.

In this dissertation, a thermodynamic based thin film gas sensor which can reliably detect various explosive compounds was developed and demonstrated. The principle of the sensors is based on measuring the heat effect associated with the catalytic decomposition of explosive compounds present in the vapor phase. The decomposition mechanism is complicated and not well known, but it can be affected by many parameters including catalyst, reaction temperature and humidity. Explosives that have relatively high vapor pressure and readily sublime at room temperature, like TATP and 2, 6-DNT, are ideal candidate for vapor phase detection using the thermodynamic gas sensor. ZnO, W_2O_3, V_2O_5 and SnO_2 were employed as catalysts.

This sensor exhibited promising sensitivity results for TATP, but poor selectivity among peroxide based compounds.

In order to improve the sensitivity and selectivity of the thermodynamic sensor, a Pd:SnO_2 nanocomposite was fabricated and tested as part of this dissertation. A combinatorial chemistry techniques were used for catalyst discovery. Specially, a series of tin oxide catalysts with continuous varying composition of palladium were fabricated to screen for the optimum Pd loading to maximize specificity. Experimental results suggested that sensors with a 12 wt.% palladium loading generated the highest sensitivity while a 8 wt.% palladium loading provided greatest selectivity. XPS and XRD were used to study how palladium doping level affects the oxidation state and crystal structure of the nanocomposite catalyst.

As with any passive detection system, a necessary theme of this dissertation was the mitigation of false positive. Toward this end, an orthogonal detection system comprised of two independent sensing platforms sharing one catalyst was demonstrated using TATP, 2, 6-DNT and ammonium nitrate as target molecules. The orthogonal sensor incorporated a thermodynamic based sensing platform to measure the heat effect associated with the decomposition of explosive molecules, and a conductometric sensing platform that monitors the change in electrical conductivity of the same catalyst when exposed to the explosive substances. Results indicate that the orthogonal sensor generates an effective response to explosives presented at part per billion level. In addition, with two independent sensing platforms, a built-in redundancy of results could be expected to minimize false positive.

ACKNOWLEDGMENTS

I would foremost like to express my grateful and sincere acknowledgement to my adviser, Dr. Otto J. Gregory, for his guidance, understanding, patience, and most importantly, his support in both academic suggestions and lifelong guidance to me. His mentorship was paramount in encouraging me to not only execute daily experiments but also grow as a self-motivated researcher and an independent thinker. His wealth of knowledge, dedicated research attitude, and rigorous academic spirit has encouraged and benefitted me throughout my graduate study. I would like to extend a heartfelt thank you, Dr. Gregory, for everything you've done for me.

A special thanks to Mr. Mike J. Platek for his remarkable contribution and timely assistance to the entire group throughout my graduate study. Thank you for making the laboratories an impeccable and wonderful place. Also, thank Dr. Oxley and her students at Chemistry Department for their cooperation and assistances.

I would like to express my appreciation to my committee members: Dr. Ghonem, Dr. Gray, Dr. Chrisman and Dr. Davis, for their guidance and invaluable time.

All the faculty members, staff and students of the Department of Chemical Engineering are greatly acknowledged. A special thanks to the students who have worked with me in the past and present, especially Matin Amani and Daniel Mellon.

Before I finish, I would like to express my deepest gratitude to my wife and my parents for their consistent understanding and encouragement in this endeavor. I would never make any achievements without your support.

PREFACE

The manuscript format has been used in the preparation of this dissertation. This dissertation is a compilation of one published manuscript, one accepted manuscript and one submitted manuscript. The first manuscript entitled "Detection of triacetone triperoxide (TATP) using a thermodynamic based gas sensor" comprises Chapter 3 of this dissertation, and provides information on the detection of TATP using a dynamic differential scanning calorimetry technique using SnO_2, ZnO, W_2O_3 and V_2O_5. It was published in *Sensors and Actuators B: Chemical* in 2012, volume 162, pages 7-13.

The second manuscript "Detection of peroxides using a Pd/SnO2 nanocomposite catalyst" was submitted to *Sensors and Actuators B: Chemical* in July 2013 and was accepted in October 2013. This manuscript comprises chapter 4 in this dissertation and discusses the effect of different Pd doping level on the sensitivity and selectivity of SnO2 catalyst toward different peroxides: H_2O_2 and TATP.

The third manuscript entitled "Detection of explosives using orthogonal gas sensors" is published by IEEE Sensors 2013 on page 12-15. This manuscript comprises Chapter 5 of this dissertation, which demonstrates an orthogonal gas sensor platform that is composed of a thermodynamic element and a conductometric element which function simultaneously for explosive detection purposes.

Chapter 6 provides a summary and conclusion of all chapters and a future outlook of this work, including study on humidity interferences, sampling and gas delivery systems, preconcentration procedures and the potential of transferring the sensor to a MEMS based platform.

TABLE OF CONTENTS

LIST OF TABLES

LIST OF FIGURES

CHAPTER 1

INTRODUCTION

The number of terrorist attacks employing improvised explosive devices (IEDs) has increased dramatically in the last 10 years. The shoe bomber in 2001, London Subway Bombing in 2005, underwear bomber in 2009, cargo plane plot in 2010 and numerous car bombs and suicide bombing incidents in Afghanistan, Pakistan and Iraq have exposed the weakness in the current system used for explosive detection and thus, initiated an urgent and compelling need to reliably detect explosives. The Intelligence Reform and Terrorism Prevention Act of 2004 directed the Department of Homeland Security (DHS) to place high priority on developing and deploying screening equipment to detect explosives on passengers and their carry-on luggage [1].

Conventional spectroscopic detection techniques, such as ion mobility spectroscopy, mass spectroscopy, Raman spectroscopy, infrared spectroscopy and nuclear magnetic resonance techniques have been used to both qualitatively and quantitatively identify explosives [2]. Some of the techniques have been incorporated by security facilities or deployed in public locations such as the entrances to major transportation centers. However, the universal application of these techniques is limited by several drawbacks, including the enormous costs in capital equipment and maintenance, costs in energy consumption, sampling, operational related expenses, and lack of continuous and real-time monitoring.

Sensors specially designed for explosive detection have addressed these disadvantages [3]. In addition, relatively small size footprints detection systems are designed as that can be manufactured into a portable device with more flexibility, capable of being linked up into a network for universal coverage, or incorporated into sensor arrays for better accuracy and reliability. A variety of sensors employing different sensing principles have been reported, including conductometric sensors, calorimetric sensors, electrochemical sensors, optical sensors, biosensors and mass sensors [4, 5]. These sensors can identify trace amount of nitroaromatic based explosives, such as DNT, TNT and RDX. However, modern IEDs are intentionally fabricated in a way that uses of materials with metallic or nitro groups are avoided but instead using more powerful but smaller compounds, such as peroxide based explosives, e.g. triacetone triperoxide (TATP). Very few of the sensing techniques can successfully detect TATP, with the exception of calorimetric sensors, which however require large space, quantified sampling and is unsuitable for real-time monitoring.

TATP has a relatively high vapor pressure and sublimes readily at room temperature. When moderately heated, TATP decomposes into acetone, O_2/O_3, water, and other smaller molecules in the presence of specific catalysts [6]. Due to the fact that under specific temperature and in presence of specific catalyst, the decomposition mechanism of TATP as well as other explosives should have their unique signature, i.e. a heat effect associated with each reaction step. *Therefore, we hypothesize that the heat effect associated with the catalytic decomposition of specific explosive molecules can be measured as a function of temperature and can thus be utilized for the unique identification of explosives*. By establishing a dynamic differential scanning

calorimetry protocol combined with of different catalysts, a wide range of target gas mixtures can be interrogated at different temperature setpoints and its heat profile will be recorded and compared with pre-established explosive database that contain a library of signatures. Techniques employing this sensor (referred as *thermodynamic sensor* here and after) exhibit the characteristic to continuously screen for explosives with both sensitivity and selectivity.

Motivations and Objectives

The overall goal of this work was to create a sensing platform that could reliably detect explosives, with nitro-based and peroxide-based explosives. To better understand the sensing mechanism associated with the solid-vapor interaction, analytical techniques were used to identify surface morphology, oxidation states and chemistry of the catalysts.

The main goals of this research were:

To fabricate and test a thermodynamic sensor and establish the characteristic response using different catalysts as a function of temperature.

To determine the detection limit and gain insight into the exact mechanism associated with detection.

To determine interference effects of explosive precursors, e.g. H_2O_2 and acetone which could lead to false positive during the detection TATP.

To optimize catalyst composition using nanocomposites of noble metals and metal oxide catalysts to enhance its selectivity and sensitivity.

To develop a sensing platform and apparatus to minimize false positives using the thermodynamic sensor.

Chapter 2 provides background information on common explosives found in improvised explosive devices that frequently used by terrorists. In addition, a literature review on conventional sensing techniques such as spectroscopy, canines and sensor technology and their applications in explosive detection is discussed.

Chapter 3 discusses the sensing theory, the fabrication and its characteristic response of the thermodynamic sensor to TATP as well as H_2O_2 and acetone. Numerous catalysts were tested including ZnO, SnO_2, V_2O_5, W_2O_3 and CuO and each exhibited a specific response or signature at a given temperature. The detection limit of the thermodynamic sensor to TATP was determined to be in the parts per million ranges. This investigation also suggested that the heat effect associated with decomposition of H_2O_2 mimics the behavior of that with TATP, implying that H_2O_2 could be one of the catalytic decomposition products of TATP. X-ray photoelectron spectroscopy (XPS) was employed to study the oxidation states of selected catalysts prior to and after exposure to the target gases. Morphology of the catalysts of the as-deposited and posted-exposure condition were characterized using scanning electron microscopy (SEM) [7].

Chapter 4 describes the fabrication and testing of Pd:SnO_2 nanocomposite catalysts for the thermodynamic sensor using combinatorial chemistry as a screening technique. SnO_2 matrix was impregnated with palladium nanoparticles at different loadings and tested to determine the optimum composition to provide maximum sensitivity and selectivity. The results of this study suggested that catalysts with a 12 wt. % palladium loading yielded highest sensitivity while an 8 wt. % palladium loading yielded the greatest selectivity between TATP and H_2O_2. Mechanisms of how

palladium loading affected the sensing behavior were discussed, based on the oxidation states of metal oxide catalysts indicated by XPS.

Chapter 5 explores the idea of an orthogonal platform to reliably track trace levels of explosives including TATP, 2,6-DNT and ammonium nitrate. The orthogonal sensor consists of a thermodynamic based sensing platform, which measures the heat effect associated with the interaction of the explosive vapor with the catalyst surface, and a conductometric sensing platform, which monitors electrical conductivity changes in the same catalyst when exposed to the target molecules. By combining these two independent techniques into a single device, the sensor signature provides a certain redundancy, which helps mitigate false positives and negatives. Responses of the orthogonal sensor to trace explosives at part per billion level was demonstrated.

Chapter 6 summarizes the achievements of this research, and the suggested directions of future work, including effect of humidity to the performance of sensor, advanced gas introduction methods and the miniaturization of well-established orthogonal sensor to a micro-electromechanical system (MEMS). The MEMS platform permits much more localized heating and cooling via a diaphragm and thus not only will miniaturize the platform but also should enhance selectivity and sensitivity as well as provide the basis for sensor arrays that will further mitigate false positives and negatives.

REFERENCES

[1] Intelliegence Reform and Terrorism Prevention Act of 2004, *Public Law,* December 2004, 108-458.

[2] J. S. Caygill, F. Davis and S. P. Higson, "Current trends in explosive detection techniques," *Talanta,* vol. 88, pp. 14-29, 2012.

[3] S. Singh, "Sensors-An effective approach for the detection of explosives," *Journal of Harzardous Materials,* vol. 144, pp. 15-28, 2007.

[4] K. Arshak, E. Moore, G. M. Lyons, J. Harris and S. Clifford, "A review of gas sensors employed in electronic nose applications," *Sensor Review,* vol. 24, pp. 181-198, 2004.

[5] N. Barsan, D. Koziej and U. Weimar, "Metal oxide-based gas sensor research: How to," *Sensors and Acutators B,* vol. 121, pp. 18-35, 2007.

[6] J. C. Oxley, J. L. Smith and H. Chen, "Decomposition of a multi-peroxidic compound: triacetone triperoxide (TATP)," *Propellants, Explosives, Pyrotechnics,* vol. 27, pp. 209-216, 2002.

[7] A. Matin, C. Yun, K. L. Waterman, C. M. Hurley, M. J. Platek and O. J. Gregory, "Detection of triacetone triperoxide (TATP) using a thermodynamic based gas sensor," *Sensors and Actuators B,* vol. 162, pp. 7-13, 2012.

CHAPTER 2

BACKGROUND

An Explosive is defined as a material that can be initiated to undergo very rapidly and self-propagating decomposition resulting in the formation of more stable material, liberation of heat or the development of sudden pressure effect [1].

This chapter will first focus on classification of explosives, commonly used military and industrial explosives and their malicious uses in terrorism. Furthermore, the conventional analytical instruments used for explosive detection have been described. Finally, the development of gas sensing platforms, including semiconducting sensor, catalytic combustion system, electrochemical sensor and thermo conductive sensor, has also been reviewed.

1. Explosives and their classification

Explosives, propellants and pyrotechnics belong to a broad group of compounds and compositions known as energetic materials. Many organic explosives consist of a carbon core incorporating covalently bonded oxidizer groups such as peroxide, nitro, nitramine, nitrate ester etc. These groups, containing bonds like O-O, N-N and N-O, have two or more atoms covalently bonded with non-bonding electrons present in p-orbitals. This creates electrostatic repulsion between the atoms, and consequently, many explosives have a positive heat of formation. On explosion an internal redox

reaction occurs where these bonds break and form gaseous products, like N_2 and CO_2, where the non-bonding electrons are tied up in stable π-bonds [2].

Explosives can be classified as primary, secondary or tertiary explosives by their sensitivity. Explosives that are extremely sensitive to mechanical or thermal stimuli such as impact, friction, stab, heat, flame, static electricity or electromagnetic radiation are known as primary explosives [3], while the ones which need the shock an explosion or a high energy impulse are recognized as secondary explosives. Primary explosives, also known as initiators, are classified as to their effectiveness in causing the detonation of less sensitive secondary explosives. Examples of commonly used primary explosives are: acetone peroxides (TATP, DADP), lead azide ($Pb(N_3)_2$), metal acetylide (Cu_2C_2, Ag_2C_2), hexamethylene triperoxide diamine (HMTD), mercury fulminate ($Hg(CNO)_2$), etc. Secondary explosives are less sensitive than primary explosives and require more energy to be ignited. Some examples of secondary explosives include pentaerythritol tetranitrate (PETN), Trinitrotoluene (TNT), cyclotrimethylenetrinitramine (RDX), cyclotetramethylenetetranitramine (HMX), urea nitrate and ethyleneglycoldinitrate (EGDN). Tertiary explosives, sometimes also classified as secondary explosives, are so insensitive to stimuli that they cannot be reliably detonated by practical quantity of primary explosives, and instead require an intermediated explosive booster, i.e. secondary explosives. Ammonium nitrate-fuel oil (ANFO) and PBXN-109 (mixture of RDX, hydroxyl-terminated polybutadiene and aluminum powder) are the most commonly used tertiary explosives.

Another way to classify an explosive is through velocity of detonation (VOD). Explosives where decomposition is propagated by deflagration (surface burning) with

a velocity less than speed of sound through the materials are classified as low explosives. Under normal condition, low explosives undergo deflagration at rates that vary from several centimeters per second to 300 meters per second [2]. Some low explosives can also detonate under confinement if initiated by the shock of another explosive. Low explosives include substances like gunpowder, smokeless powder and gun propellants. Correspondingly, chemical reactions of high explosives are more rapid and undergo the physical phenomenon of detonation, which means that the high-pressure shock wave travels through the substance at a supersonic speed. High explosives typically detonate at a rate between 4000-9500 meters per second [2] and this VOD is used to compare the performance of different explosives.

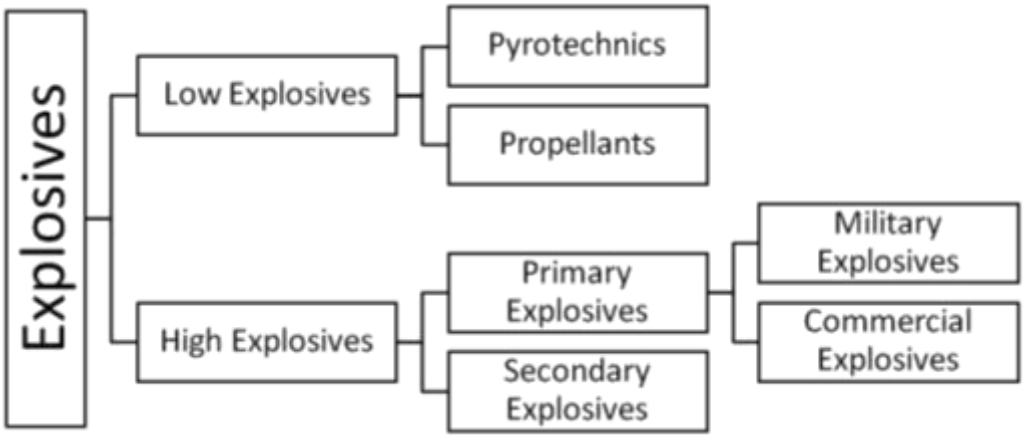

Table 2.1 Classification of explosives based on structure and performance [1].

Oxygen balance (OB) is defined as the ratio of the oxygen content of a compound to the total oxygen required for the complete oxidation of all carbon, hydrogen and other oxidisable elements to CO_2, H_2O etc. and is used to classify energetic materials as either oxygen deficient or oxygen rich. A positive oxygen balance indicates that the molecule contains more oxygen than needed and vice versa. The sensitivity and

brisance (VOD) of an explosive are somewhat dependent upon OB and tend to approach their maxima as OB approaches zero. Nitroglycerin ($C_3H_5N_3O_9$) [4], for example, contains enough oxygen to burn all its own carbon and hydrogen (OB%=3.5%) and is, therefore, capable of an extremely rapid combustion.

2. Introduction of high explosives

2.1 Military high explosives

For military purposes high explosives are used as filling for shell (propellant explosives), bombs and warheads of rockets. Such explosives are required to have high power in per unit weight and unit volume, high VOD, long-term stability and insensitivity to environmental stimuli. The most important properties of the commonest military explosives are listed in *Table 2.2* [5].

Explosive	M.P. (℃)	Density (g/mm^3)	Weight Strength % Blasting gelatine	Maximum detonation velocity (m/s)
TNT	80.7	1.63	67	6950
PETN	141.3	1.77	97	8300
RDX	204	1.73	100	8500

Table 2.2 Properties of common military explosives.

Trinitrotoluene (TNT) is the 2, 4, 6-ismore of the following constitution (*Figure 2.1*). It was fist fabricated in 1863 by German scientist and was originally used as a dye instead of explosives, due to its insensitivity to detonate. And since it's relatively safe to handle and of low toxicity, nowadays TNT has become one of the most commonly used explosives in military and industrial applications. In industry, TNT is nitrated from toluene in three steps, employing nitric acid and sulphuric acid mixtures

as nitrating agent. TNT has a negative OB, meaning it contains insufficient oxygen to give complete combustion of the carbon on detonation. It can, therefore, usefully be mixed with ammonium nitrate, which has an excess of oxygen. The resulting explosives, known as amatols, are more powerful and cheaper than TNT itself, but in general have a lower VOD. A proportion of 60% ammonium nitrate is the commonest of these compositions [4].

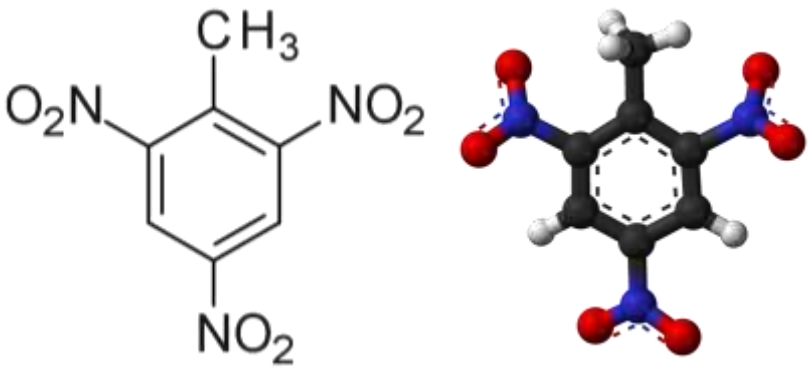

Figure 2.1 Molecular structure of trinitrotoluene.

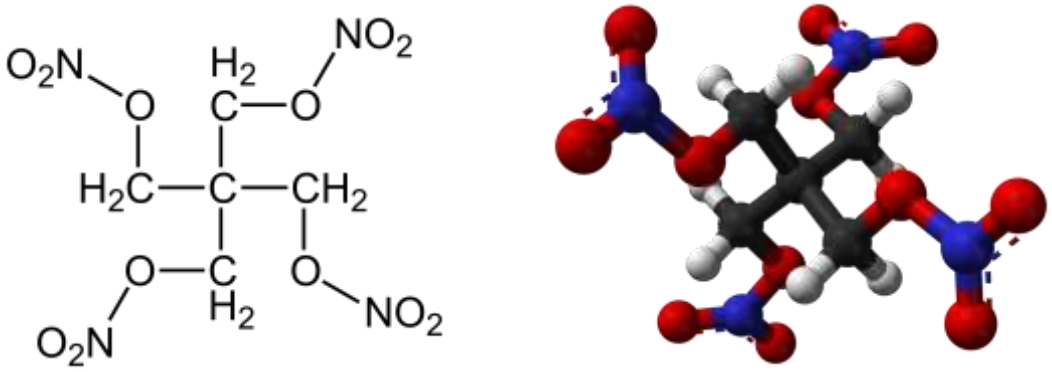

Figure 2.2 Molecular structure of pentaerythritol tetranitrate (PETN).

PETN was first synthesized in 1895 and then used as a military explosive in World War I. Pentaerythritol is made commercially by the reaction of formaldehyde

and acetaldehyde in the presence of alkali. It is then nitrated by adding it to strong nitric acid at temperatures below about 30 ℃. PETN is very stable both chemically and thermally, but is sensitive to shock and friction. Upon ignition, the oxygen atoms in the nitrate sub-group terminals oxidize the carbon and hydrogen in the interior. PETN, mixed with TNT, is largely used as a secondary explosive in military applications. Associated with triacetone triperoxide (TATP) as an initiator, PETN is also used in terrorism attacks.

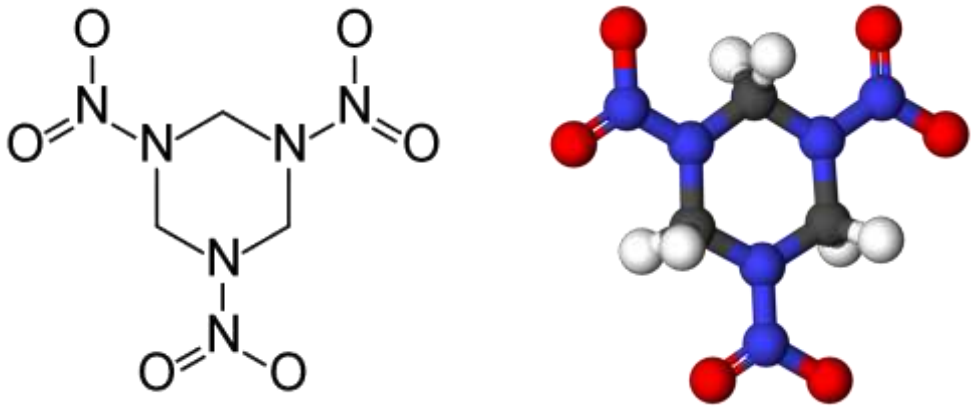

Figure 2.3 Molecular structure of cyclotrimethylenetrinitramine (RDX).

Originally discovered in 1899, RDX attained military importance during the World War II owing to its lower sensitiveness than PETN. It is a white crystalline powder made by the nitration of hexamine (hexamethylenetetramine) with nitric acid and ammonium nitrate below 30 ℃. RDX is widely used as in both military and industries as a base component of explosives compounds, such as plastic explosives, and is considered one of the most stable and powerful high explosives. It can be used alone in pressed charges, or in admixture with TNT.

2.2 Commercial high explosives

The major applications of blasting explosives in commercial applications are in mining, quarrying and civil engineering work such as is encountered in hydroelectric schemes, road building and controlled demolition. In all these cases the general procedure is to drill a hole into the solid rock or coal, insert cartridges of explosives with a detonator and thereby use the explosives to fracture and bring down the rock. For commercial purposes, explosives do not need to have the high purity demanded for the military product, but otherwise the material is identical. Besides TNT, PETN and RDX described above, the most frequently used commercial explosives include ammonium nitrate, nitroglycerine and nitrocellulose, etc.

Ammonium nitrate (NH_4NO_3) is commonly used in agriculture as a nitrogen fertilizer, and also as an oxidant agent in explosives (OB%=20%). Ammonium nitrate is made by the neutralization of nitric acid with ammonia in different production processes depending on its particular application in explosives. For use in explosives sensitized by high explosive ingredients, ammonium nitrate should be of a dense and non-absorbent character, while for uses in conjunction with fuel oil, an absorbent form of ammonium nitrate is required. Ammonium nitrate is the main component of ammonium nitrate fuel oil (ANFO), a widely used bulk industrial explosive mixture which accounts for 80% of the explosives used annually in North America [6]. ANFO is used in coal mining, quarrying, metal mining and civil construction in undemanding applications. The popularity of ANFO is largely attributable to its low cost and high stability.

3. IEDs and terrorist attacks using IEDs

An improvised explosive device (IED) is a homemade bomb constructed and deployed in ways other than conventional military action. Nowadays, terrorism has become a grave threat to national security and lives of individuals around the world, and the usage of IEDs could cause massive destruction and injuries. Explosives used

for IEDs usually require readily available raw material and relatively simple synthesis processes other than the benefits offered by military explosives such as high VOD, water resistance, oxygen balance and power per unit volume. Due to the ease of manufacturing and readily available starting materials, TATP and HMTD have becoming increasingly popular among terrorists as primary explosives or initiators for the detonation of high explosives such as PETN, ANFO, urea nitrate, etc.

3.1 Common primary explosives used by terrorists

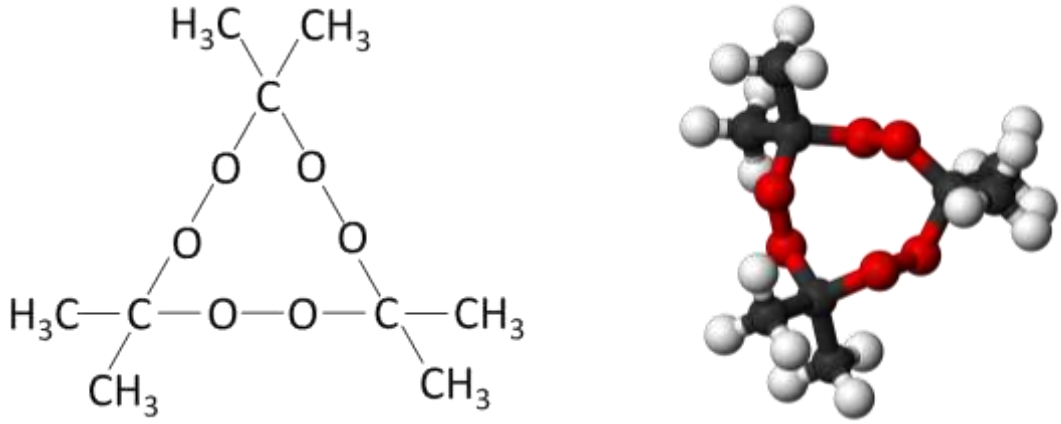

Figure 2.4 Molecular structure of triacetone triperoxide.

TATP is an organic peroxide explosive which is extremely sensitive to heat, shock and friction. It is produced from hydrogen peroxide (H_2O_2) and acetone (C_3H_6O) in presence of strong acid (sulfuric acid). In mildly acid or neutral condition, the reaction will produce more diacetone diperoxide (DADP) or even acetone peroxide monomer than TATP. TATP has a relatively high vapor pressure which allows it sublime under room temperature. Also, it is a very powerful explosive which produces approximately 80% of outward force that TNT produces with the same amount of exposive. Due to its readily available material and easy to synthesize, TATP has been

used as the initiator in many terrorist attacks. Some of the notorious examples are as follows.

On July 26th 1994, TATP was employed as trigger of a car bomb attack at the *London Israeli Embassy*, causing massive widespread damage. 20 civilians were injured during the attack.

Richard Reid, known as the "*shoe bomber*", attempted to detonate PETN using TATP as trigger while on board of *American Airlines Flight 63* on December 22nd 2001.

TATP and HMTD were employed on *July 7th 2005 the London Subway Bombing* incident, in which 52 civilians and 4 bombers were killed.

Umar Farouk Abdulmutallab, known as the "*underwear bomber*", attempted to detonate a mixture of PETN and TATP while on board of *Northwest Airlines Flight 253* on December 25th, 2009.

TATP and PETN were employed in the bomb plot on two cargo planes, one in UK and the other in Dubai in October 2010.

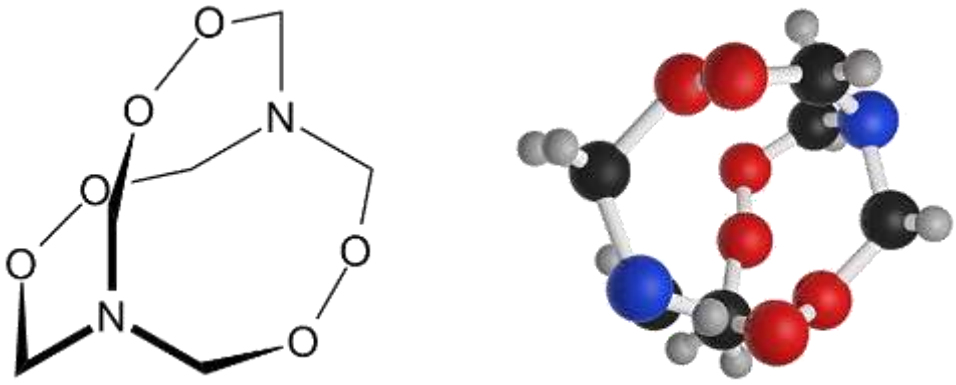

Figure 2.5 Molecular structure of HMTD.

HMTD is another common homemade primary explosives used by terrorists in suicide bombings and other attacks. It is made from hydrogen peroxide (H_2O_2) and

Hexamethylenetetramine ($(CH_2)_6N_4$) in presence of citric acid or dilute sulfuric acid as catalyst. HMTD is extremely sensitive to shock, heat and friction, making it dangerous to manufacture but ideal as a detonator. HMTD has been used in a large number of suicide bombing and other terrorist attacks all over the world. For example, HMTD was one of the components in the *2000 millennium attack plots*, in the *July 7th 2005 London Subway Bombing* and in the *2006 transatlantic aircraft plot*.

3.2 Common secondary explosives used by terrorists

Ammonium nitrate fuel oil (ANFO) described above in section 2.2 as a common commercial explosive is also frequently used by terrorist due to its low price, ease of use and availability. Some of the examples are as follows.

On April 19th 1995, hundreds of kilograms of ammonium nitrate were used during the *Oklahoma City Bombing*. 168 people were killed and 680 injured. The bombing caused an estimated of $650 million damage.

On March 16th 2001, ammonium nitrate was employed during the *Shijiazhuang Series Bombings* in China, causing a total of 108 deaths and 38 injuries.

An ammonium nitrate and nitromethane mixture, enriched with alumina powder, was used in the *Oslo Bombing* during *2011 Norway Attacks* on July 22nd 2011, claiming a total of 77 lives.

Similar to ammonium nitrate, urea nitrate ($(NH_2)_2COH\text{-}NO_3$) is another fertilizer-based high explosive that has been used in IEDs in many terrorist attacks, including the car bombs in Israel, Iraq and Afghanistan, and various other attacks elsewhere in the world. Urea nitrate can be produced by simply mixing urea and nitric acid under

controlled temperature. Urea nitrate is used in the World Trade Center Bombing on February 26th 1993, causing 6 deaths and 1042 injuries.

1. Spectroscopic approaches for the detection of explosives

Traditional security measures, at the airport, for example, have been using metal detectors to identify any concealed weapon in conjunction with X-ray machines to reveal the contents of baggage. However, explosives, especially modern IEDs, are not easily detectable using conventional approaches for the reason that terrorist groups have adapted to avoid using metals, and instead started using smaller but more powerful compounds and more deceptive devices, such as *shoe bombs*, *backpack bombs* and *underwear bombs*. Spectroscopic approaches, such as infra-red spectroscopy, ion mobility spectroscopy, mass spectroscopy, nuclear magnetic resonance spectroscopy, Raman spectroscopy, and terahertz spectroscopy, have proved to be an accurate and reliable way for identification of explosives [7]. However, these detection approaches employing analytical instruments share the same disadvantages, which lie in the cost of equipment, maintenance, complicated sampling and endless sample preparation period, which thus made them not applicable for continuous monitoring.

4.1 Infra-red spectroscopy

Infra-red (IR) spectroscopy exploits the IR region (10^{-3}-10^{-6}m) of electromagnetic spectrum to identify molecules with characteristic bonds or functional groups. When the transition energy of these bonds or groups that vibrate matches the radiation at specific frequency, the molecule then absorbs such radiation due to resonance. One

challenge of this technology is its specificity to distinguish different molecules with similar groups. Fourier transform infrared (FTIR) spectroscopy is a technique that has been largely used to replace the more traditional dispersive instruments [7]. By scanning all IR frequencies simultaneously, considerable decrease in the time taken for sample analysis is achieved with FTIR, enabling demonstration of absorption spectrum at different wavelength of radiation.

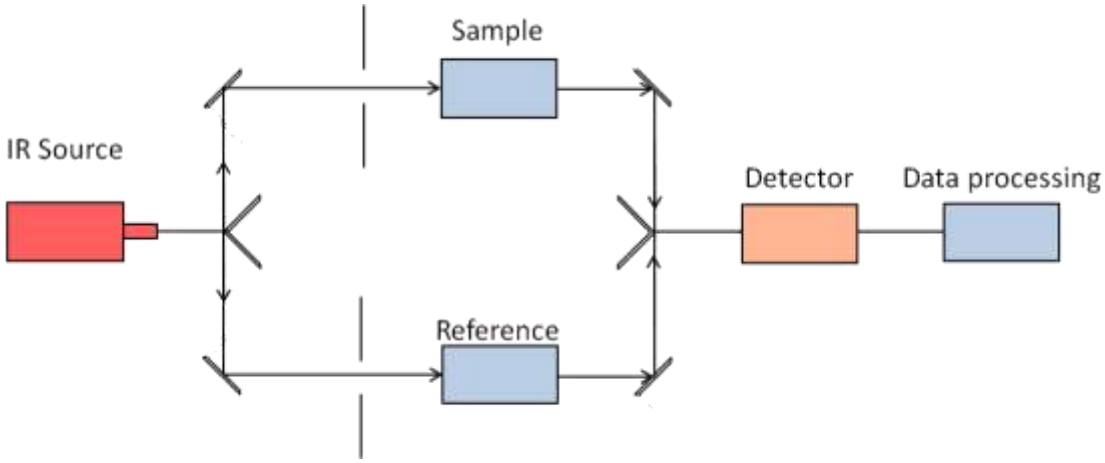

Figure 2.6 Simplified schematic of infrared spectrometer.

The IR band intensities of vibrational transitions in TNT, RDX and PETN vapors were reported by Janni, et al. [8]. They also suggested that ammonium nitrate cannot be detected since it dissociates to smaller fragments. Banas, et al. provided a way of post-blast detection of TNT, RDX and PETN using FTIR [9]. Their technique exhibited a high sensitivity and repeatability results with trace amounts of sample and relatively short analyzing period. Primera-Pedrozo et al. reported a technique for the detection and quantification of high explosives residues on metallic surfaces using fibre optic coupled reflection/absorption IR spectroscopy (RAIRS) [10]. This technique enabled analysis of samples in situ rather than within the spectrometer

sample chamber. Low detection limits were reported of 160 ng/cm^2 for TNT and Tetryl; 220 ng/cm^2 for PETN and DNT; 400 ng/cm^2 for HMX absorbed on the metal surface.

4.2 Ion mobility spectroscopy

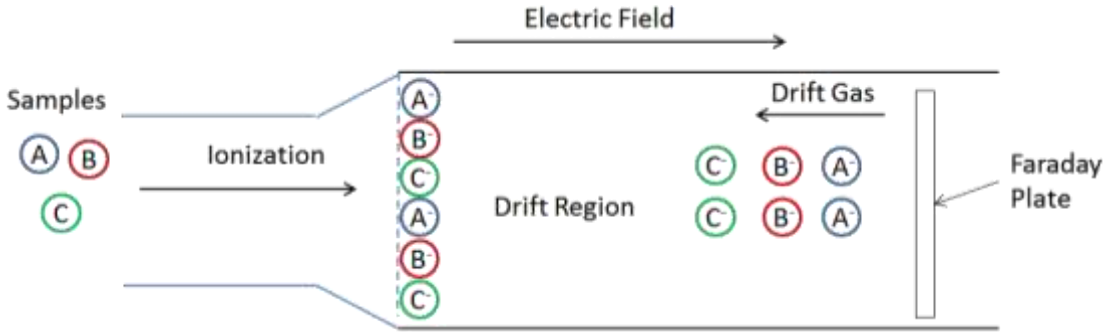

Figure 2.7 Simplified schematic of ion mobility spectrometer for detection of solids.

Ion mobility spectroscopy (IMS) is the most successful and widely used technology for the detection of trace level nitro-organic explosives on handbags and carry on-luggage in airports throughout the US [11]. A simplified schematic of ion mobility spectrometer is shown in *Figure 2.6*. ^{63}Ni or ^{241}Am is typically used as the ionization source. The sample vapors are ionized at atmospheric pressure before electronically injected into the drift region. Under the influence of applied electric field (about 200 V/cm), ions move toward the detector, usually a Faraday plate, creating a signal such as current flow. The drift times are related to the mass of the ions and by determining the mass/charge ratio, it is possible to identify components within the sample through comparison with known standards. In practice, the coefficient of mobility, κ, in units of cm^2/(V·s) is used to replace drift time. Reagent gases are used to create alternate reactant ions that provide additional selectivity in response.

TNT, 2,4-DNT and 2,6-DNT, RDX, PETN and TATP have been widely studied with IMS technology [12-20]. The properties of TNT and its ion behavior showed favorable response in IMS compared with any other explosives. This is because the gas phase chemistry of TNT is relatively simple and product ions have good thermal and chemical stability. The mobility spectrum could be affected by the type of supporting gas and the sensitivity of response was increased with oxygen.

Investigations into sensitivity and accuracy enhancement have increased over recent years. Kanu, et al presented new approaches in reducing false positive interferences in explosive detection using IMS by a rapid pre-separation of potential interference after ionization prior to detection and minimizing the influence of interferents by extending retention time [21]. A detection limit as low as 10 picogram of TNT with a sensitivity of 12 A/g were reported in their work. A pre-concentrating process employing a micro-hotplate coated with a sorbent polymer prior to analysis with IMS was reported [22]. This technique enhanced sensitivity by at least an order of magnitude.

Miniaturization of the IMS apparatus to smaller size for field deployment has also drawn the attention of researchers [23]. A planar ion-focusing aspiration condenser which allows fluidic focusing of ion carrier gas by means of geometric constrains before separation was described [24]. This apparatus consumes less power and has much smaller size, making it a potential device to be incorporated into a hand-held system.

4.3 Mass spectroscopy

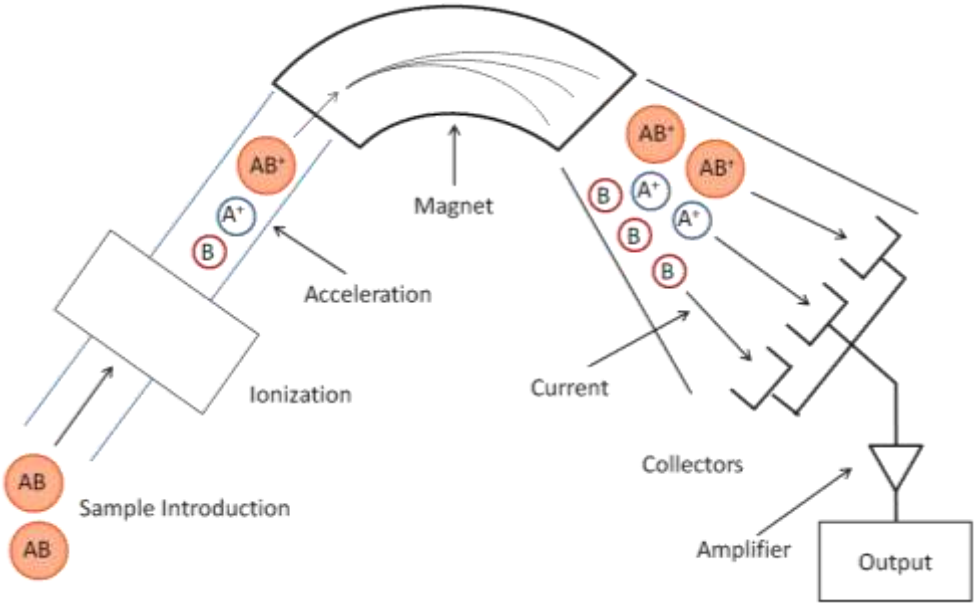

Figure 2.8 Simplified schematic of mass spectroscopy.

Mass spectrometry (MS) has been widely used in explosive detection due to its excellent specificity in identifying substance, both qualitatively and quantitatively, and the speed at which the analysis are completed. The principle of mass spectrometry is that when traveling through the analyzer, the speed and direction of ionized molecules and their fragments of the samples are altered in presence of electric and magnetic field (as shown in *Figure 2.7*). The magnitude of deflection of the moving ion's trajectory is determined by its mass-to-charge ratio, and thus the chemical composition of substance can be separated and analyzed. Various forms of mass spectrometry used for the detection of explosives include ion traps, quadrupoles and time-of-flight mass analyzers, and combinations such as Tandem mass spectrometry system [25]. Detection of explosives using these technologies has been reported [26]. However, this technology is limited in identifying molecules that produce similar fragmented ions.

Coupled technology has been used to enhance the mass resolving capability of mass spectrometry in identifying hydrocarbon compounds. One common combination is gas chromatography-mass spectrometry (GC/MS). Different particles are pre-separated with a gas chromatograph prior being introduced into ion source of mass spectrometer. Bench scale analysis of trace level explosives including ethylene glycol dinitrate (EGDN), DNT, TNT, PETN, RDX and Tetryl have been reported [27-29]. Simulated field detection was reported Holmgren, et al. [30]. They demonstrated an approach for detection of extracted explosives from soil by GC/MS using a negative chemical ionization. Their work required relatively short sample preparation time and achieved a limit of detection of 0.5 μg/g.

An isotope-ration mass spectrometry (IRMS) is a technique that measures relative abundance of isotope in given samples. In addition to identify unknown substance with mass spectrometer, this technology also provides the capability to distinguish one source of the same substance from the other, and thus has been widely used in forensic analysis [31, 32].

4.4 Nuclear magnetic resonance and nuclear quadrupole resonance spectroscopy

Nuclear magnetic resonance (NMR) spectrometry has long been recognized as a powerful tool for structural analysis. NMR is a phenomenon in which nuclei absorb and re-emit electromagnetic radiation at specific resonance frequency in presence of a magnetic field. This technology can be used to study molecular physics, crystals and non-crystalline materials. However, it has been unable to compete with other commonly used analytical methods for the examination of explosives due to lack of

sensitivity. Very limited number of materials using NMR spectrometry has been published to date [33, 34].

Nuclear quadrupole resonance (NQR) spectroscopy is similar in concept to NMR except that it does not require externally applied static magnetic field. Instead, NQR studies the interaction between the quadrupole moment of the electric distribution around the nuclei and the electric field gradient (EFG) applied from outside. Compared with NMR, NQR offers more advantages in explosive detection, for the reason that it is more accurate, more selective and does not rely on external magnetic field which could cause irreversible changes in the molecules under study [35-37].

Most explosives contain nitrogen atoms, which makes it possible to detect the most common isotope ^{14}N using NQR spectrometry. There have been a number of general papers written describing the use of ^{14}N NQR to observe explosives [38-41]. When a suspect sample is scanned by probe coil, an adequate sequence of RF pulses near the NQR frequency of interest is applied, and a return signal will then be detected if the expected chemical specimen is present. One problem is that the return signal from some explosives lasts very short time (i.e. less than 1 ms for TNT [42]) and is not long enough to allow the electrical reverberation (known as magneto-acoustic ringing), an interfering signal, to decay to negligible levels. Several approaches can be taken to solve this problem, such as spin echo sequences, composite pulse sequences, two-photon or three-frequency excitation [43-45]. Another fundamental problem is that the return signals are generally very weak and comparable in magnitude to thermal noise. Measures can be taken to improve the signal-to-noise ratio (SNR) as

well as detection time by employing steady state free precession (SSFP) or continuous wave free precession pulse (CWFP) techniques [46, 47].

4.5 Raman spectroscopy

Raman spectroscopy is a widely used analytical technology which studies the vibrational or rotational transition of molecules by monitoring the inelastic scatted laser photons applied and collected. An energy difference between the incident and scattered photons can be observed when the molecule is excited by photon from ground state to excited state, or the other way around. Raman spectra obtained from Fourier transform techniques can offer a fingerprint of the item under analysis that can identify individual components of the sample.

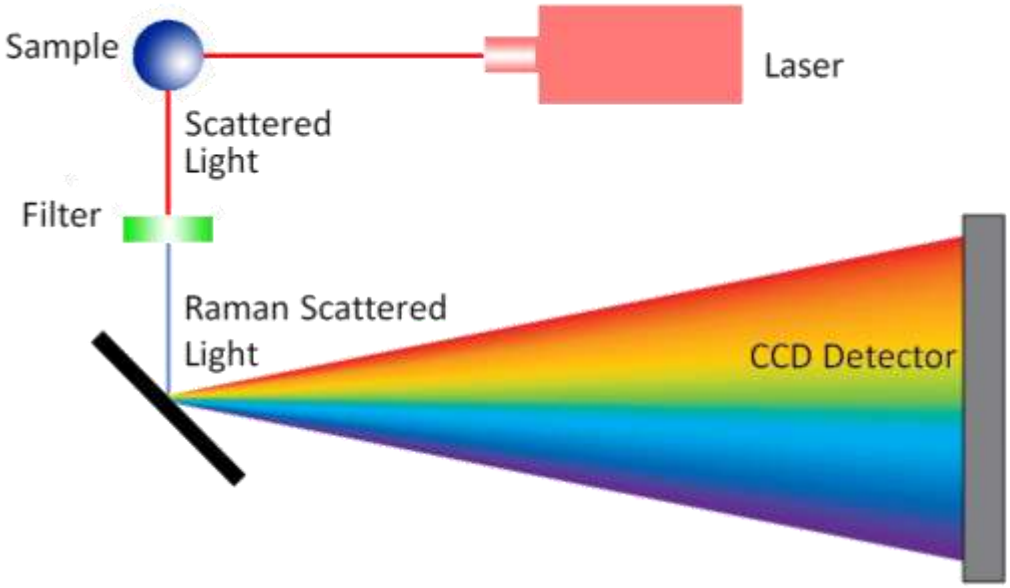

Figure 2.9 Simplified schematic of Raman spectroscopy.

Due to the near instantaneous results and possible stand-off capacity, allowing samples to be analyzed at some distance from the instrumentation, the potential of this technique for use as an explosive detection method has led to considerable work

within this area [7]. Several literatures that describe standoff direct Raman spectroscopy and its various applications have been published recently [48-54].

Miniaturization of this technology has also been widely studied and reported [49-56]. A number of portable Raman devices are commercially available, which can identify small amounts of most kinds of explosives in the field. However, some issues like fluorescence and background mitigation, and possible ignition of dark or deeply colored explosives still exist, limiting its complete application for field uses [56].

4.6 Terahertz spectroscopy

Terahertz technology has demonstrated the capabilities to both detect and identify trace and bulk explosives. Terahertz region usually refers to the frequency range of electromagnetic radiation between 0.1 and 10 THz. The most commonly used methods for terahertz spectroscopy are Fourier transform infrared (FTIR) spectroscopy and terahertz time-domain (THz-TDS) spectroscopy. Compared with FTIR, THz-TDS spectroscopy has the advantage of more frequency coverage and higher signal-to-noise ratio (SNR). With advances in laser technology, small time-domain systems are available for handheld or remote detection [57, 58]. Other techniques for generation of THz radiation include photomixing and electronic spectroscopy.

Detection of 2,4-DNT, 2,6-DNT, TNT, RDX, PETN and ammonium nitrate using terahertz spectroscopy in both gas phase and solid phase have been widely reported [59-67]. However, this technology suffers from several drawbacks that include: the frame rate speed, a loss of attenuation as distance from sample increases, and power requirements for the system [67].

2. Explosive detection using canines

Explosive	Vapor pressure (Torr) at 25 ℃	Vapor pressure (Torr) at 100 ℃
HMTD	-	-
DADP	1.3×10^{-1}	-
TATP	5.1×10^{-2}	-
EGDN	2.8×10^{-2}	22.2
NG	4.4×10^{-4}	3.9×10^{-1}
TNT	7.1×10^{-6}	6.9×10^{-2}
PETN	1.4×10^{-8}	8.0×10^{-4}
RDX	4.6×10^{-9}	1.6×10^{-4}

Table 2.3 Vapor of potential explosives that can be detected by dogs. Symbol "-" indicates that the vapor pressure of such compound is not measurable at given temperature due to decomposition.

Since World War II, dog-handler teams have been used extensively by the military to locate explosives [68]. Sniffer dogs are capable of giving fast and real-time response due to their highly developed sense of smell. Nowadays, the use of canines as a method of detection of explosives is well established worldwide and those applying this technology range from police forces and military to humanitarian agencies in the developing world. A number of studies have been performed to study the sensing ability, sensing mechanism and reliability of canines in explosive detection, as well as training and maintenance related issues [69].

Dogs are able to identify a number of explosives as listed in *Table 2.3*, especially the ones with relatively high vapor pressure and special odor. Both theoretical and experimental scientific evidence demonstrate that the sense of smell is the major sense used by dogs in detection of explosives, compared with sense of hearing and sight [68, 70, 71]. The reliability of dogs in detection of explosives is still a big challenge.

Factors such as breed, fatigue, health, type of explosive material, searching environment (temperature, pressure, humidity, noise level, etc.) and training stage are all important factors that can affect the reliability of the results [72-74]. In order to improve their detection capability and minimize false positive, many new breeding and training protocols have been discussed and developed [75-82].

3. Sensors for explosive detection

A gas sensor, or gas detector, usually refers to a qualitative but non-quantitative analytical device which detects the presence of various gases. Compared with spectroscopic instruments, gas sensors have the capability to perform continuous and real-time monitoring but require much less cost in manufacture, operation and maintenance. In addition, with much smaller geometric dimension, autonomous gas sensors can be deployed in series or groups to form networks for the purpose of general coverage over essential area, or can be incorporated into portable devices with better mobility and flexibility.

The earliest form of gas sensor was invented in the early 19^{th} century by Japanese scientists based on light wave interference. A real sensor era has started in 1970s during which semiconductor combustible gas sensor, solid electrolyte oxygen sensors and humidity sensors were commercialized for civil uses [83]. Till now, extensive efforts have been complied in development and improvement of gas sensors with features of high safety, accuracy, mobility, energy conservation and so on. This technology is becoming a mature application indicated by industrial statistics results. For example, US sales of sensors are forecast to climb at a 6.1% annual rate through

2016 to $14.9 billion [84]. Besides these mature platforms, innovative and effective gas sensors, such as sensors specially designed for explosive detection, have been developed in recent years.

It has been widely discussed that the detection of explosive compounds is a highly significant task in public safety, forensics, antiterrorist activities and global de-mining projects [7]. Continuous monitoring of explosives with high mobility is preferred as it provides an appropriate feedback during the measurement or characterization of sites with security risks and offers rapid warning in presence of suspicious compounds. Not only this, identification and quantification of explosives has constituted an emerging and important topic of interest due to their relevant role in security threat. Accordingly, extensive efforts have been devoted to the development of innovative and effective sensors that are capable of monitoring explosives both in time and location.

6.1 Conductometric sensors

A conductivity sensor is a sensing system that measures the change in conductivity due to the interaction between sensing material and explosive molecules. Conducting polymer composites, intrinsically conducting polymers and metal oxides (mostly semiconductors) are three of the most commonly utilized classes of sensing materials in conductivity sensors [85]. *Figure 2.10* demonstrates typical schematics of a conductometric sensor.

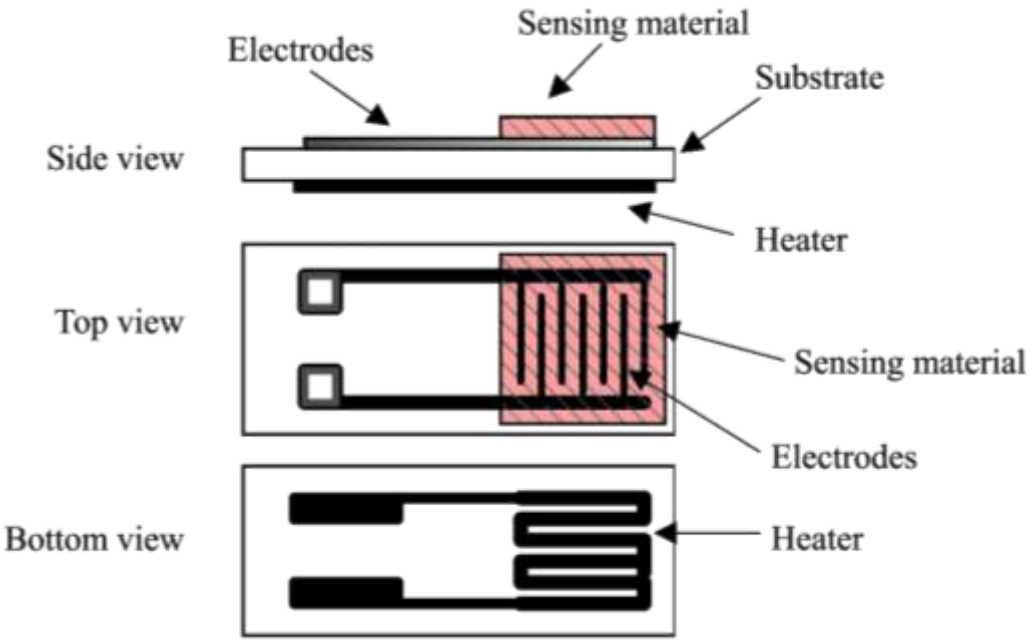

Figure 2.10 Schematics of a typical conductometric sensor.

Conducting polymer composites consist of conducting particles interspersed in an insulating polymer matrix. When exposed to a vapor, some of the gas molecules diffuse into the polymer and causes the polymer film to expand. As a result, this expansion causes a reduction of the conducting pathways for charge carriers, leading to an increase in the electrical resistance of the composite [86]. In addition, chemical reaction between target vapor and filling conductive materials also contributes to the conductivity changes [87]. Compared with other conductometric sensors, conducting polymer composites have the advantage of applicability in humid environment and no heating element is required for detection. The drawbacks of this technique are their constrained detection range from certain gases, and limited lifetime. Intrinsically conducting polymers (ICPs) are composed of unsaturated monomers that can be doped as semiconductors or conductors [88]. When target gas molecules are absorbed into the polymer, the intrachain conductivity as well as intermolecular conductivity is

altered [89]. ICP also works at room temperature and is sensitive to polar compounds, but is vulnerable to humidity interference. Due to their limitations, very limited numbers of literatures can be found which employs the above mentioned two conductivity techniques for explosive detection.

Metal oxide gas sensors based on measuring the conductivity change of the semiconducting materials, or known as conductometric sensors, are one of the most investigated groups of gas sensors due to their low cost and flexibility associated to their production, simplicity of their use and wide possible application fields [90, 91]. The cause of change of sensor conductivity can be traced down to two major causes: physical process and chemical process. One is that when the chemicals are physically adsorbed to the surface of metal oxide, transfer of charge carriers (electrons or holes) between semiconductor and adsorbed species or their catalytic decomposition products leads to the conductivity changes. The other reason is that the chemicals or their catalytic decomposition products is very reactive, either oxidizing or reducing the metal oxide to a different oxidation state which will then alter the electrical property of the semiconducting material.

The sensitivity of conductometric sensor depends on many parameters, including film quality (thickness, density, grain size, crystal structure and defects, etc.), type and loading of dopants, temperature at which the sensor is operated and species of target molecules [85, 92, 93]. Film quality varies from selected deposition approaches, including chemical vapor deposition (CVD), RF sputtering and spin-coating, etc., and post-deposition treatment protocols such as heat treatment and chemical rinse [94-96]. The sensitivity can be improved by adding noble metals to the metal oxide; however,

excessive doping can reduce sensitivity [97-99]. Detection of explosives, including DNT, TNT, RDX, PETN, etc., using conductometric sensor has been widely reported [100-102], with detection limit as low as part per billion. However, conductometric sensor has one major defect being that lack of selectivity to molecules with similar functional groups and thus, limiting its application in explosive recognition. One way to improve its identification capability is by forming sensor arrays or networks with different types of metal oxides that work independently and simultaneously, providing a redundancy of results for analytical purposes [102].

6.2 Calorimetric sensors

Since all chemical reactions and physical changes are associated with generation or consumption of energy, mostly in the form of heat, a quantification of thermal energy provides a simple and universal method for characterizing chemical or physical processes [103]. Based upon this theory, thermal analysis or calorimetry becomes a widely used technique for obtaining both qualitative and quantitative information about thermal transitions associated with a particular material or process. Explosives and energetic materials are designed to provide enormous amount of energy during chemical reaction leading to explosion, making calorimetry an ideal technique for their detection [104]. Besides, as the procurement of traditional explosives becomes difficult with increasingly stricter regulations and security, terrorists have been seeking to utilize novel IEDs such as TATP, which contains neither nitro/nitrate group nor metallic atoms, making conventional detection techniques less effective. As a result, much work has been done recently on calorimetric technique to enhance

detection performance and miniaturize the size of device, i.e. by using MEMS device [103-109].

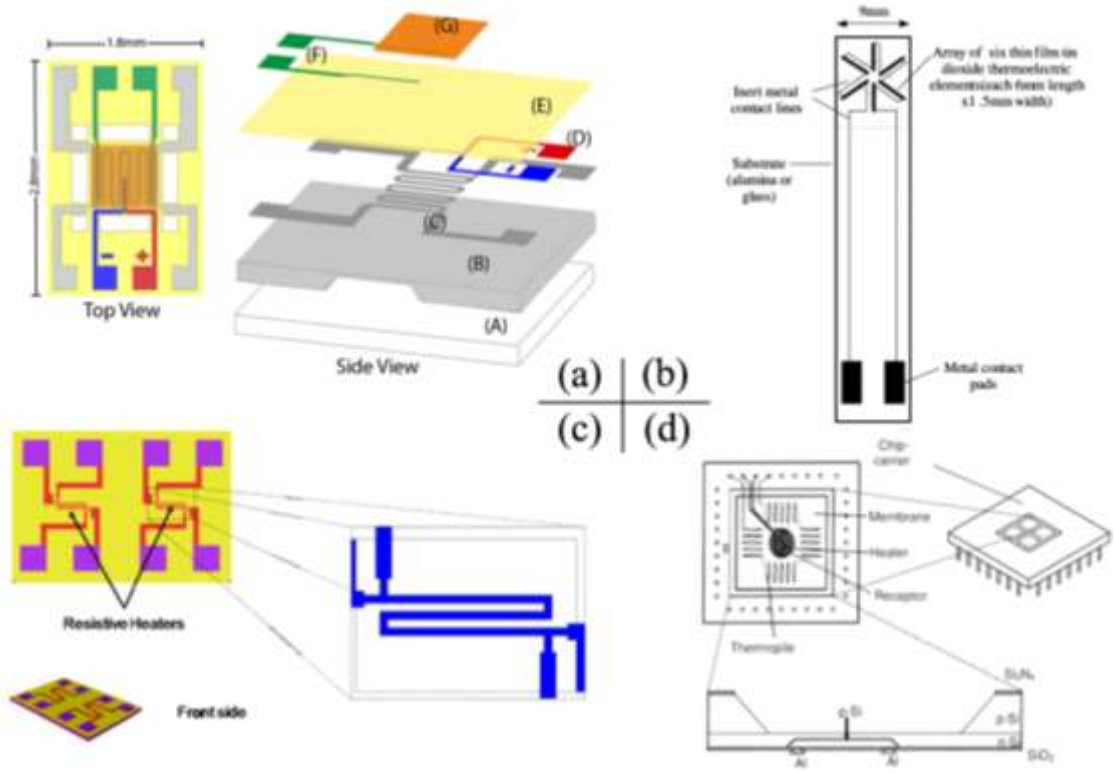

Figure 2.11 Schematics of several calorimetric sensor platforms: (a) MEMS system developed by us (b) sensor platform developed by Casey et al. [107] (c) sensor platform developed by Carreto-Vazquez et al. [108] (d) sensor platform developed by Lerchner et al. [109].

Calorimetric sensor has one major disadvantage that its detection is required to be in a constrained and isolated space for accurate measurements, and thus is not suitable for continuous and real-time monitoring. A differential scanning calorimetry (DSC) technique is then developed to meet all the challenges. It measures the differential heating power between a sample and a reference material as their temperature is varied in a range of interest, directly determining the thermodynamic properties of the sample [110]. Several researches are reported using DSC technique for explosive detection

[111-113]. Still, DSC technique suffers from several drawbacks such as lack of stability and incapability of quantitative analysis.

6.3 Electrochemical sensors

Electrochemical sensors detect change of signal caused by electric currents or electric potential through electrodes when substances interact with electrodes. This technique differs from conductivity sensor because the measurement involves chemical reaction of the explosive molecules or their decomposition product. Since the changes of electrical output result from a flow of electrons or ions during chemical reaction, the inherent redox properties of certain substances, i.e. nitroaromatic explosives and peroxide explosives, make themselves ideal candidate for this technique [1, 114]. Electrochemical sensors are fast in response, inexpensive with high sensitivity and a viable option for miniaturization [115].

Detection of military high explosives that contain nitro groups such as DNT, TNT, RDX and Tetryl are widely reported using electrochemical sensors [116-121]. In Zang, et al.'s work, TNT is reported to be readily detected at 0.2 parts per billion level employing ordered mesoporus carbon [117]. Detection of peroxide based primary explosives, usually TATP and HMTD, are also studied and reported [122, 123]; detection limit is reported at part per million level.

6.4 Optical sensors

Optical sensor is a general term of a vast number of optical transduction techniques, including absorption, fluorescence, phosphorescence, etc. [124-126]. Due to reliability and number of approaches, these techniques have been used in explosive detection in recent years and can be classified into either direct or indirect detection

methods. Direct detection techniques utilize any light-wave which the sample may emit itself or through inducement with a chemical reaction. Indirect detection involves the implication of explosive being present through their effect on a fluorescent material, i.e. via quenching [127]. Depending on the nature of the application and desired sensitivities, different choices of particular optical method can be made. One major disadvantage of optical sensors is their lack of selectivity and incapable of providing reliable results from multiple interference such as temperature and humidity.

Fluorescence is the phenomenon of the emission of light quanta by a molecule or a material (fluorophore) after initial excitation in a light-absorption process. After excitation, a molecule resides for some time in the exited state and its fluorescence emission can be observed with a lower energy (longer wavelength) [128]. Based upon this principle, fluorescence sensors have been widely used in detecting heavy metals, ions, combustible and toxic gases, etc. Due to its high sensitivity and ease of operation, fluorescence sensor has also been used in identification of nitroaromatic explosives in recent years, including TNT, DNT, PETN, etc. [129-131]. Miniaturization has also been studied and Caron et al. were able to detect trace amount of TNT on a piece of cotton using a portable fluorescent device [130].

Fiber optics is usually coupled with other optical techniques composing a integrated sensor that uses optical fiber to detect chemicals by monitoring the changes in the frequency or intensity of electromagnetic radiation. Trace amount of DNT, TNT, PETN and RDX were reported being detected employing fiber optic sensors [132-134].

6.5 Biosensors

Research on controlled animals such as dogs, rats, honeybees and pigs for explosive detection purposes have been studied by different research groups around the world [135]. With more accurate and sensitive detection capability, biologically inspired detection technology has the potential to compete with or be used in conjunction with other artificial technology to complement performance strengths. A biosensor is an analytical device that integrates a biological element on a solid-state surface, enabling a reversible biospecific interaction with the analyte and a signal transducer. The major advantage of biosensor is associated with high sensitivity and specificity of biomolecules for their target substrate. However, they often lack storage and operational stability because they are based on a fragile biological recognition element: an enzyme or antibody.

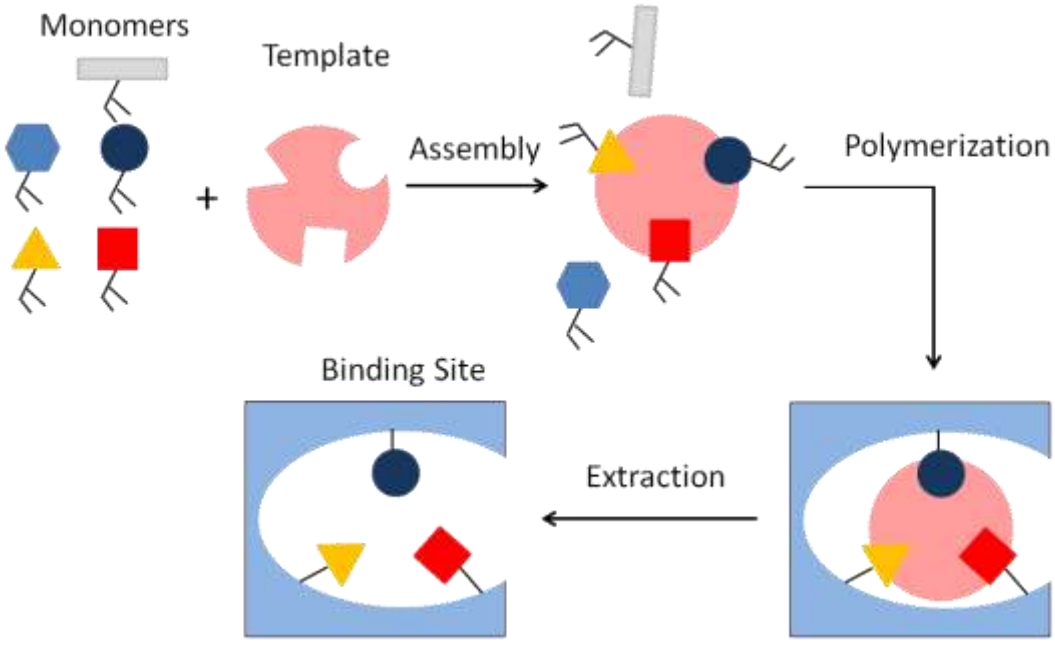

Figure 2.12 The principle of molecular imprinting process.

Computational method has been developed to engineer proteins that can specifically detect a wide array of chemicals from TNT to brain chemicals involved in neurological disorders. A rapidly developing field that takes advantage of nano-scale templating is known as molecular imprinting (*Figure 2.12* [135]). This technique starts with dissolving preselected monomers together with template molecules. During polymerization process, monomers interact with the template and polymer forms around the template. After extraction of the template molecules, a cavity (recognition site) with size, shape and chemical functionality matching to the original template molecules forms and can selectively bind to molecules of interest [136].

Immunosensor is an example of imprinted biosensors and it involves the use of antibodies as biosensing element by measuring the reaction between a target analyte and a specific antibody [137-140]. The detection limit to certain explosive species, TNT for example, is at sub-ppm level.

6.6 Mass sensors

Mass sensors typically adsorb the chemicals of interest onto the surface and the device detects change in mass. The detection can be accomplished through changes in surface acoustic waves (SAW devices) or by actual bending or a change in the shape of the device as mass is accumulated (micro-cantilever devices) [1].

SAW sensor is composed of a piezoelectric substrate with an input and output interdigital transducer deposited on top of the substrate. The sensitive membrane (polymeric or liquid crystal) is placed between the transducers measuring the disturbance in sound wave caused by a chemical across the membrane [141, 142]. If a vapor is present on the surface, it will interact and alter the properties of the wave,

such as frequency, amplitude, phase, etc. The measurement of changes in the surface wave characteristics is a sensitive indicator of the properties of the vapor. SAW devices have been used for detection of explosives, including DNT and TNT [142-144].

Quartz crystal microbalance (QCM) sensor is a typical micro-cantilever sensor that measures the surface force on micro-cantilever induced by the interaction between surface and substance [85]. If such interactions are restricted to on surface, then the resulting differential stress leads to the bending of the cantilever. This QCM sensor has the advantage of superior mass sensitivity, smaller size and low cost. Explosives including TNT, RDX, TATP and PETN have been reported of successful detection using QCM sensors [145-147].

REFERENCES

[1] S. Singh, "Sensors-An effective approach for the detection of explosives," *Journal of Harzardous Materials,* vol. 144, pp. 15-28, 2007.

[2] J. P. Agrawal and R. D. Hodgson, Organic Chemistry of Explosives, Chichester, UK: John Wiley & Sons, Ltd, 2007.

[3] R. Matyas, J. Selesovsky and T. Musil, "Sensitivity to friction for primary explosives," *Journal of Hazardous Materials,* Vols. 213-214, pp. 236-241, 2012.

[4] S. Fordham, High Explosives and Propellants, Fordham, Stanley, UK: Pergamon Press Ltd., 1980.

[5] T. Urbanski, Chemistry and Technology of Explosives, London: Pergamon Press, 1964.

[6] E. M. Green, "Explosives Regulation in the USA," *Industrial Minerals,* vol. 465, p. 78, 2006.

[7] J. S. Caygill, F. Davis and S. P. Higson, "Current trends in explosive detection techniques," *Talanta,* vol. 88, pp. 14-29, 2012.

[8] J. Janni, B. D. Gilbert, R. W. Field and J. I. Steinfeld, "Infrared absorption of explosive molecule vapors," *Spectrochimica Acta Part A: Molecular and Biomolecular Spectroscopy,* vol. 53, pp. 1375-1381, 1997.

[9] A. Banas, K. Banas, M. Bahou, H. O. Moser, L. Wen, P. Yang, Z. J. Li, ang, Z.J. Li, M. Cholewa, S.K. Lim, Ch.H. Lim, M. Cholewa, S. K. Lim and C. H. Lim, "Post-blast detection of traces of explosives by means of Fourier transform infrared spectroscopy," *Vibrational Spectroscopy,* vol. 51, pp. 168-176, 2009.

[10] O. M. Primera-Pedrozo, Y. M. Soto-Feliciano and L. C. Pacheco-Londo, "Detection of high explosives using reflection absorption infrared spectroscopy with fiber coupled grazing angle probe/FTIR," *Sensing and Imaging,* vol. 10, pp. 1-13, 2009.

[11] R. G. Ewing, D. A. Atkinson, G. A. Eiceman and G. J. Ewing, "A critical review of ion mobility spectrometry for the detection of explosives and explosive related compounds," *Talanta,* vol. 54, pp. 515-529, 2001.

[12] F. W. Karasek and D. W. Denney, "Detection of 2,4,6-trinitrotoluene vapours in air by plasma chromatography," *Journal of Chromatography,* vol. 93, pp. 141-147, 1974.

[13] G. E. Spangler and P. A. Lawless, "Ionization of nitrotoluene compounds in Negative ion plasma chromatography," *Analytical Chemistry,* vol. 50, pp. 884-892, 1978.

[14] S. D. Huang, L. Kolaitis and D. M. Lubman, "Detection of explosives using

laser desorption in ion mobility spectrometry/mass spectrometry," *Applied Spectroscopy,* vol. 41, pp. 1371-1376, 1987.

[15] G. E. Spangler, J. P. Carrico and D. N. Campbel, "Recent advances in ion mobility spectrometry for explosives vapor detection," *Journal of Testing and Evaluation,* vol. 13, pp. 234-240, 1985.

[16] G. R. Asbury, J. Klasmeier and H. H. Hill, "Analysis of explosives using electrospray ionization/ion mobility spectrometry (ESI/IMS)," *Talanta,* vol. 50, pp. 1291-1298, 2000.

[17] G. A. Eiceman, D. Preston, G. Tiano, J. Rodriguez and J. E. Parmeter, "Quantitative calibration of vapor levels of TNT, RDX, and PETN using a diffusion generator with gravimetry and ion mobility spectrometry," *Talata,* vol. 45, pp. 57-74, 1997.

[18] T. Khayamian, M. Tabrizchi and M. T. Jafari, "Analysis of 2,4,6-trinitrotoluene, pentaerythritol tetranitrate and cyclo-1,3,5-trimethylene-2,4,6-trinitramine using negative corona discharge ion mobility spectrometry," *Talanta,* vol. 54, pp. 515-529, 2001.

[19] T. L. Buxton and P. B. Harrington, "Rapid multivariate curve resolution applied to identification of explosives by ion mobility spectrometry," *Analytica Chimica Acta,* vol. 434, pp. 269-282, 2001.

[20] G. A. Buttigieg, A. K. Knight, S. Denson, C. Pommier and M. B. Denton,

"Characterization of the explosive triacetone triperoxide and detection by ion mobility spectrometry," *Forensic Science International*, vol. 135, pp. 53-59, 2003.

[21] A. B. Kanu, C. Wu and H. H. Hill Jr., "Rapid preseparation of interferences for ion mobility spectrometry," *Analytica Chimica Acta*, vol. 610, pp. 125-134, 2008.

[22] M. Martin, M. Crain, K. Walsh, R. A. McGill, E. Houser, J. Stepnowski and S. Stepnows, "Microfabricated vapor preconcentrator for portable ion mobility spectroscopy," *Sensors and Actuators B*, vol. 126, pp. 447-454, 2007.

[23] A. Zalewska, W. Pawlowski and W. Tomaszewski, "Limits of detection of explosives as determined with IMS and field asymmetric IMS vapour detectors," *Forensic Science International*, vol. 226, pp. 168-172, 2013.

[24] S. Zimmermann, N. Abel, W. Baether and S. Barth, "An ion-focusing aspiration condenser as an ion mobility spectrometer," *Sensors and Actuators B*, vol. 125, pp. 428-434, 2007.

[25] J. Yinon, "Analysis and detection of explosives by mass spectrometry," in *Aspects of Explosives Detection*, Oxford, UK, Elsevier, 2009, pp. 147-169.

[26] F. Rowell, J. Seviour, A. Y. Lim, C. G. Elumbaring-Salazar, J. Loke and J.

Ma, "Detection of nitro-organic and peroxide explosives in latent fingermarks by DART- and SALDI-TOF-mass spectrometry," *Forensic Science International,* vol. 221, pp. 84-91, 2012.

[27] J. M. Perr, K. G. Furton and J. R. Almirall, "Gas chromatography positive chemical ionization and tandem mass spectrometry fot the analysis of organic high explosives," *Talanta,* vol. 67, pp. 430-436, 2005.

[28] J. A. Mathis and B. R. McCord, "The analysis of high explosives by liquid chromatography/electrospray ionization mass spectrometry: multiplexed detection of negative ion adducts," *Rapid Communications in Mass Spectrometry,* vol. 19, pp. 99-104, 2005.

[29] O. L. Collin, C. M. Zimmermann and G. P. Jackson, "Fast gas chromatography negative chemical ionization tandem mass spectrometry of explosive compounds using dynamic collision-induced dissociation," *Mass Spectrometry,* vol. 279, pp. 93-99, 2009.

[30] E. Holmgren, S. Ek and A. Colmsjo, "Extraction of explosives from soil followed by gas chromatography–mass spectrometry analysis with negative chemical ionization," *Journal of Chromatography A,* vol. 1222, pp. 109-115, 2012.

[31] S. Benson, C. Lennard, P. Maynard and C. Roux, "Forensic applications of isotope ratio mass spectrometry—A review," *Forensic Science International,*

vol. 157, pp. 1-22, 2006.

[32] D. Wakelin, Isotopic ratio analysis of explosives traces – a new type of evidence, UK: United Kingdom Defence Evaluation and Research Agency report, 2000.

[33] D. T. Burns and R. J. Lewis, "Analysis and characterisation of nitroglycerine based explosives by proton magnetic resonance spectrometry," *Analytica Chimica Acta,* vol. 300, pp. 221-225, 1995.

[34] J. A. Smith, T. J. Rayner, M. D. Rowe, J. Barras, N. F. Peirson, A. D. Stevens and K. Althoefer, "Magnetic field-cycling NMR and ^{14}N, ^{17}O quadrupole resonance in the explosive pentaerythritol tetranitrate (PETN)," *Journal of Megnetic Resonance,* vol. 204, pp. 139-144, 2010.

[35] J. B. Miller, "Chapter 7 - Nuclear quadrupole resonance detection of explosives," in *Counterterrorist Detection Techniques of Explosives*, Oxford, UK, Elsevier, 2007, pp. 157-198.

[36] J. N. Latosinska, "Nuclear Quadrupole Resonance spectroscopy in studies of biologically active molecular systems - a review," *Journal of Pharmaceutical and Biomedical Analysis,* vol. 38, pp. 577-587, 2005.

[37] T. M. Osan, L. M. Cerioni, J. Forguez and J. M. Olle, "NQR: From imaging to explosives and drugs detection," *Physica B: Condensed Matter,* vol. 389,

pp. 45-50, 2007.

[38] A. N. Garroway, M. L. Buess, J. P. Yesinowski and J. B. Miller, "Narcotics and explosive detection by ^{14}N pure NQR," *Proceedings of SPIE*, vol. 2092, pp. 318-327, 1993.

[39] V. S. Grechishkin and N. Y. Sinyavskii, "New technologiesnuclear quadrupole resonance as an explosive and narcotic detection technique," *Physics Uspekhi*, vol. 40, pp. 393-406, 1997.

[40] A. N. Garroway, M. L. Buess, J. B. Miller, B. H. Suits, A. D. Hibbs, G. A. Barrall, R. Matthews and L. J. Burnett, "Remote sensing by nuclear quadrupole resonance," *IEEE Transactions, Geoscience and Remote Sensing*, vol. 39, pp. 1108-1118, 2001.

[41] J. A. Smith, M. Blanz, T. J. Rayner, M. D. Rowe, S. Bedford and K. Althoefer, "^{14}N quadrupole resonance and ^{1}H T1 dispersion in the explosive RDX," *Journal of Magnetic Resonance*, vol. 213, pp. 98-106, 2011.

[42] V. T. Mikhaltsevitch and T. N. Rudakov, "On the NQR detection of nitrogenated substances by multi-pulse sequences," *Physica Status Solidi (b)*, vol. 241, pp. 411-419, 2004.

[43] Y. Millot and P. P. Man, "Determination of quadrupole parameters with a composite pulse for spurious signal suppression," *Journal of Magnetic*

Resonance, vol. 150, pp. 10-16, 2001.

[44] P. T. Eles and C. A. Michal, "Two-photon excitation in nuclear quadrupole resonance," *Chemical Physics Letters,* vol. 376, pp. 268-273, 2003.

[45] K. L. Sauer, B. H. Suits, A. N. Garroway and J. B. Miller, "Three-frequency nuclear quadrupole resonance of spin-1 nuclei," *Chemical physics Letters,* vol. 342, pp. 362-368, 2001.

[46] S. S. Kim, J. R. Jayakody and R. A. Marino, "Experimental investigations of the strong off resonant comb (SORC) pulse sequence in ^{14}N NQR," *Verlag der Zeitschrift für Naturforschung (A),* vol. 47, pp. 415-420, 1993.

[47] L. M. Cerioni and D. J. Pusiol, "A new method to obtain frequency offsets in NQR multi-pulse sequences," *Hyperfine Interactions,* vol. 159, pp. 389-393, 2005.

[48] M. Wu, M. Ray, K. H. Fung, M. W. Ruckman, D. Harder and A. J. Sedlacek, "Stand-off Detection of Chemicals by UV Raman Spectroscopy," *Applied Spectroscopy,* vol. 54, pp. 196-220, 2000.

[49] M. D. Ray, A. J. Sedlacek and M. Wu, "Ultraviolet mini-Raman lidar for stand-off, in situ identification of chemical surface contaminants," *Review of Scientific Instruments,* vol. 71, pp. 3485-3489, 2000.

[50] N. Gupta and R. Dahmani, "AOTF Raman spectrometer for remote detection

of explosives," *Spectrochimica Acta A,* vol. 56, pp. 1453-1456, 2000.

[51] J. C. Carter, S. M. Angel, M. Lawrence-Snyder, J. Scaffidi, R. E. Whipple and J. G. Reynolds, "Standoff Detection of High Explosive Materials at 50 Meters in Ambient Light Conditions Using a Small Raman Instrument," *Applied Spectroscopy,* vol. 59, pp. 120-138, 2005.

[52] S. K. Sharma, A. K. Misra and B. Sharma, "Portable remote Raman system for monitoring hydrocarbon, gas hydrates and explosives in the environment," *Spectrochimica Acta A,* vol. 61, pp. 2404-2412, 2005.

[53] S. K. Sharma, A. K. Misra, P. G. Lucey, S. M. Angel and C. P. McKay, "Remote Pulsed Raman Spectroscopy of Inorganic and Organic Materials to a Radial Distance of 100 Meters," *Applied Spectroscopy,* vol. 60, pp. 871-876, 2006.

[54] C. Eliasson, N. A. Macleod and P. Matousek, "Noninvasive detection of concealed liquid explosives using Raman spectroscopy," *Analytical Chemistry,* vol. 79, pp. 8185-8189, 2007.

[55] E. L. Izake, "Forensic and homeland security applications of modern portable Raman spectroscopy," *Forensic Science International,* vol. 202, pp. 1-8, 2010.

[56] D. S. Moore and R. J. Scharff, "Portable Raman explosive detection," *Analytical and Bioanalytical Chemistry,* vol. 393, pp. 1571-1578, 2009.

[57] J. Xu, H. Liu, T. Yuan, R. Kersting and X.-C. Zhang, "Advanced terahertz time-domain spectroscopy for remote detection and tracing," *Proceedings of SPIE,* vol. 5070, pp. 17-27, 2003.

[58] M. R. Leahy-Hoppa, M. J. Fitch and R. Osiander, "Terahertz spectroscopy techniques for explosives detection," *Analytical and Bioanalytical Chemistry,* vol. 395, pp. 247-257, 2009.

[59] Y. Hu, P. Huang, L. Guo, X. Wang and C. Zhang, "Terahertz spectroscopic investigations of explosives," *Physics Letters A,* vol. 359, pp. 728-732, 2006.

[60] T. Yuan, H. Liu, J. Xu, F. Al-Douseri, Y. Hu and X.-C. Zhang, "Terahertz time-domain spectroscopy of atmosphere with different humidity," *Proceedings of SPIE,* vol. 5070, pp. 28-37, 2003.

[61] R. J. Foltynowicz, R. E. Allman and E. Zuckerman, "Terahertz absorption measurement for gas-phase 2,4-dinitrotoluene from 0.05 THz to 2.7 THz," *Chemical Physics Letters,* vol. 431, pp. 34-38, 2006.

[62] W. R. Tribe, D. A. Newnham, P. F. Taday and M. C. Kemp, "Hidden object detection: security applications of terahertz technology," *Proceedings of SPIE,* vol. 5354, pp. 168-176, 2004.

[63] M. C. Kemp, P. F. Taday, B. E. Cole, J. A. Cluff, A. J. Fitzgerald and W. R. Tribe, "Security applications of terahertz technology," *Proceedings of SPIE,*

vol. 5070, pp. 44-52, 2003.

[64] J. F. Federici, B. Schulkin, F. Huang, D. Gary, R. Barat, F. Oliveira and D. Zimdars, "THz imaging and sensing for security applications—explosives, weapons and drugs," *Semiconductor Science and Technology*, Vols. S266-S280, p. 20, 2005.

[65] D. J. Cook, B. K. Decker, G. Maislin and M. G. Allen, "Through container THz sensing: applications for explosives screening," *Proceedings of SPIE*, vol. 5354, pp. 55-62, 2004.

[66] Y. Chen, H. Liu, M. J. Fitch, R. Osiander, J. B. Spicer, M. Shur and X.-C. Zhang, "THz diffuse reflectance spectra of selected explosives and related compounds," *Proceedings of SPIE*, vol. 5790, pp. 19-24, 2005.

[67] H. Liu, Y. Chen, G. J. Bastiaans and X. Zhang, "Detection and identification of explosive RDX by THz diffuse reflection spectroscopy," *Optics Express*, vol. 14, pp. 415-423, 2006.

[68] K. G. Furton and L. J. Myers, "The scientific foundation and efficacy of the use of canines as chemical detectors for explosives," *Talanta*, vol. 54, pp. 487-500, 2011.

[69] L. P. Waggoner, "Chapter 3 – Detection of Explosives by Dogs," in *Aspects of Explosives Detection*, Oxford, UK, Elsevier, 2009, pp. 27-40.

[70] W. Neuhaus, "Uber die Riechscharfe des Hundes fur Fettsauren," *Zeitschrift Fur Vergleichende Physiologie,* vol. 35, p. 527, 1953.

[71] I. Gazit and J. Terkel, "Domination of olfaction over vision in explosives detection by dogs," *Applied Animal Behaviour Science,* vol. 82, pp. 65-73, 2003.

[72] I. Gazit and J. Terkel, "Explosives detection by sniffer dogs following strenuous physical activity," *Applied Animal Behaviour Science,* vol. 81, pp. 149-161, 2003.

[73] T. Jezierski, E. Adamkiewicz, M. Walczak, M. Porkopczyk and M. Wziatek, "Factors affecting drugs and explosives detection by dogs in experimental tests," *Journal of Veterinary Behavior: Clinical Applications and Research,* vol. 8, p. e33, 2013.

[74] G. Diesel, D. Brodbelt and D. U. Pfeiffer, "Reliability of assessment of dogs' behavioural responses by staff working at a welfare charity in the UK," *Applied Animal Behaviour Science,* vol. 115, p. 171–181, 2008.

[75] T. G. Berntsen, "Global training centre of mine detection dogs in Bosnia: Breeding and training program," *Journal of Veterinary Behavior: Clinical Applications and Research,* vol. 4, p. 245–246, 2009.

[76] 1. T. F. Michael Ben Alexandera, M. B. Alexandera, T. Friend and L. Haug, "Obedience training effects on search dog performance," *Applied Animal Behaviour Science,* vol. 132, pp. 152-159, 2011.

[77] A. Haverbeke, B. Laporte, E. Depiereux, J. M. Giffroy and C. Diederich, "Training methods of military dog handlers and their effects on the team's performances," *Applied Animal Behaviour Science,* vol. 113, pp. 110-122, 2008.

[78] R. J. Harper, J. R. Almirall and K. G. Furto, "Identification of dominant odor chemicals emanating from explosives for use in developing optimal training aid combinations and mimics for canine detection," *Talanta,* vol. 67, pp. 313-327, 2005.

[79] M. Williams and J. M. Johnston, "Training and maintaining the performance of dogs (Canis familiaris) on an increasing number of odor discriminations in a controlled setting," *Applied Animal Behaviour Science,* vol. 78, pp. 55-65, 2002.

[80] J. Riva, S. P. Marelli, V. Redaelli, E. Sforzini, F. Luzi and G. P. Bondio, "Effect of training on behavioral reactivity and neurotransmitter levels in drug detection dogs," *Journal of Veterinary Behavior: Clinical Applications and*

Research, vol. 5, pp. 38-39, 2010.

[81] N. J. Hall, D. W. Smith and D. L. Wynne, "Training domestic dogs (Canis lupus familiaris) on a novel discrete trials odor-detection task," *Learning and Motivation,* p. In press, 2013.

[82] L. A. Guerrero, "Quick Learning Techniques: Dogs used to detect narcotics and explosives," *Journal of Veterinary Behavior: Clinical Applications and Research,* vol. 4, p. 253, 2009.

[83] N. Yamazoe, "Toward innovations of gas sensor technology," *Sensors and Actuators B ,* vol. 108, pp. 2-14, 2005.

[84] Industry Report, Sensors Markets 2016, Freedonia, 2013.

[85] K. Arshak, E. Moore, G. M. Lyons, J. Harris and S. Clifford, "A review of gas sensors employed in electronic nose applications," *Sensor Review,* vol. 24, pp. 181-198, 2004.

[86] B. C. Munoz, G. Steinthal and S. Sunshine, "Conductive polymer-carbon black composites-based sensor arrays for use in an electronic nose," *Sensor Review,* vol. 19, pp. 300-305, 1999.

[87] K. J. Albert, N. S. Lewis, C. L. Schauer, G. A. Sotzing, S. E. Stitzel, T. P. Vaid and D. R. Walt, "Cross reactive chemical sensor arrays," *Chemical Reviews,* vol. 100, pp. 2595-2626, 2000.

[88] A. J. Heeger, "Semiconducting and metallic polymers: the fourth generation of polymeric materials," *Current Applied Physics,* vol. 1, pp. 247-267, 2001.

[89] J. M. Charlesworth, A. C. Partridge and N. Garrard, "Mechanistic studies on the interactions between poly (pyrrole) and organic vapors," *Journal of Physical Chemistry,* vol. 97, pp. 5418-5423, 1993.

[90] D. E. Williams, "Semiconducting oxides as gas-sensitive resistors," *Sensors and Actuators B,* vol. 57, pp. 1-16, 1999.

[91] N. Barsan, D. Koziej and U. Weimar, "Metal oxide-based gas sensor research: How to," *Sensors and Acutators B,* vol. 121, pp. 18-35, 2007.

[92] E. Schaller, J. O. Bosset and F. Escher, "Electronic noses and their application to food," *LebensmittelWissenschaft und-Jechnologie,* vol. 31, pp. 305-316, 1998.

[93] G. Gaggiotti, A. Galdikas, S. Kaciulis, G. Mattogno and A. Setkus, "Temperature dependencies of sensitivity and surface chemical composition

of SnO_x gas sensors," *Sensors and Actuators B,* vol. 25, p. 516–519, 1995.

[94] J. Huang, D. Kuo and B. Shew, "The effects of heat treatment on the gas sensitivity of reactively sputtered SnO_2 films," *Surface and Coatings Technology,* vol. 79, pp. 263-267, 1996.

[95] Y. Hu, O. K. Tan, J. S. Pan, H. Huang and W. Cao, "The effects of annealing temperature on the sensing properties of low temperature nano-sized $SrTiO_3$ oxygen gas sensor," *Sensors and Actuators B,* vol. 108, p. 244–249, 2005.

[96] K. Kato, H. Omoto, T. Tomioka and A. Takamatsu, "Optimum packing density and crystal structure of tin-doped indium oxide thin films for high-temperature annealing processes," *Applied Surface Science,* vol. 257, p. 9207–9212, 2011.

[97] G. Korotcenkov and B. K. Cho, "Engineering approaches for the improvement of conductometric gas sensor parameters: Part 1. Improvement of sensor sensitivity and selectivity," *Sensors and Actuators B,* vol. 188, pp. 709-728, 2013.

[98] G. Korotcenkov, I. Boris, V. Brinzari, S. H. Han and B. K. Cho, "The role of doping effect on the response of SnO_2-based thin film gas sensors: Analysis

based on the results obtained for Co-doped SnO2 films deposited by spray pyrolysis," *Sensors and Actuators B,* vol. 182, pp. 112-124, 2013.

[99] S. J. Ippolito, S. Kandasamy, K. Kalantar-zadeh and W. Wlodarski, "Hydrogen sensing characteristics of WO_3 thin film conductometric sensors activated by Pt and Au catalysts," *Sensors and Actuators B,* vol. 108, pp. 154-158, 2005.

[100] J. W. Gardner and P. N. Bartlett, Electronic Noses – Principles and Applications, Oxford, UK: Oxford University Press, 1999.

[101] J. Yinon, "Detection of explosives by electronic noses," *Analytical Chemistry,* vol. 75, pp. 99-105, 2003.

[102] K. Brudzewski, S. Osowski and W. Pawlowski, "Metal oxide sensor arrays for detection of explosives at sub-parts-per million concentration levels by the differential electronic nose," *Sensors and Actuators B,* vol. 161, pp. 528-533, 2012.

[103] P. Bunyan, C. Baker and N. Rurner, "Application of heat conduction calorimetry to high explosives," *Thermochimica Acta,* vol. 401, pp. 9-16, 2003.

[104] Y. Liu, V. M. Ugaz, S. W. North, W. J. Rogers and S. Mannan, "Development of a miniature calorimeter for identification and detection of explosives and other energetic compounds," *Journal of Hazardous Materials,* vol. 142, pp. 662-668, 2007.

[105] J. O. A. Grevea, A. Greve, J. Olsen, N. Privorotskaya, L. Senesac, T. Thundat, W. P. King and A. Boisen, "Micro-calorimetric sensor for vapor phase explosive detection with optimized heat profile," *Microelectronic Engineering,* vol. 87, p. 696–698, 2010.

[106] A. Zark, D. Kaplan and S. Kendler, "A MEMS-based microthermal analysis of explosive materials," *Sensors and Actuators A,* vol. 199, pp. 129-135, 2013.

[107] V. Casey, J. Cleary, G. D'Arcy and J. B. McMonagle, "Calorimetric combustible gas sensor based on a planar thermopile array: fabrication, characterisation, and gas response," *Sensors and Actuators B,* vol. 96, p. 114–123, 2003.

[108] V. H. Carreto-Vazquez, A. K. Wojcik, Y. Liu, D. B. Bukur and M. S. Mannan, "Miniaturized calorimeter for thermal screening of energetic materials," *Microelectronics Journal,* vol. 41, pp. 874-881, 2010.

[109] J. Lerchner, D. Caspary and G. Wolf, "Calorimetric detection of volatile

organic compounds," *Sensors and Actuators B,* vol. 70, pp. 57-66, 2000.

[110] B. Wang and Q. Lin, "Temperature-modulated differential scanning calorimetry in a MEMS device," *Sensors and Actuators B,* vol. 180, pp. 60-65, 2013.

[111] M. Amani, Y. Chu, K. L. Waterman, C. M. Hurley, M. J. Platek and O. J. Gregory, "Detection of triacetone triperoxide (TATP) using a thermodynamic based gas sensor," *Sensors and Actuators B,* vol. 162, pp. 7-13, 2012.

[112] D. J. Whelan, R. J. Spear and R. W. Read, "The thermal decomposition of some primary explosives as studied by differential scanning calorimetry," *Thermochimica Acta,* vol. 80, p. 149–163, 1984.

[113] A. Burger and K. D. Wehrstedt, "Azodicarboxylates: Explosive properties and DSC measurements," *Journal of Loss Prevention in the Process Industries,* vol. 23, p. 734–739, 2010.

[114] J. Wang, "Electrochemical Sensing of Explosives," *Electroanalysis,* vol. 19, p. 415–423, 2007.

[115] P. Rabenecker and K. Pinkwart, "A Look Behind Electrochemical Detection of Explosives," *Propellants, Explosives, Pyrotechnics,* vol. 34, p. 274–279, 2009.

[116] W. Chen, Y. Wang, C. Bruckner, C. Li and Y. Lei, "Poly[meso-tetrakis(2-

thienyl)porphyrin] for the sensitive electrochemical detection of explosives," *Sensors and Actuators B,* vol. 147, p. 191–197, 2010.

[117] J. Zang, C. Guo, F. Hu, L. Yu and C. Li, "Electrochemical detection of ultratrace nitroaromatic explosives using ordered mesoporous carbon," *Analytica Chimica Acta,* vol. 683, p. 187–191, 2011.

[118] R. Blue, Z. Vobeck, P. J. Skabara and D. Uttamchandani, "The development of sensors for volatile nitro-containing compounds as models for explosives detection," *Sensors and Actuators B: Chemical,* vol. 176, pp. 534-542, 2013.

[119] K. Masunaga, K. Hayama, T. Onodera, K. Hayashi, N. Miura, K. Matsumoto and K. Toko, "Detection of aromatic nitro compounds with electrode polarization controlling sensor," *Sensors and Actuators B,* Vols. 427-434, p. 108, 2005.

[120] K. B. Lee, M. B. Gu and S. H. Moon, "Degradation of 2,4,6-trinitrotoluene by immobilized horseradish peroxidase and electrogenerated peroxide," *Water Research,* vol. 37, pp. 983-992, 2003.

[121] S. Y. Ly, D. H. Kim and M. H. Kim, "Square-wave cathodic stripping voltammetric analysis of RDX using mercury-film plated glassy carbon electrode," *Talanta,* Vols. 919-926, p. 58, 2002.

[122] D. A. Cagan, R. A. Munoz, T. Tangkuaram and J. Wang, "Highly sensitive

electrochemical detection of trace liquid peroxide explosives at a Prussian-blue ‘artificial-peroxidase’ modified electrode," *Analyst,* vol. 131, pp. 1279-1281, 2006.

[123] S. Parajuli and W. Miao, "Sensitive Determination of Hexamethylene Triperoxide Diamine Explosives, Using Electrogenerated Chemiluminescence Enhanced by Silver Nitrate," *Analytical Chemistry,* vol. 81, pp. 5267-5272, 2009.

[124] V. Lopez-Avila and H. H. Hill, "Field analytical chemistry," *Analytical Chemistry,* vol. 69, pp. 289-306, 1997.

[125] J. Janata, M. Josowicz, P. Vanysek and D. Michael DeVaney, "Chemical sensors," *Analytical Chemistry,* vol. 70, p. 179–208, 1998.

[126] M. S. Meaney and V. L. McGuffin, "Luminescence-based methods for sensing and detection of explosives," *Analytical and Bioanalytical Chemistry,* vol. 391, pp. 2557-2576, 2008.

[127] F. Chu and J. Yang, "Study of nitro aromatic explosives sensor based on fluorescence quenching," *Optik - International Journal for Light and Electron Optics,* vol. 122, pp. 2246-2248, 2011.

[128] A. P. Demchenko, Introduction to Fluorescence Sensing, Netherland: Springer Netherlands, 2009.

[129] J. Cho, A. Anandakathir, A. Kumar, J. Kumar and P. U. Kurup, "Sensitive and fast recognition of explosives using fluorescent polymer sensors and pattern recognition analysis," *Sensors and Actuators B,* vol. 160, p. 1237–1243, 2011.

[130] T. Caron, M. Cuillemot, P. Montmeat, F. Veignal, F. Perraut, P. Prene and F. Serein-Spirau, "Ultra trace detection of explosives in air: Development of a portable fluorescent detector," *Talanta,* vol. 81, p. 543–548, 2010.

[131] M. P. Monterola, B. W. Smith, N. Omenetto and J. D. Winefordner, "Photofragmentation of nitro-based explosives with chemiluminescence detection," *Analytical and Bioanalytical Chemistry,* vol. 391, pp. 2617-2626, 2008.

[132] X. Li, Q. Li, H. Zhou, H. Hao, T. Wang, S. Zhao, Y. Lu and G. Huang, "Rapid, on-site identification of explosives in nanoliter droplets using a UV reflected fiber optic sensor," *Analytica Chimica Acta,* vol. 751, pp. 112-118, 2012.

[133] K. J. Albert and D. R. Walt, "High speed fluorescence detection of explosive like," *Analytical Chemistry,* vol. 72, p. 1947–1955, 2000.

[134] L. C. Shriver-Lake, C. H. Patterson and S. K. Van Bergen, "New Horizons: explosive detection in soil extracts with a fiber-optic biosensor," *Field*

Analytical Chemistry and Technology, vol. 4, pp. 239-245, 2000.

[135] M. K. Habib, "Controlled biological and biomimetic systems for landmine detection," *Biosensors and Bioelectronics,* vol. 23, pp. 1-18, 2007.

[136] D. Kriz and R. J. Ansell, "Man Made Mimics of Antibodies and their Application in Analytical Chemistry," *Molecularly Imprinted Polymers,* vol. 23, p. 417–436, 2001.

[137] D. R. Shankaran, K. V. Gobi, T. Sakai, K. Matsumoto, K. Toko and N. Miura, "Surface plasmon resonance immunosensor for highly sensitive detection of 2,4,6-trinitrotoluene," *Biosensors and Bioelectronics,* vol. 20, p. 1750–1756, 2005.

[138] P. T. Charles and A. W. Kusterbeck, "Trace level detection of hexahydro-1,3,5-trinitro-1,3,5-triazine (RDX) by microimmunosensor," *Biosensors and Bioelectronics,* vol. 14, p. 387–396, 1999.

[139] M. Park, L. N. Cella, W. Chen, N. V. Myung and A. Mulchandani, "Carbon nanotubes-based chemiresistive immunosensor for small molecules: Detection of nitroaromatic explosives," *Biosensors and Bioelectronics,* vol. 26, p. 1297–1301, 2010.

[140] R. Wilson, C. Clavering and A. Hutchinson, "Paramagnetic bead based enzyme electrochemiluminescence immunoassay for TNT," *Journal of Electroanalytical Chemistry,* vol. 557, pp. 109-118, 2003.

[141] Z. P. Khlebarov, "Surface acoustic wave gas sensor," *Sensors and Actuators B,* vol. 8, pp. 33-40, 1992.

[142] A. Afzal, N. Iqbal, A. Mujahid and R. Schirhagl, "Advanced vapor recognition materials for selective and fast responsive surface acoustic wave sensors: A review," *Analytica Chimica Acta,* vol. 787, pp. 36-49, 2013.

[143] G. K. Kannan, A. T. Nimal, U. Mittal, R. D. Yadava and J. C. Kapoor, "Adsorption studies of carbowax coated surface acoustic wave (SAW) sensor for 2,4-dinitro toluene (DNT) vapour detection," *Sensors and Actuators B,* vol. 101, pp. 328-334, 2004.

[144] A. T. Nimal, U. Mittal, M. Singh, M. Khaneja, G. K. Kannan, J. C. Kapoor, V. Dubey, P. K. Gutch, G. Lal, K. D. Vyas and D. C. Gupta, "Development of handheld SAW vapor sensors for explosives and CW agents," *Sensors and Actuators B,* vol. 135, pp. 399-410, 2009.

[145] L. A. Pinnaduwage, V. Boiadjiev, J. E. Hawk and T. Thundat, "Sensitive detection of plastic explosives with self-assembled monolayer-coated microcantilevers," *Applied Physics Letters,* vol. 83, pp. 1471-1473, 2003.

[146] P. G. Datskos, N. V. Lavrik and M. J. Sepaniak, "Detection of explosive compounds with the use of microcantilevers with nanoporous coatings," *Sensor Letters,* vol. 1, pp. 25-32, 2003.

[147] D. Lubczyk, C. Siering, J. Lorgen, Z. B. Shifrina, K. Mullen and S. R. Waldvogel, "Simple and sensitive online detection of triacetone triperoxide explosive," *Sensors and Actuators B,* vol. 143, pp. 561-566, 2010.

[148] "CHAPTER 3 Training methods of military dog handlers and their effects on the team's performances," *Applied Animal Behaviour Science,* vol. 113, pp. 110-122, 2008.

CHAPTER 3

"Detection of Triacetone Triperoxide (TATP) Using a Thermodynamic Based Gas Sensor"

by

Matin Amani[1]; Yun Chu[2]; Kellie Waterman[3]; Caitlin Hurley[4]; Michael J. Platek[5] and

Otto J. Gregory[6]

Is published in Sensors and Actuators B, vol.162, pp.727-736 (2012)

---

[1] MS Candidate, Department of Electrical, Computer and Biomedical Engineering, The University of Rhode Island, Kingston, RI 02881. Email: matin.amani@gmail.com

2 PhD Candidate, Department of Chemical Engineering, The University of Rhode Island, Kingston, RI 02881. Email: yun.z.chu@gmail.com

3 Undergraduate student, Department of Chemical Engineering, The University of Rhode Island, Kingston, RI 02881. Email: kh2oman19@gmail.com

4 Undergraduate student, Department of Chemical Engineering, The University of Rhode Island, Kingston, RI 02881. Email: caitmhurley@gmail.com

5 Electrical Materials Engineer, Department of Electrical, Computer and Biomedical Engineering, The University of Rhode Island, Kingston, RI 02881. Email: platek@ele.uri.edu

6 Distinguished Professor, Department of Chemical Engineering, The University of Rhode Island, Kingston, RI 02881. Email: gregory@egr.uri.edu

1. Introduction

Triacetone triperoxide (TATP) has been widely used in IEDs by terrorists, since its precursors (acetone, hydrogen peroxide and a strong acid) are readily available and its preparation is relatively simple. For example, in 2001 a suicide bomber targeted American Airlines with a TATP trigger and it is also believed that TATP was used in the 2005 London subway bombings [1]. Consequently, the reliable detection of TATP using a portable, small footprint sensor continues to draw interest; however, relatively few studies have been published to date.

Unlike many other explosives, TATP contains neither metallic elements nor nitro groups, and therefore, has no significant absorption in the ultraviolet region and does not fluoresce [2]. This makes it very difficult to detect with conventional spectroscopy techniques, especially when combined with its instability and molecular structure. Specifically, the presence of peroxide bonds makes the TATP molecule sensitive to extreme shock, heat and friction, but at the same time this makes it degrade readily. TATP is typically a crystalline solid compound at low temperatures but sublimes readily at room temperature, which makes it an ideal material for vapor phase detection. Several studies have been published on detecting TATP, including ion mobility spectra (IMS) combined with Raman spectrometry, mass spectrometry (MS), nuclear magnetic resonance (NMR), fluorescence spectroscopy and absorption spectroscopy [3-8]. Each of these detection methods has limitations, which include slow responses and/or low sensitivity [2], and all these techniques require large scale analytical instrumentation which is very difficult to implement at venues where a portable or hand held device is required. TATP analysis by high performance liquid

chromatography has been touted as an improved technique, coupled with UV irradiation and electrochemical detection [9], but it still requires considerable analysis time and is not suitable for in situ monitoring under field conditions. Finally, all these techniques are based on the detection of solid TATP and often involve swabbing techniques, thus cannot be used for continuous in situ monitoring. More recently, sensor platforms based on colorimetric sensor arrays have been developed which have detection limits as low 2 ppb [10]; however, this method is based on a one-time use, swabbing technique, and cannot be used for continuous real time detection. Capua et al. have also recently demonstrated a multisensory array capable of detecting ppb quantities of TATP vapor continuously, in real time [11].

Metal oxide based gas sensors have been extensively studied and have been implemented in several commercial applications, such as O_2 and CO detection in internal combustion engine exhaust systems as well as the detection of other toxic, inflammable gases such as NH_3, NO_2, SO_2 and H_2 at concentrations as low as 1 ppm [12, 13]. These sensor platforms also offer several advantages, such as compatibility with conventional CMOS processing, low cost and small dimensions, but have been criticized for their lack of long term stability and poor selectivity. The majority of these platforms operate by monitoring the changes in the electrical properties of the catalyst due reactions with a target gas [14]. However, these reactions are typically observed at relatively high temperatures, and the electrical properties of the catalyst film tend to vary due to issues such as cracking or sintering of the film. While these issues are still of concern in the thermodynamic sensors described here, the heat effect generated by the catalyst is relatively constant over time compared to the electrical

response and provides a more stable response which should provide additional information when coupled with a conductometric sensor.

In order to satisfy the need for a fast and accurate method of continuously screening TATP, extensive efforts have been devoted to developing an innovative and effective sensor platform that is capable of monitoring explosives, such as TATP, in real time [15]. TATP sublimes readily due to its relatively high vapor pressure, and forms a complex vapor upon decomposition [16, 17]. Preliminary studies suggest that using our gas sensor platform, TATP has a similar response to hydrogen peroxide, one of its decomposition products, but also exhibits its own characteristic signal. Consequently, by selecting metal oxide catalysts sensitive to the peroxide bonds in TATP, as well as its organic by-products, a reliable sensor with high sensitivity and high selectivity can be produced.

In this study, a thermodynamic based gas sensor was developed for the detection of TATP and its precursors. This sensor measures the heat generated or absorbed by a metal oxide catalyst in the presence of TATP and its decomposition products in air at very low concentrations. The technique employs a digital control system which enables a thin film microheater, coated with a metal oxide catalyst, to be scanned over a selected temperature range. The electrical power difference due to catalytic reaction (power difference between the microheater in air and the microheater in the presence of TATP) was measured as a function of temperature for various metal oxide catalysts. Utilizing arrays of microheaters, each with a different catalyst it was possible to uniquely identify TATP in real time, while simultaneously minimizing false positives.

2. Experimental

2.1. Fabrication of thermodynamic gas sensors

Catalyst	Cu_2O	Cu_2O–CuO	SnO_{2-x}	ZnO	V_2O_5	WO_3–TiO_2
Target diameter (mm)	150	150	150	150	125	150
Target material	Cu	CuO	SnO_2	ZnO	V	W–Ti
Power density (W/cm^2)	1.77	1.98	1.98	1.98	2.45	1.77
Voltage (V)	1100	900	1150	950	1600	1400
Gas pressure (Pa)	Ar: 1.1 O_2: 0.3	Ar: 1.4	Ar: 1.4	Ar: 1.4	Ar: 1.1 O_2: 0.3	Ar: 1.1 O_2: 0.3
Deposition rate (μm/h)	0.17	0.9	0.8	1.1	0.06	0.13

Table 3.1 Sputtering Conditions for various metal oxide catalysts.

Over a hundred thin film microheaters were fabricated on perforated 96% pure compact alumina substrates using an MRC 822 sputtering system to deposit 2 μm thick nickel films at room temperature. The wafer was then annealed at 900 ℃ in nitrogen for 5 h to densify and stabilize the electrical resistivity of the nickel films. Various metal oxide catalysts having a nominal thickness of 0.5 μm were then deposited directly over the nickel microheaters using either metal or ceramic targets in a MRC 8667 sputtering system. The detailed sputtering conditions for the deposition of the metal oxide catalysts are listed in *Table 3.1*. The sensors were subsequently annealed in air at 650 ℃ to further improve their stability. Prior to and after testing, the oxidation state of the metal oxide catalysts was characterized using XPS and the morphology of the oxide catalysts was followed using SEM.

2.2. Gas sensor testing apparatus and protocol

A schematic of the test bed used for all the gas sensor experiments is shown in *Figure 3.1*, where multiple Alicat Scientific mass flow controllers were used to mix the target gases at various concentrations while maintaining a constant flow rate of

100 SCCM. H_2O_2 and acetone were introduced into the system by bubbling air through sealed flasks containing the liquid precursors, while TATP was introduced into the system by passing air over filter paper impregnated with nanogram quantities of TATP crystals. The sensors were mounted using a standard DB-9 connector mounted in a 13 mm diameter PVC tube.

A digital control system employing a LabView program was used to heat the microheaters to a series of predetermined set point temperatures. These temperatures were selected using the temperature coefficient of resistance (TCR) of the nickel film, which was independently calibrated. After the sensor reached equilibrium at each temperature set point, the total power dissipation was recorded for a period of 75 s. The average amount of heat generated or absorbed by the catalyst in the presence of the target gas was calculated as the power required to maintain the sensor at a constant temperature, as well as the percent response which was the fraction of total power generated by the catalyst. These tests were conducted using both a dynamic pulsed gas scheme, where the sensor is initially run in air, followed by 2 min in various concentrations of the target gas, and then run in air again, without changing temperature. Static testing was also performed by determining the power dissipation in air at each temperature, cooling the sensor to room temperature and running again in the target gas at the same temperatures. Using the static test protocol, the sensitivity of electronics and drift in the resistance of the thin film microheaters allow for power differences greater than 8 mW to be reliably detected, while the dynamic response technique allows for power differences as low as 1 mW to be reliably detected.

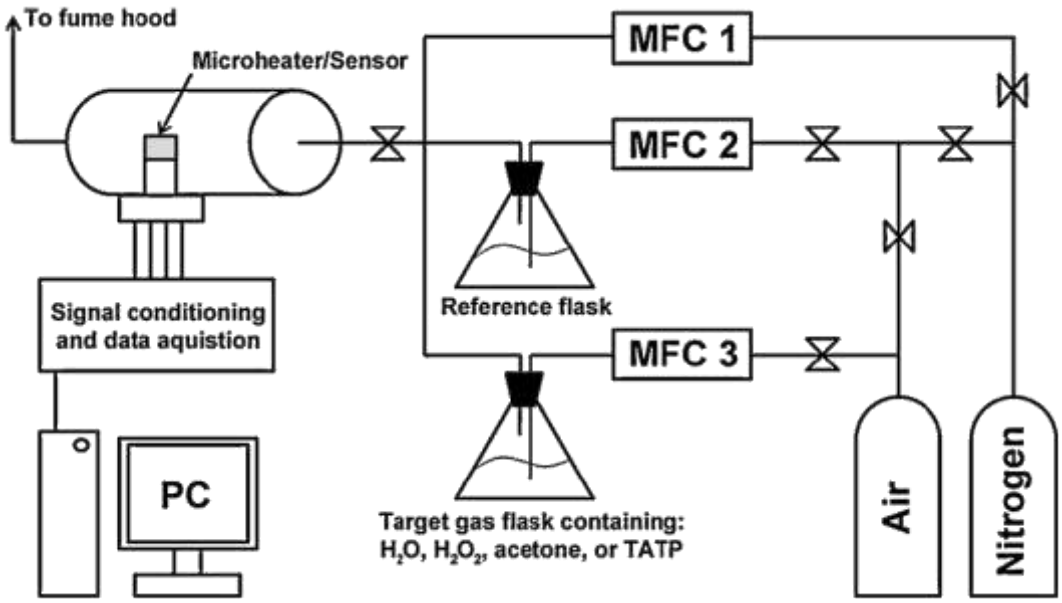

Figure 3.1 Schematic of apparatus used for the detection of TATP, H_2O_2 and acetone using a thermodynamic gas sensor.

3. Results and discussion

3.1. Chemical characterization

The oxidation states of the copper oxide catalysts prepared from ceramic and metallic targets were determined by XPS (*Figure 3.2*). It can be seem from *Figure 3.2* that the Cu 2p spectra of those copper oxide films prepared by reactive sputtering in an Ar/O_2 plasma from a metallic target (dashed line) were compared to copper oxide films prepared by sputtering in an Ar plasma from a CuO target (solid line).

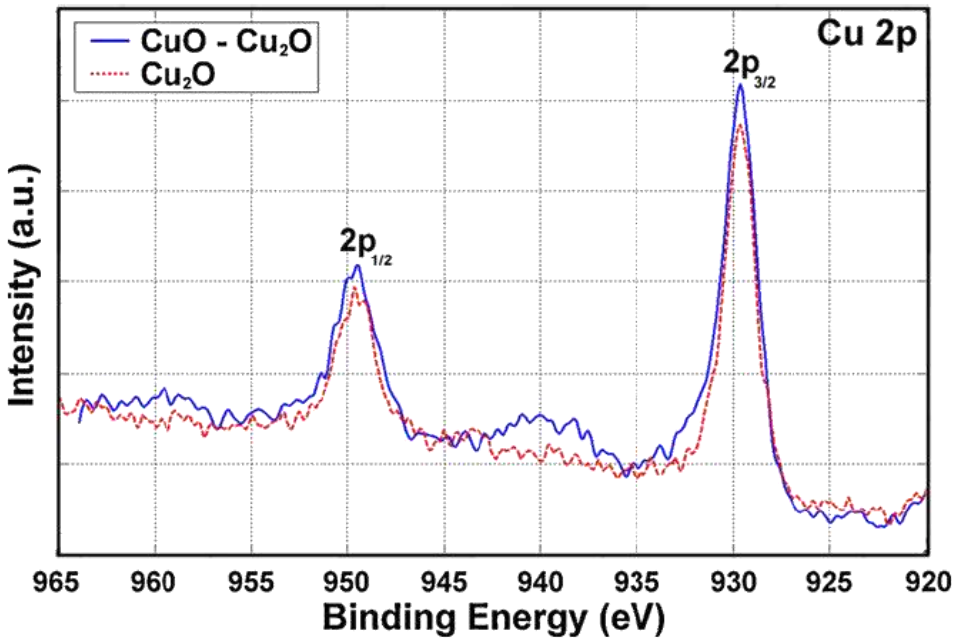

Figure 3.2 XPS spectra of Cu_2O films prepared by sputtering in an Ar/O_2 plasma from a metal target and CuO–Cu_2O films prepared by sputtering in an Ar plasma from a CuO target.

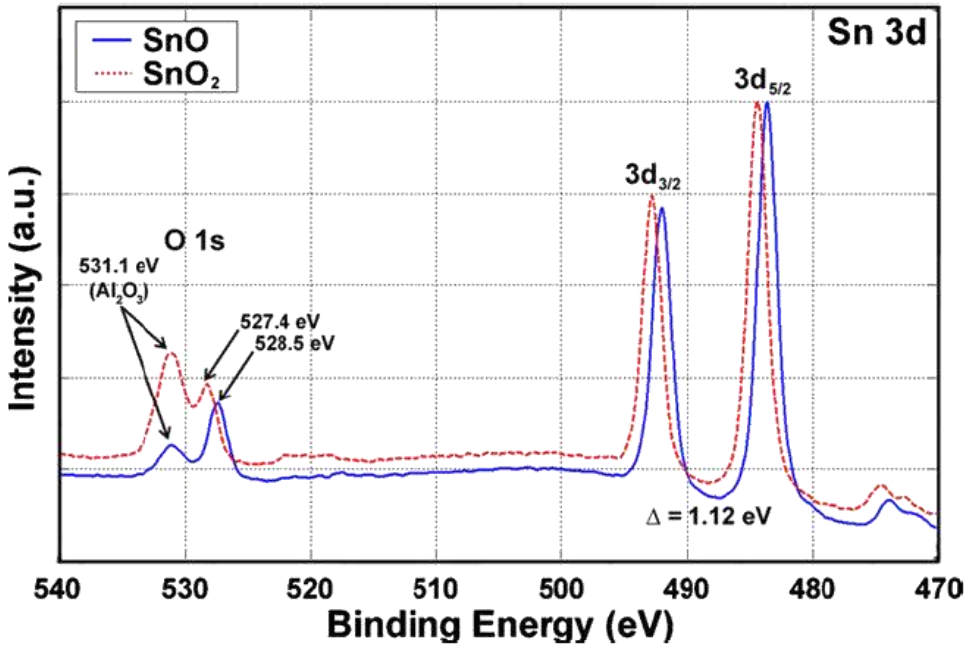

Figure 3.3 XPS spectra of stoichiometric SnO_2 films prepared by sputtering in an Ar/O_2 plasma from a ceramic target and non-stoichiometric SnO_{2-x} films prepared by sputtering in an Ar plasma from a SnO_2 target.

The significant difference between the spectra is that the films prepared from ceramic targets contain satellite peaks which are typically found 7–10 eV above the main peaks associated with the copper $2p^{3/2}$ and $2p^{1/2}$ electrons, respectively for Cu^{2+} compounds, and correspond to shake-up electrons with $2p^{3d9}$ character [18]. In this film, the copper $2p^{3/2}$ and $2p^{1/2}$ peaks were found at 929.65 and 949.15 eV (Cu^{+}), respectively; furthermore, curve fitting of the main $2p_{3/2}$ peak revealed a second peak with lower amplitude at 931 eV (Cu^{2+}). The broadening of the $2p^{3/2}$ peak towards higher binding energies combined with the presence of the satellite peaks suggests that these copper oxide films prepared by sputtering from ceramic targets in an Ar plasma have mixed oxidation states [19].

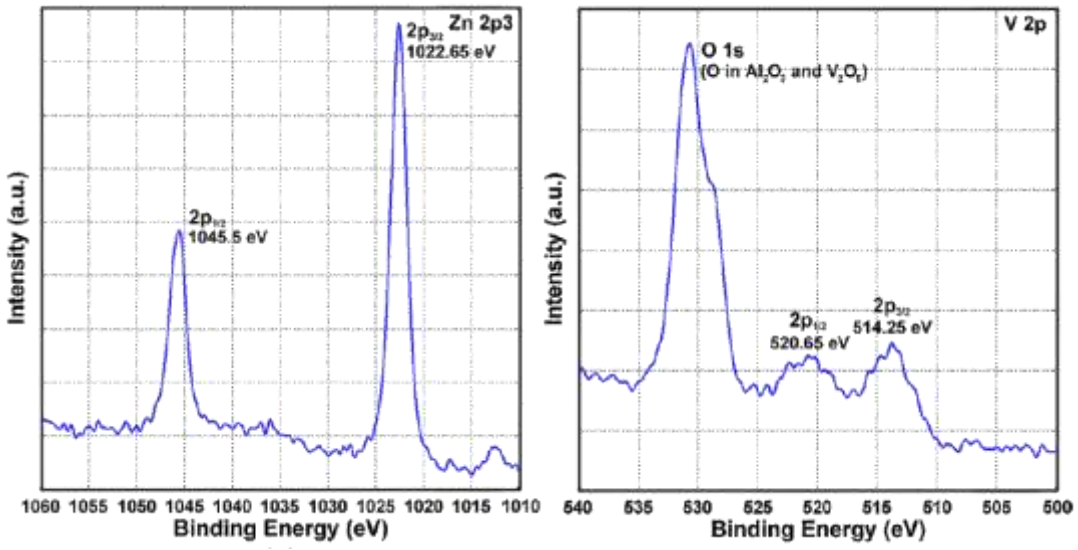

Figure 3.4 XPS spectra of ZnO (left) and V_2O_5 (right) films.

On the other hand, by sputtering in Ar/O_2 plasma from a metal target, a narrow $2p^{3/2}$ peak at 929.65 eV was observed and no satellite peaks were present, in the spectra indicating that the film is largely composed of Cu_2O. Non-stoichiometric SnO_{2-x} films were also prepared by sputtering from an oxide target in an argon

plasma. A 1.12 eV shift in both the O 1s and the Sn 3d peaks was observed relative to those peaks for a SnO2 reference film, as shown in *Figure 3.3*. This is consistent with the shift typically described in the literature, for SnO [20]. *Figure 3.4* shows the XPS spectra of the 3d and 2p electrons in (a) ZnO and (b) V_2O_5. The Zn $2p^{3/2}$ and $2p^{1/2}$ peaks were found at 1022.65 eV and 1045.5 eV, respectively. In the spectra for vanadium oxide, the $2p^{3/2}$ and $2p^{1/2}$ core levels were found at 514.25 eV and 520.65 eV, respectively, both of which are in agreement with those values typically observed in ZnO and V_2O_5 films [21, 22]. Moreover, no significant shifting of these peaks was observed after testing at a maximum temperature of 650 ℃.

3.2. Structural characterization

Figure 3.5 shows the microstructure of several oxide catalysts sputtered from metallic and ceramic targets in different Ar/O_2 partial pressures. CuO–Cu_2O films with mixed oxidation states, were sputtered from a ceramic target in argon plasma, and show surfaces devoid of any fine structure. They also exhibit relatively smooth rounded protuberances with minimal surface area, typical of an as-sputtered film (*Figure 3.5a*). However, the Cu_2O films reactively sputtered from a metallic target in Ar/O_2 mixtures, exhibited a microcrystalline surface morphology within the rounded protuberances of the as-deposited films, unlike those films prepared from a ceramic target (*Figure 3.5b*). When this catalyst surface was exposed to various target gases, including H_2O_2 and TATP at a high temperature, there was no apparent change in the fine microstructure but instead an increase in the cluster/grain size was observed (*Figure 3.5c*).

The reactively sputtered V_2O_5 catalysts prepared from a metallic vanadium target in an Ar/O_2 plasma (*Figure 3.5c*), revealed the formation of acicular needles as well as a very fine fibrous morphology or nano-hair on the surface of the sensor. The surface area of these very fine microstructural features, associated with reactively sputtered films produced from metallic targets, was estimated to be orders of magnitude greater than that of typical sputtered film morphology. SnO_{2-x} and ZnO films were also deposited from a ceramic target by sputtering in an argon plasma (*Figure 3.5e* and *3.5f*), and a morphology more similar to that of sputtered CuO–Cu_2O (*Figure 3.5a*) was observed. In the case of SnO_{2-x}, some micro-cracking of the films due to thermal stress due to high temperature testing became apparent over time.

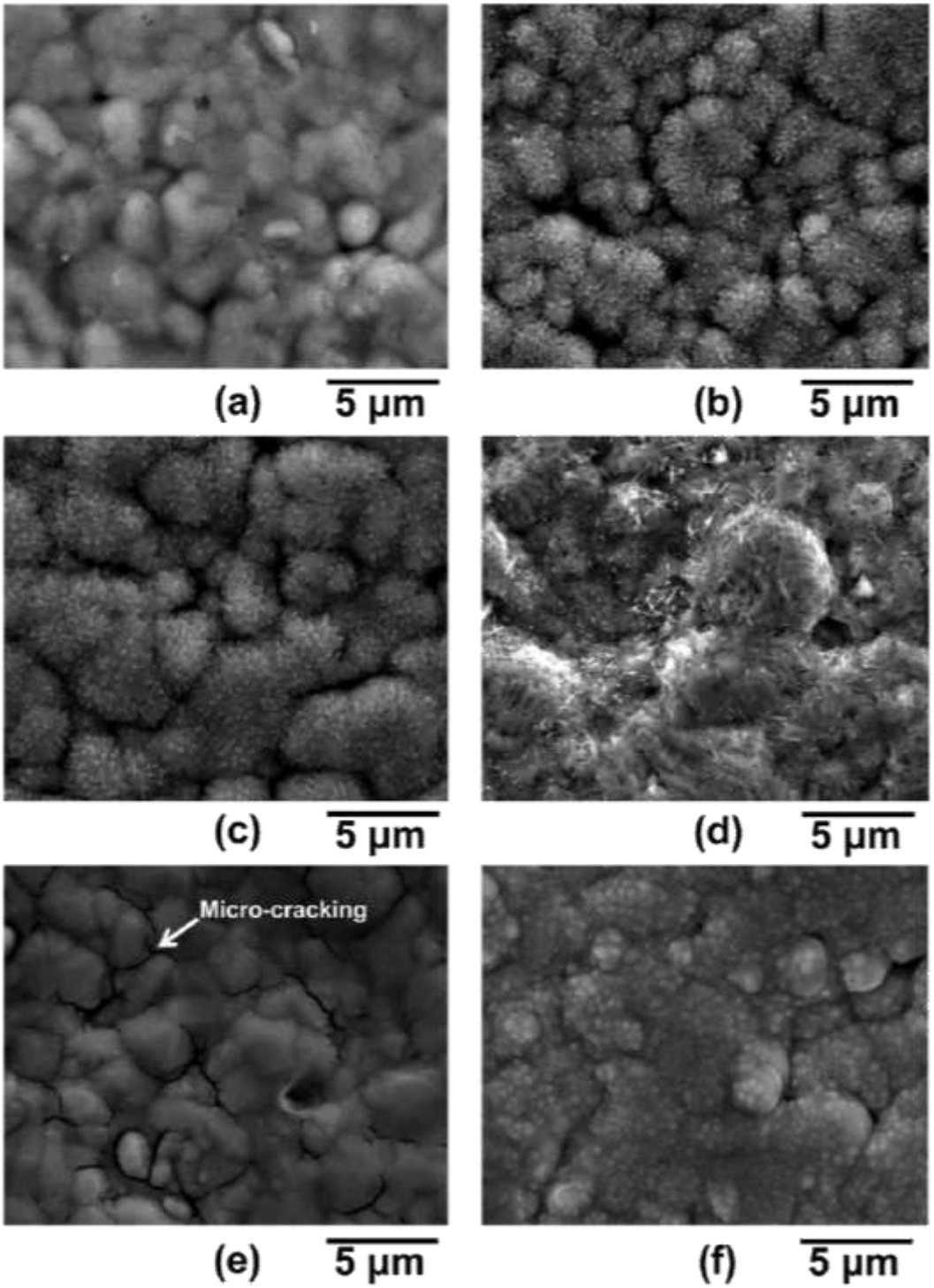

Figure 3.5 SEM micrographs of (a) CuO–Cu_2O after testing, Cu_2O (b) before and (c) after testing and (d) V_2O_5, (e) ZnO and (f) SnO_{2-x} after testing.

3.3. Gas sensing properties

The responses of a tin oxide catalyst and a tungsten oxide catalyst to TATP and hydrogen peroxide are shown in *Figure 3.6*. Here, the percent response to 8 ppm TATP and 9 ppm H_2O_2 as a function of temperature were measured using the static testing approach. A precipitous drop in the response for tin oxide occurs until a temperature of 300 ℃, at which point the response increases dramatically as a function of temperature. We believe this is due to the decomposition of TATP by the catalyst, for which the response peaks at 400 ℃. It should be noted that the response for hydrogen peroxide using the same catalyst has a similar behavior and tracks the TATP response closely.

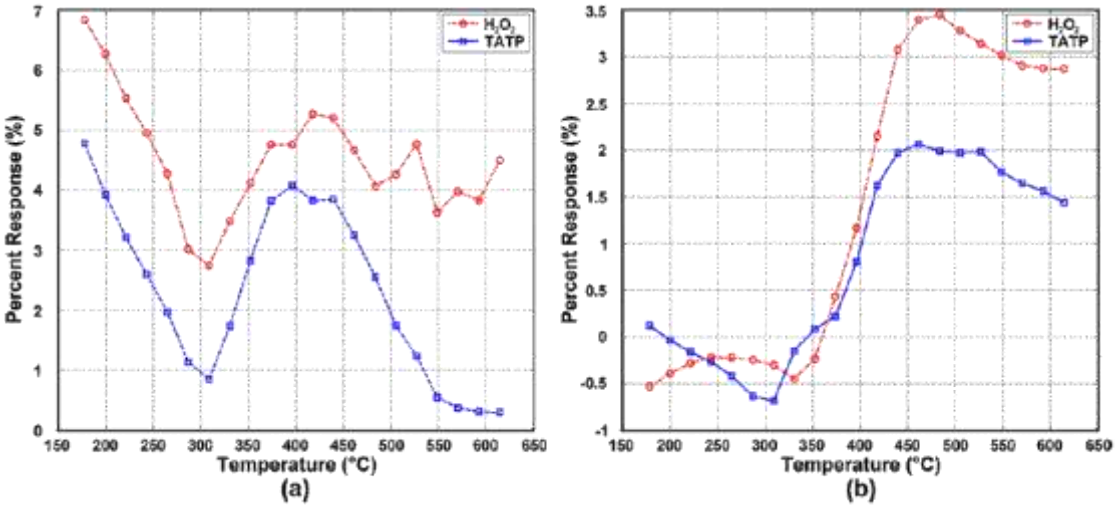

Figure 3.6 Percent response in 8 ppm TATP and 9 ppm H_2O_2 as a function of temperature for (a) tin oxide and (b) tungsten oxide catalysts, measured using the static testing approach.

The response of a tungsten oxide catalyst to TATP and hydrogen peroxide is shown in *Figure 3.6b* and has very different characteristics than that of tin oxide. No significant response was observed at temperatures below 380 ℃, at which point the response then increased dramatically until a maxima was observed at 460 ℃. As was the case for the tin oxide catalyst, the response of the sensor to H_2O_2 was very similar

and closely tracks the TATP response. In both cases the response to hydrogen peroxide was larger in magnitude as might be expected since the decomposition of the TATP is not complete during the test cycle and the starting concentration of TATP is 8 ppm whereas the starting concentration of H_2O_2 is 9 ppm.

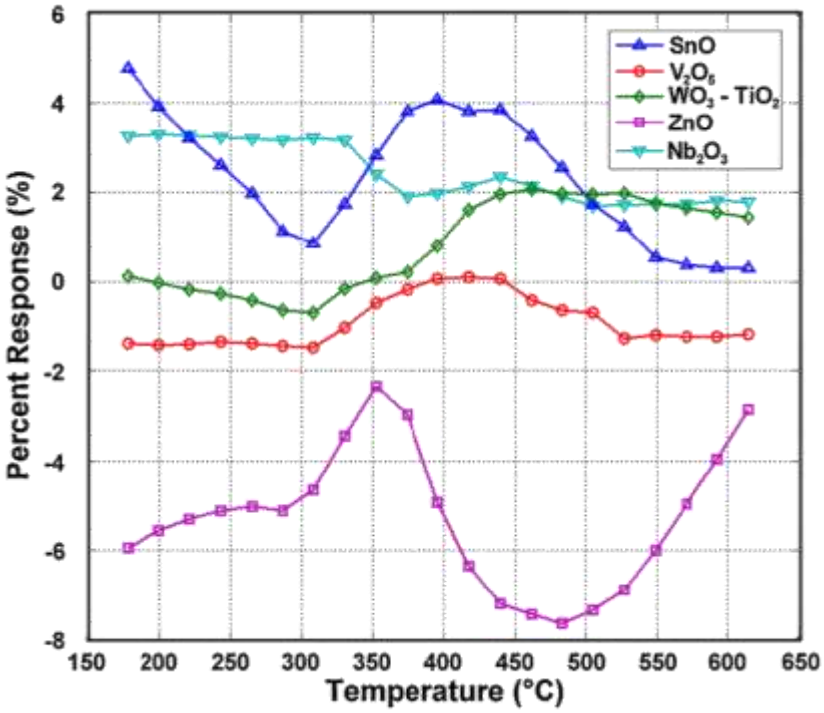

Figure 3.7 Response as a function of temperature using several catalysts to detect TATP (8 ppm) including WO3–TiO2, V2O5, SnO2−x and ZnO, measured using the static testing approach.

The gas sensor response to TATP using a number of different catalysts is shown in *Figure 3.7*. Here, the response to 8 ppm TATP as a function of temperature using several catalysts including WO_3–TiO_2, V_2O_5, SnO_{2-x}, Nb_2O_3 and ZnO was measured using the static testing approach. Each of the five oxide catalysts show a unique response as a function of temperature, and show features ranging from almost no peak response for Nb_2O_3 to well defined peaks for ZnO. Due to the catalytic decomposition of TATP, it is expected that the target gas consists not only of a mixture of air and

TATP vapor, but also contains some H_2O_2 vapor. To verify this, several experiments were undertaken to investigate if TATP is indeed decomposing into H_2O_2 in the vicinity of the catalyst, which is not the primary decomposition product based on a number of related studies. For example, Oxley and Smith [16, 17] have determined that acetone and not hydrogen peroxide is the predominant decomposition product of high purity TATP in air and they have measured the activation energy and determined the decomposition kinetics for the degradation of TATP.

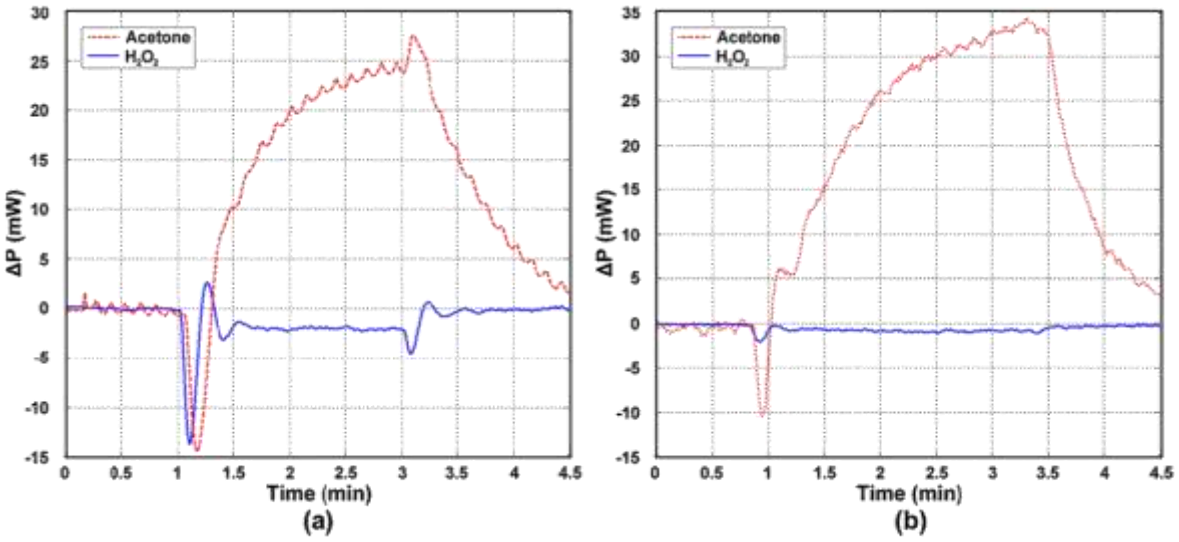

Figure 3.8 Response of (a) CuO–Cu2O and (b) Cu2O in acetone and H2O2 at 330 ◦C.

Figure 3.8 shows the response of a CuO–Cu_2O and Cu_2O catalyst to 8 ppm acetone and H_2O_2 at 330 ℃ after a 2-min exposure to the target gas. From this figure it can be seen that the relative response to acetone is considerably greater than that of H_2O_2, which is consistent with other investigations using thermodynamic based gas sensors for detection [23]. These studies support our findings that significant exothermic heat effects are observed for hydrocarbons. Not only is the magnitude of the response to acetone for both CuO–Cu_2O and Cu_2O significantly greater than that of hydrogen peroxide but it is also of opposite sign, which implies that the sensitivity

of the thermodynamic sensor platform to acetone is significantly greater than that of the other gaseous products derived from the decomposition of TATP. Furthermore, this figure indicates that CuO–Cu_2O (*Figure 3.8a*) is a more selective catalyst for hydrogen peroxide than that of Cu_2O (*Figure 3.8b*), since both a smaller heat of reaction in the presence of acetone and a more negative heat of reaction for H_2O_2 were observed. All of this suggests that these results can be further improved upon by tailoring the sputtering conditions and thus, the oxidation state of the catalyst films.

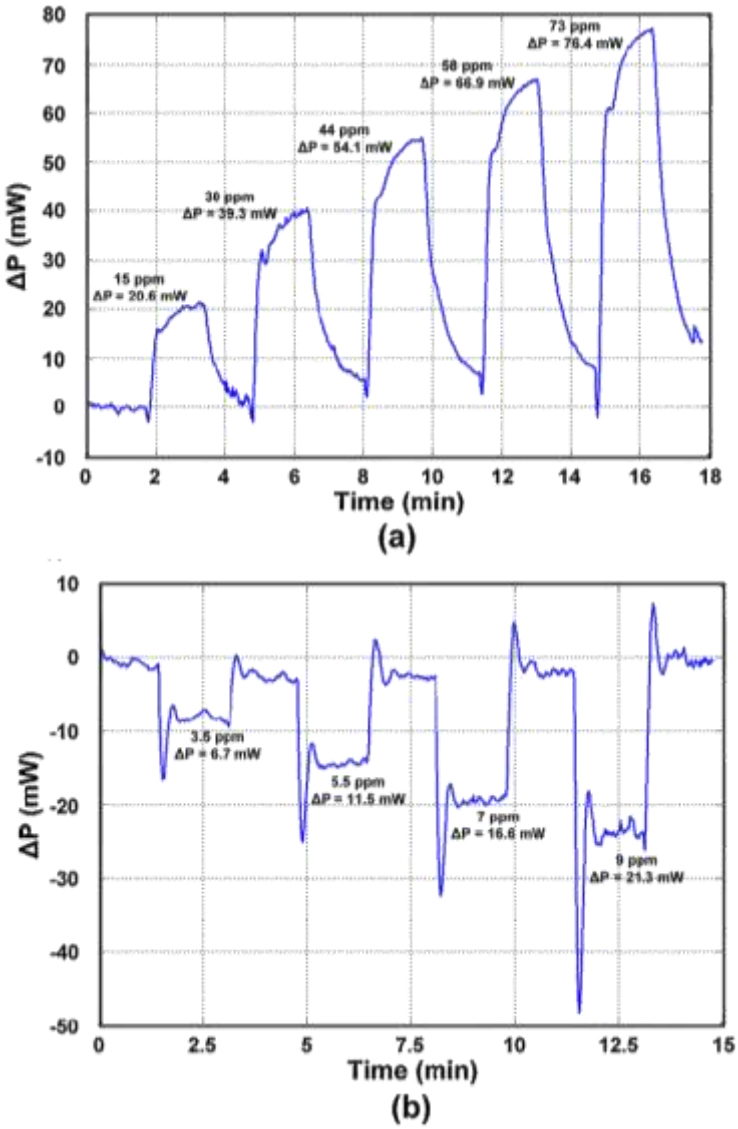

Figure 3.9 Response of SnO_{2-x} in several concentrations of (a) acetone and (b) H_2O_2 at 415 ◦C.

The effect of acetone and H_2O_2 concentration on the magnitude of the response using tin oxide as the catalyst is shown in *Figure 3.9,* where the temperature was held constant at 415 ℃ (maximum sensitivity to H_2O_2 and TATP shown in *Figure 3.6a*). Again the responses are of opposite sign, and it was found that the TATP response tracks that of hydrogen peroxide, which can be readily detected at concentrations as low as 3.5 ppm. Based on the results presented in *Figure 3.9,* we should also be able to reliably detect low levels of acetone in the gas stream generated by the decomposition of TATP. Since we do not see any evidence of acetone in the output signal, we can conclude that the TATP is detected as hydrogen peroxide. However, it has also been extensively cited in the literature [16, 17] that under ambient conditions TATP primarily decomposes into acetone. Therefore, we believe that we are sensing the catalytic decomposition of TATP, which is a much more specific reaction than the decomposition of TATP to acetone in air ambient, and this specific mechanism should help mitigate false positives using this sensor platform.

4. Conclusion

A small footprint, thermodynamic based gas sensor capable of detecting TATP at ppm levels in air under ambient conditions was demonstrated. This robust sensor platform has the potential of exhibiting the necessary sensitivity, selectivity and response time to be used for the continuous monitoring of TATP and its precursors. This would be particularly important in closed spaced venues where the public may be exposed to potential threats from IEDs employing TATP as the triggering device. A number of metal oxide catalysts were able to detect TATP using the thermodynamic

based gas sensor described within. We have shown that TATP vapor at concentrations of 8 ppm in air can be detected readily using SnO_{2-x} and ZnO catalysts, and its peroxide and acetone precursors were able to be detected at even lower concentrations.

Based on our preliminary results, arrays of microheater sensors can be fabricated using multiple catalysts and combining the characteristic response curves to uniquely identify the target molecules of interest. In addition, the current thermodynamic detection scheme can easily be integrated into an existing micro-hotplate based MEMS metal oxide gas sensing platforms by modifying the heater electronics and adding a mass flow controller to eliminate hydrodynamic effects. This can add a second independent variable to minimize false positives and improve long term stability in existing gas sensor systems.

REFERENCES

[1] F. Dubnikova, R. Kosloff, Y. Zeiri and Z. Karpas, "Novel approach to the detection of triacetone triperoxide (TATP), its structure and its complexes with ions," *Journal of Physical Chemistry A*, vol. 106, p. 4951–4956, 2002.

[2] I. Cotte-Rodriguez, H. Chen and R. G. Cooks, "Rapid trace detection of triacetone triperoxide (TATP) of complexation detections of desorption electrospray ionization," *Chemical Communications,* vol. 5, pp. 953-955, 2006.

[3] G. A. Buttigieg, A. K. Knight, S. Denson, C. Pommier and M. B. Denton, "Characterization of the explosive triacetone triperoxide and detection by ion mobility spectrometry," *Forensic Science International,* vol. 135, pp. 53-59, 2003.

[4] R. Rasanen, M. Nousiainen, K. Parakorpi, M. Sillanripaa, L. Polari, O. Anttalainen and M. Utriainen, "Determination of gas phase triacetone triperoxide with aspiration ion mobility spectrometry and gas chromatography–mass spectrometry," *Analytica Chimica Acta,* vol. 623, p. 59–65, 2008.

[5] J. Wilkinson, C. T. Konek, J. S. Moran, E. M. Witko and T. M. Korter, "Terahertz absorp spectrum of triacetone triperoxide (TATP)," *Chemical Physics Letters,* vol. 478, pp. 172-174, 2009.

[6] A. Stambouli, A. E. Bouri, T. Bouayoun and M. A. Bellimam, "Headspace

GC/MS detection of TATP traces in post-explosion debris," *Forensic Science International* , vol. 146S, pp. 191-194, 2004.

[7] C. Mullen, A. Irwin, B. V. Pond, D. L. Huestis, M. J. Coggiola and H. Oser, "Detection of explosives and explosives-related compounds by single photon laser ionization time-of-flight mass spectrometry," *Analytical Chemistry*, vol. 78, p. 3807–3814, 2006.

[8] C. Shen, J. Li, H. Han, H. Wang, H. Jiang and Y. Chu, "Triacetone triperoxide using low reduced-field proton transfer reaction mass spectrometer," *International Journal of Mass Spectrometry*, vol. 285, pp. 100-103, 2009.

[9] R. S. Ladbeck and U. Karst, "Determination of triacetone triperoxide in ambient air," *Analytical Chemistry,* vol. 482, pp. 183-188, 2003.

[10] H. Lin and K. S. Suslick, "A colorimetric sensor array for detection of triacetone triperoxide vapor," *Journal of American Chemistry Society,* vol. 132, pp. 15519-15521, 2010.

[11] E. Capua, R. Cao, C. N. Sukenik and R. Naaman, "Detection of triacetone triperoxide (TATP) with an array of sensors based on non-specific interactions," *Sensors and Actuators B,* vol. 140, p. 122–127, 2009.

[12] N. Barsan, D. Koziej and U. Weimar, "Metal oxide-based gas sensor research: How to," *Sensors and Acutators B,* vol. 121, pp. 18-35, 2007.

[13] N. L. Hung, H. Kim, S. K. Hong and D. Kim, "Enhancement of CO gas sensing properties of ZnO thin films deposited on self-assembled Au nanodots," *Sensors and Actuators B,* vol. 151, pp. 127-132, 2010.

[14] G. Eranna, B. C. Joshi, D. P. Runthala and R. P. Gupta, "Oxide materials for development of integrated gas sensors: a comprehensive review," *Critical Reviews in Solid State and Mateirals Sciences,* vol. 29, pp. 111-188, 2004.

[15] W. H. Zhang, W. D. Zhang and L. Y. Chen, "Highly sensitive detection of explosive triacetone triperoxide by an In2O3 sensor," *Nanotechnology,* vol. 21, p. 315502, 2010.

[16] J. C. Oxley, J. L. Smith, K. Shinde and J. Moran, "Determination of the vapor density of triacetone triperoxide (TATP) using a gas chromatography headspace technique," *Propellants, Explosives, Pyrotechnics,* vol. 30, pp. 127-130, 2005.

[17] J. C. Oxley, J. L. Smith and H. Chen, "Decomposition of a multi-peroxidic compound: triacetone triperoxide (TATP)," *Propellants, Explosives, Pyrotechnics,* vol. 27, p. 209–216, 2002.

[18] W. Y. Yang, W. G. Kim and S. W. Rhee, "Radio frequency sputter deposition of single phase cuprous oxide using Cu_2O as a target material and its resistive switching properties," *Thin Solid Films,* vol. 517, pp. 967-971, 2008.

[19] C. I. Pearce, R. A. Pattrick, D. J. Vaughan, C. M. Henderson and G. van der Laan, "Copper oxidation state in chalcopyrite: mixed Cu d^9 and d^{10} characteristics," *Geochimica,* vol. 70, p. 4635–4642, 2006.

[20] S. Hwang, Y. Y. Kim, J. H. Lee, D. K. Seo, J. Y. Lee and H. K. Cho, "Irregular electrical conduction types in tin oxide thin films induced by nanoscale phase separation," *Journal of the American Ceramic Society,* vol.

95, pp. 324-332, 2012.

[21] S. Uthanna, T. K. Subramanyam, B. S. Naidu and G. M. Rao, "Structure–composition–property dependence of reactive magnetron sputtered ZnO thin films," *Optical Materials,* vol. 19, p. 461–469, 2002.

[22] G. Silversmit, D. Depla, H. Poelman, G. B. Marin and R. Gryse, "Determination of the V^{2p} XPS binding energies for different vanadium oxide oxidation states (V^{5+} to V^{0+})," *Journal of Electron Spectroscopy and Related Phenomena,* vol. 135, p. 167–175, 2004.

[23] E. Vereshchaginam, R. A. Wolters and J. G. Gardeniers, "Measurement of reaction heats using a polysilicon based microcalorimetric sensor," *Sensors and Actuators A,* vol. 169, p. 308–316, 2001.

CHAPTER 4

"Detection of Peroxides Using a Pd/SnO_2 Nanocomposite Catalyst"

by

Yun Chu[1]; Daniel Mallin[2]; Matin Amani[3]; Michael J. Platek[4]; and Otto J. Gregory[5]

Sensors and Actuators B, In press.

---

[1] PhD Candidate, Department of Chemical Engineering, The University of Rhode Island, Kingston, RI 02881. Email: yun.z.chu@gmail.com

[2] MS Candidate, Department of Electrical, Computer and Biomedical Engineering, The University of Rhode Island, Kingston, RI 02881. Email: daniel.p.mallin@gmail.com

[3] MS Candidate, Department of Chemical Engineering, The University of Rhode Island, Kingston, RI 02881. Email: matin.amani@gmail.com

[4] Electrical Materials Engineer, Department of Electrical, Computer and Biomedical Engineering, The University of Rhode Island, Kingston, RI 02881. Email: platek@ele.uri.edu

[5] Distinguished Professor, Department of Chemical Engineering, The University of Rhode Island, Kingston, RI 02881. Email: gregory@egr.uri.edu

1. Introduction

Triacetone triperoxide (TATP) is a peroxide-based compound commonly used as an initiator in improvised explosive devices (IED's) that employ other high-energy explosives such as pentaerythritol tetranitrate (PETN). Due to its ease of manufacture from readily available precursors and its simple preparation technique [1], it is an energetic material widely used by terrorists. The detection of TATP using bench-scale analytical instrumentation has been successfully demonstrated using a number of techniques. Specifically, ion mobility spectrometry [2, 3, 4], terahertz absorption spectrometry [5], mass spectrometry [4, 6, 7, 8] and fluorescence spectroscopy [9] have all been used to successfully detect TATP. They exhibit adequate sensitivity and stability for low-level detection. However, the aforementioned techniques are somewhat limited for field use since they cannot be adapted in a small footprint platform and are not capable of continuously monitoring the environment for these threat molecules. Therefore, a low cost, small footprint sensor that exhibits adequate selectivity and sensitivity without introducing false positives is highly desired for field use where the continuous monitoring at low levels is desired.

A number of investigators have reportedly employed metal oxide catalysts in a variety of gas sensor platforms. Metal oxide semiconductors, for example, have been successfully used to detect trace levels of toxic gases such as CO, H_2S, H_2 and NO_x [10-12]. A vast majority of these sensors employed metal oxide catalysts, and as such exhibited responses that depend on changes in the electrical properties of the catalyst when exposed to the target gas; these include changes in electrical conductivity [10-12], changes in dielectric constant of the metal oxide [13], change in work function

[14, 15]. Others reflect changes in optical properties of the metal oxide catalyst [16, 17]. However, one major disadvantage in using metal oxides, as well as all other types of solid-state gas sensors, is their poor selectivity due to their inability to distinguish between complex target molecules [10]. In a previous study, we demonstrated a gas sensor, which was capable of detecting TATP at trace levels using a SnO_2 catalyst based on the catalytic decomposition of TATP to form hydrogen peroxide (H_2O_2) [18]. However, these sensors exhibited little or no selectivity between TATP and H_2O_2, making them somewhat susceptible to false positives in the presence of other peroxides and related precursors such as acetone.

A number of researchers [17, 19] have reported that the sensitivity of metal oxide based sensors can be enhanced by the direct exchange of electrons between the oxide semiconductor and noble metals such as Pd, Au, and Pt. The addition of such metals increased the rate of specific reactions on the surface of oxide crystals due to spill-over effects, which actually changed the reaction mechanism in some cases through modification of surface energy states [17, 19]. In our case, additions of palladium to SnO_2 catalysts may not only lower the detection limit by increasing the decomposition rate of TATP, but may also provide a different reaction path to avoid forming intermediates, such as H_2O_2 and thus, provide a sensor response to TATP that is significantly different from H_2O_2. Consequently, a gas sensor employing metal oxide catalysts with improved sensitivity and selectivity over H_2O_2 was the motivation for this study.

In the present investigation, we utilized combinatorial chemistry techniques to screen Pd:SnO_2 nanocomposites with various palladium loadings for the purpose of

optimizing sensor sensitivity and selectivity. Our thermodynamic sensor platform employs a digital control system to measure the heat effect associated with the interaction of a target gas molecule with a metal oxide catalyst deposited over the surface of a microheater. The heat effect associated with the catalytic decomposition of TATP was monitored by thermally scanning the microheater from room temperature to 450˚C. The characteristic heat affects were measured as the target molecules of interest such as TATP, H_2O_2 and acetone were passed over the catalyst coated microheater. In this way, the controlled addition of palladium to a SnO_2 matrix was used to systematically investigate sensor response to TATP and selectivity of TATP over that of H_2O_2.

2. **Experimental**

2.1 Sensor fabrication and characterization

Thin film nickel microheaters having a nominal thickness of 4.5 μm were deposited onto laser-perforated alumina substrates using a MRC Model 822 sputtering system. The nickel microheaters were annealed in flowing nitrogen at 900℃ for 5 hours to improve the electrical stability and eliminate point defects in the nickel microheaters as a result of the sputtering process. A 1μm thick alumina film was then deposited over the nickel microheaters to prevent electrical shorts between the Ni heating element and the oxide catalyst. The alumina film was also used to prevent the microheaters from interacting with oxygen and other gases present in the atmosphere. SnO_2/Pd nanocomposite catalysts were co-sputtered from simultaneously energized SnO_2 and Pd targets in pure argon onto an array of microheater sensors on alumina supports in an MRC Model 8667 sputtering machine. A schematic of sensor placement

relative to the sputtering targets is shown in *Figure 4.1* and the sputtering parameters used for the deposition of the nanocomposite catalyst are given in *Table 4.1*. This approach generated a large number of essentially different catalysts with a continuously varying, spatially dependent chemistry.

	SnO_2	Pd
Diameter of targets (mm)	150	100
Vertical distance between specimen and target (mm)	75	75
Forward voltage (V)	480	480
Power density (W/cm^2)	1.70	3.8
Sputtering gas	Ar	Ar
Pressure (Torr)	$9*10^{-4}$	$9*10^{-4}$
Deposition rate (μm/hr)	0.49	0.28

Table 4.1 Parameters applied to SnO_2 and Pd targets during co-sputtering.

Palladium loadings ranged from 1 wt.% to 25 wt.% in the nanocomposite film. A cutaway view of the various layers comprising the sensor is shown in *Figure 4.2*. Following deposition, the films were annealed at 550℃ in air to promote crystallization and further stabilize the oxide catalysts. The chemical composition and morphology of these catalysts were characterized using scanning electron microscopy (SEM) equipped with energy dispersive X-ray spectroscopy (EDS). The catalysts were also characterized using X-ray diffraction (XRD) and X-ray photoelectron spectroscopy (XPS). Pure tin oxide films were also prepared as catalysts for comparison purposes, using the deposition conditions presented in reference [19].

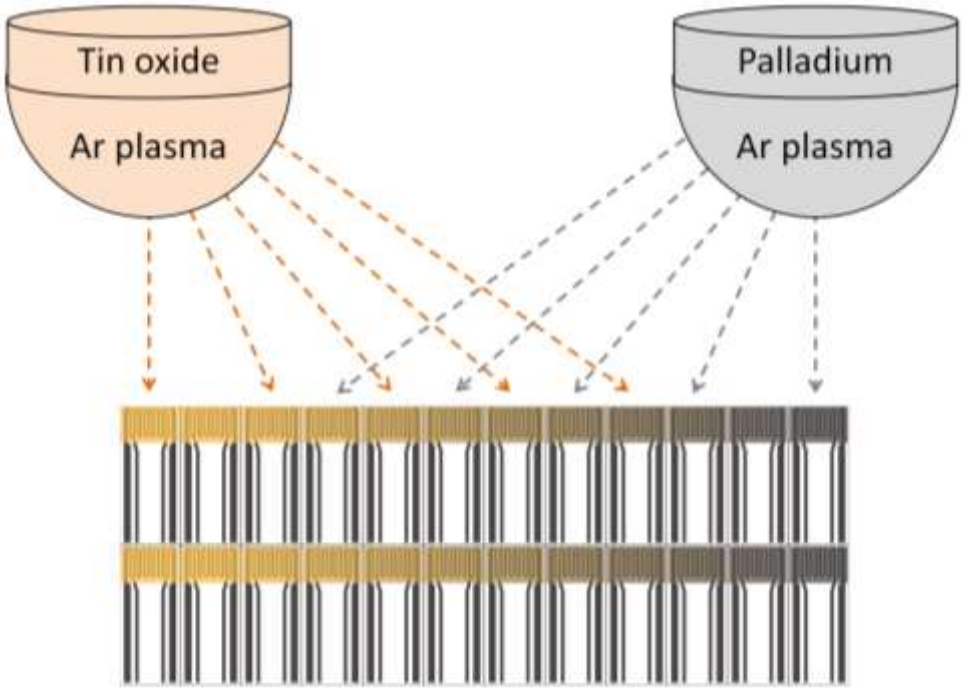

Figure 4.1 Overview of the Pd:SnO_2 co-sputtering process, in which an array of sensors were placed between two energized targets, resulting in that the sensors were coated with varying composition of catalysts.

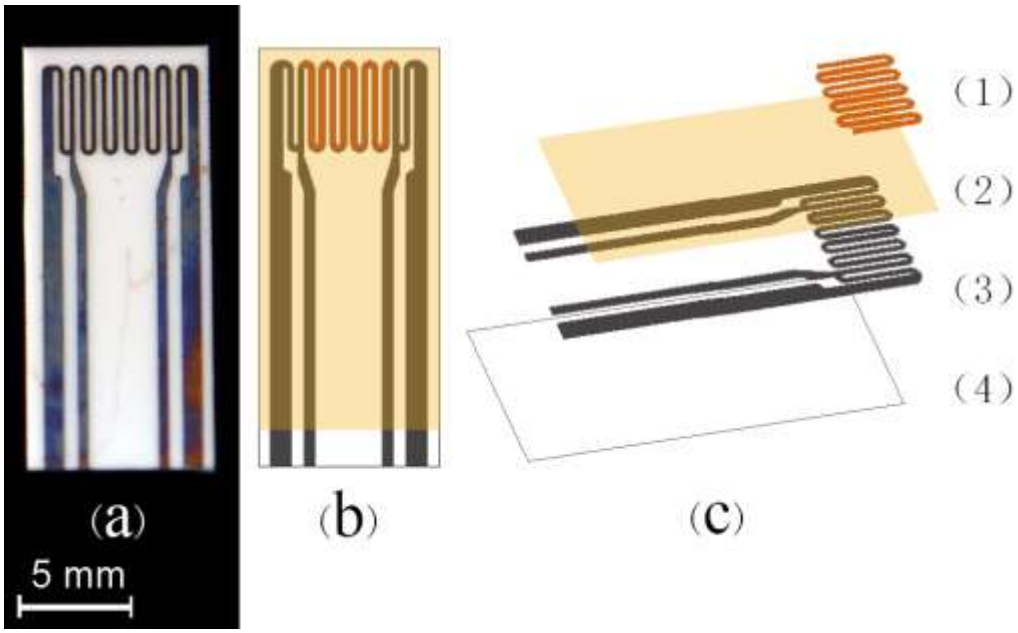

Figure 4.2 Actual picture and schematic demonstrating the size and structure of thermodynamic based sensor platform: (a) an actual picture, (b) top view and (c) expended view of schematic of the sensor showing catalyst film (1), alumina passivation layer (2), nickel microheater (3) and alumina substrate (4).

2.2 Testing apparatus and protocol

The flow rate of inert gas (dry air) and target gas was precisely metered into the test chamber using two mass flow controllers and a digital flow meter, which produced a constant mass flow and allowed precise control over the target gas and inert gas mixtures delivered to the testbed. The desired vapor phase concentration of TATP (e.g. 0.68 μg/ml) was achieved by passing a carrier gas over a piece of filter paper impregnated with high purity TATP crystals in a flask maintained at constant temperature. When the target molecules were derived from liquid-based chemical solutions such as H_2O, or acetone in deionized water, air was bubbled through the flask containing dilute solutions to establish an equilibrium partial pressure in the vapor phase. A schematic of the test bed used to evaluate sensor performance is shown in *Figure 4.3*.

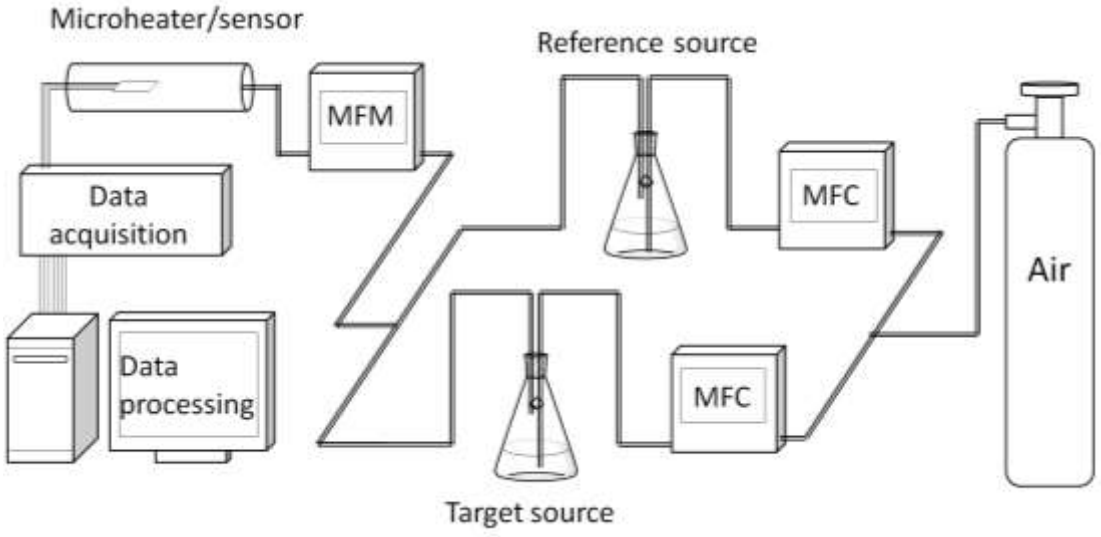

Figure 4.3 Apparatus used for the detection of TATP and H_2O_2 using a micro-calorimetric sensor.

The catalytic response was determined by measuring the heat affect associated with the interaction of the target molecules with a catalyst using a dynamic testing

protocol. The catalyst-coated microheater was heated to a number of predetermined temperature set points by controlling the electrical resistance of the microheater, using a four-point probe method. The temperature coefficient of resistance (TCR) of the nickel microheater was independently calibrated and verified prior to each sensor test. The gas delivery system consisted of a series of mass flow controllers interfaced to a computer. In addition, a data acquisition system was also interfaced to a computer and controlled using LabView software. After reaching each temperature set point, the sensor was allowed to equilibrate for 360 seconds under constant inert gas flow. The target gas was then introduced into the test chamber for 180 seconds and then the reference gas was introduced for 180 seconds before the microheater was ramped to the next temperature set point. This testing sequence is referred to as an "off-on-off" protocol. The power required to maintain the sensor at a particular temperature was recorded after the target gas was introduced and this temperature was maintained until the start of next step increase in temperature. The heat effect at each temperature set point was measured by taking the difference in power required to maintain the temperature in the presence of the target gas and the power required to maintain the temperature in the presence of the inert gas. Prior to measuring the sensor response, the background power (sensor drift) was subtracted from the sensor response. Typically, all responses smaller than ±1.0 mW were considered background (noise), which is due to small variations in the target and inert gas flow rates, drift in the baseline resistance of the nickel microheaters and other electrical instabilities.

3. Results

3.1 Chemical characterization and surface morphology

The morphology of the different nanocomposite catalysts were characterized by SEM and TEM, as shown in *Figure 4.4*. While most of the as-deposited catalysts are featureless, as might be expected given the non-equilibrium deposition processes used to form the composites, extensive micro-cracking was observed after annealing. This was attributed to the large volume change associated with crystallization of the amorphous phases in the nanocomposite [25]. In addition, as the palladium content in the nanocomposite was increased, the density of micro-cracks diminished and eventually disappeared from the microstructure when palladium loadings greater than 25 wt.%. EDS analysis was used in conjunction with TEM to confirm the chemistry of the dark, spherical particles observed in the SnO_2 matrix. These palladium particles had an average diameter of 20 nm, and EDS confirmed these were palladium particles in the SnO_2 matrix.

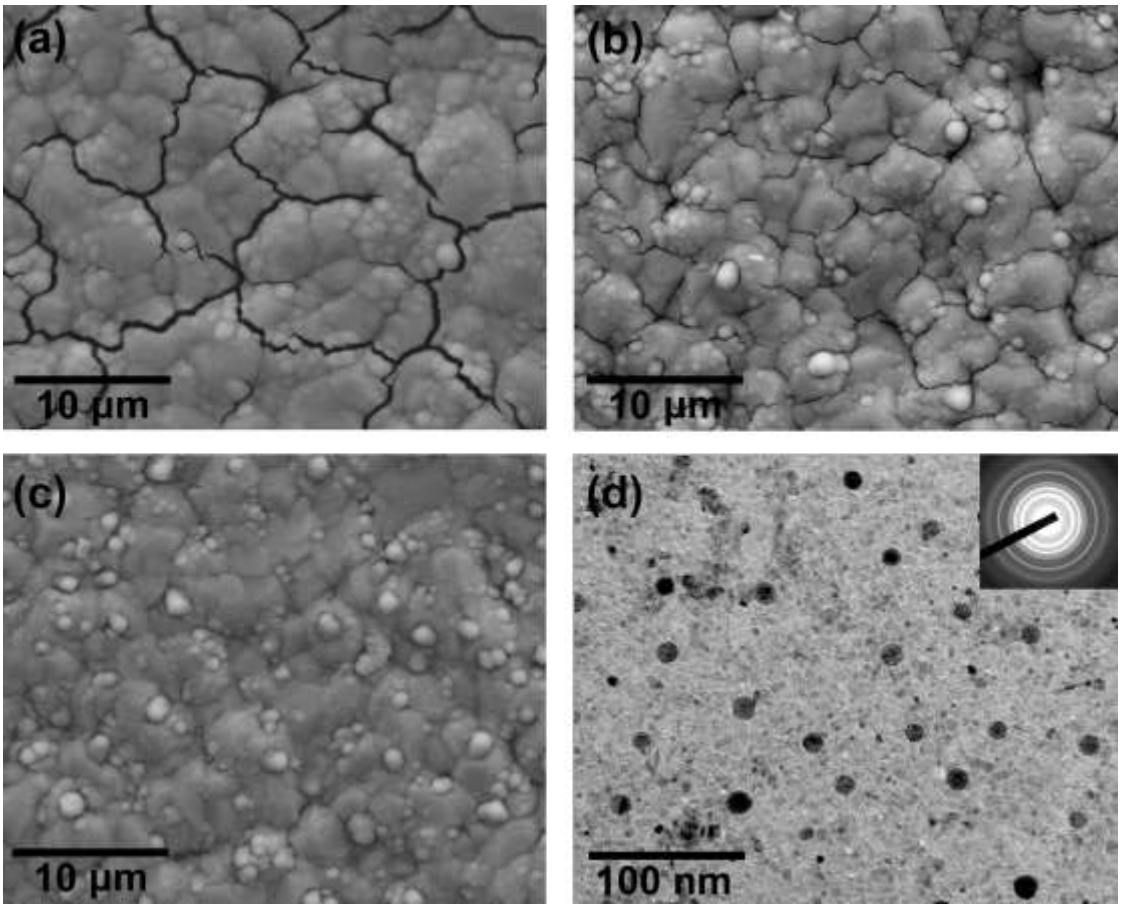

Figure 4.4 SEM image of as-annealed nanocomposite catalyst with palladium doping amount of (a) 2.2% wt.%, (b) 8 wt.% and (c) 12 wt.%, and (d) TEM micrographs of as-annealed nanocomposite catalyst with a 12 wt.% palladium loading.

The nano-composite catalysts, comprised of palladium nanoparticles in a tin oxide matrix, were characterized by XRD, in the as-deposited and annealed condition (*Figure 4.5*). All nanocomposite catalysts, regardless of palladium loading, were amorphous in the as-deposited condition and became partially or fully crystalline after subsequent annealing steps. Peaks corresponding to the tetragonal form of SnO_2 were observed in the XRD patterns of the annealed catalysts with no preferred orientation or texture evident. A uniform 2θ shift of (0.01Å) was observed for the SnO_2 diffraction peaks relative to the literature values, which was likely caused by substitutional defects in the oxide [20]. The PdO (101) peak was observed in all Pd "alloyed"

nanocomposites. However, the Pd (110) and Pd (220) peaks observed at higher palladium loadings all but disappear as the Pd loading decreases, as shown in Figs. 4(3) through 4(5). To further explore this phenomenon, the oxidation states of the as-annealed nanocomposite catalysts were characterized using XPS. As shown in *Figure 4.6*, the XPS spectra of pure SnO_2 and Pd:SnO_2 nanocomposites exhibited the same Sn $3d_{5/2}$ core level peak at 486.5 eV, suggesting that tin was present in +4 oxidation states in both specimens. Pure SnO_2 contains the +2 Sn state as indicated by the lower intensity and slight shifting of the main Sn peak. The Pd $3d_{5/2}$ peaks in the 2.2 wt.% nanocomposite were observed at 336.4 eV and 337.5 eV respectively, which is in good agreement with literature values corresponding to palladium in the +2 and +4 states [20-24]. The exact composition (at.%) was 0.17:0.83 (PdO_2:PdO), based on the peak area. As the palladium loading was increased to 12 wt.%, metallic palladium began to phase separate and the composition of PdO_2:PdO:Pd phases tended towards 0.084:0.723:0.193, respectively. When the palladium loading reached 32 wt.%, the metallic phase became dominant and the PdO_2 and PdO peaks disappeared. This was attributed to the differences in oxidation between palladium single crystals, which are more difficult to oxidize and the palladium particles in the SnO_2 [22]. This finding was in agreement with the disappearance of the palladium (110) and (220) peaks in the XRD patterns shown in *Figure 4.5*. It should be noted that XPS was also performed after the catalysts were exposed to peroxides, in which case the oxidation state of palladium remained the same (figure not shown).

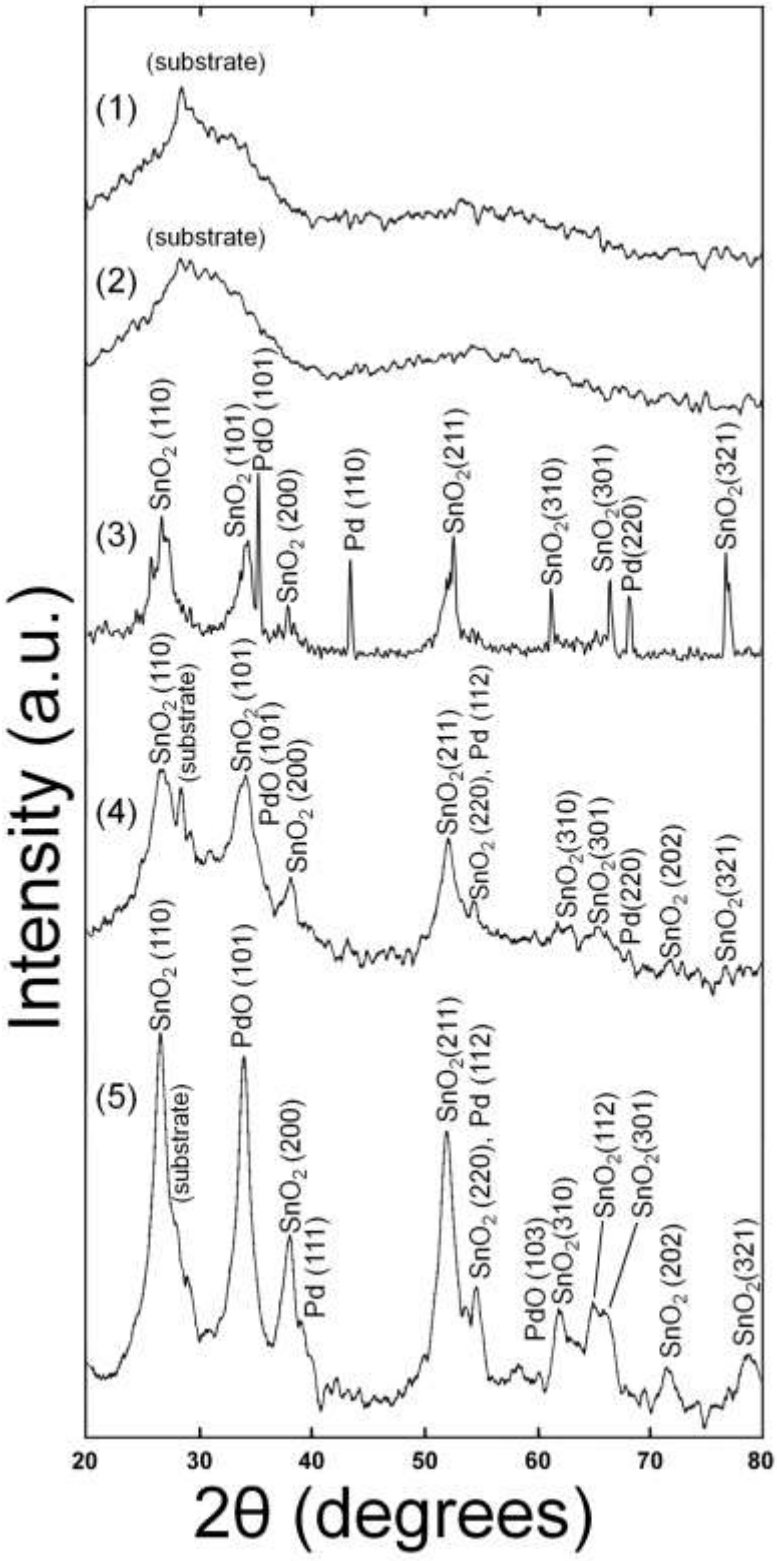

Figure 4.5 XRD patterns of as-deposited film with (1) 12 wt.% and (2) 2.2 wt.% loading palladium and annealed films with (3) 12 wt.% loading Pd, (4) 8 wt.% loading Pd, and (5) 2.2 wt.% loading Pd in the Pd:SnO_2 nanocomposite catalyst.

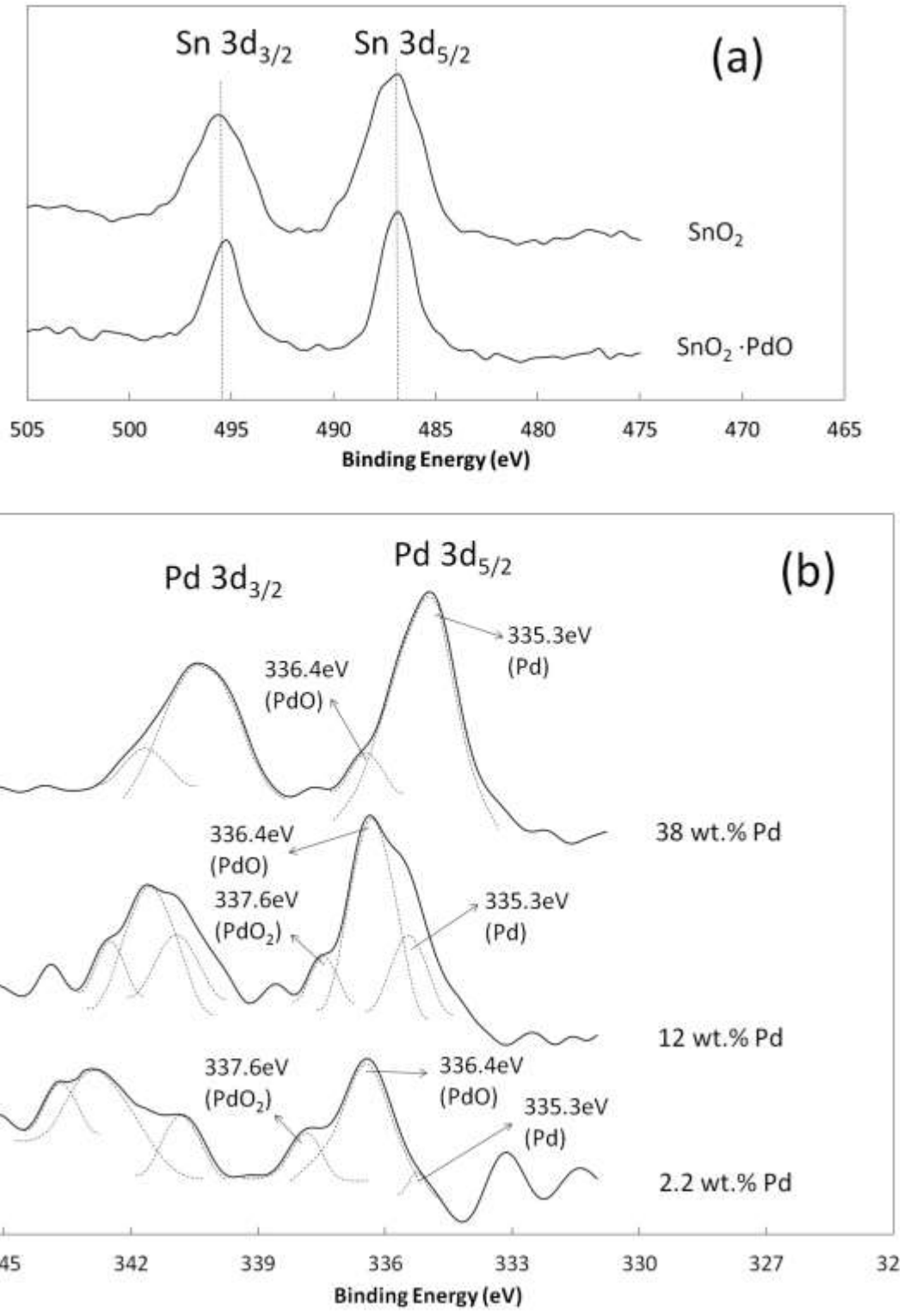

Figure 4.6 XPS spectra of (a) Sn $3d_{3/2}$ and $3d_{5/2}$ doublet for Pd doped and un-doped SnO_2, and (b) Pd $3d_{3/2}$ and $3d_{5/2}$ doublet corresponding to 2.2 wt.% loading Pd, 12 wt.% loading Pd and 38 wt.% loading Pd in the $PdSnO_2$ nanocomposite.

3.2 Sensor Measurements

Control experiments using un-doped SnO_2 catalysts at several temperature set points in the presence of 0.68 μg/ml TATP were conducted. *Figure 4.7(a)* illustrates the "off-on-off" testing protocol used for each run. Power difference (ΔP) was used to describe the sensor response, and was defined as power used to maintain temperature in presence of target gas at each stage (P_R) minus power used to maintain temperature in presence of an inert gas at the same stage (P_0) (expressed as: $\Delta P = P_R - P_0$). At temperatures below 240 ℃, a slightly exothermic reaction was observed at the surface of the SnO_2 catalyst, which was due to the decomposition reaction of TATP into diacetone diperoxide (DADP), acetone, H_2O and O_2/O_3 [15]. However, as the temperature was increased beyond 240 ℃, the reaction tended to become endothermic and peaked at 395˚C. Accompanying this change in sign of the response was a change in the reaction kinetics, which was apparent from the reduced response time for the exothermic reaction compared to the endothermic sensor response. As the temperature was increased, TATP and its intermediate decomposition products continued to oxidize in the presence of air and a large amount of H_2O was generated. Heat absorbed by H_2O overwhelmed the heat released by the decomposition and oxidation reactions of TATP, which led to a power increase to maintain temperature. These sign changes are very telling with respect to the uniqueness of the sensor response (signature) and along with the magnitude of response can alleviate false positives. The details of reaction path remained unknown to researchers to date due to the complexity of the reaction.

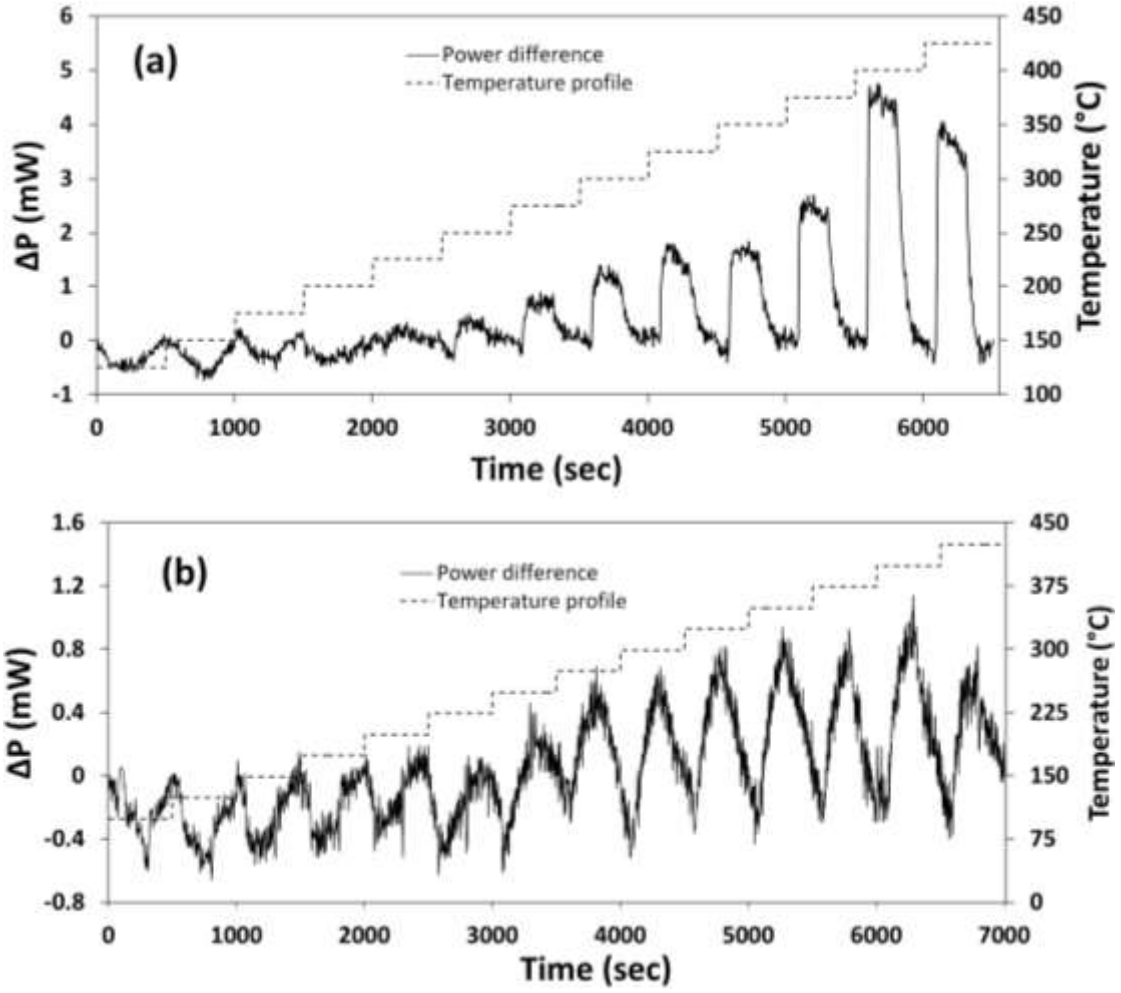

Figure 4.7 Response of thermodynamic sensor to 0.68 μg/ml TATP using a SnO_2 catalyst, which was thermally scanned various temperature steps between 135 ℃ – 435 ℃ using (a) compressed dry air and (b) compressed nitrogen as carrier gas.

A comparative experiment was conducted to confirm this conclusion by using nitrogen as carrier gas to get the TATP molecules into the gas stream. As shown in *Figure 4.7(b)*, the heat effect in the low temperature range (120 ℃ – 240 ℃) exhibited the same sign and magnitude (response), and the same transition temperature; i.e. from a negative heat effect to a positive heat effect compared with results in *Figure 4.7(a)*. This indicates that the same catalytic decomposition process was taking place. However, the magnitude of the response to TATP at high temperature range (280 ℃ – 455 ℃) when using nitrogen as the carrier gas was much smaller which suggests that

much less heat was consumed by H_2O to maintain temperature. This is because TATP was not completely oxidized due to the absence of an oxidant and thus, much less H_2O was generated.

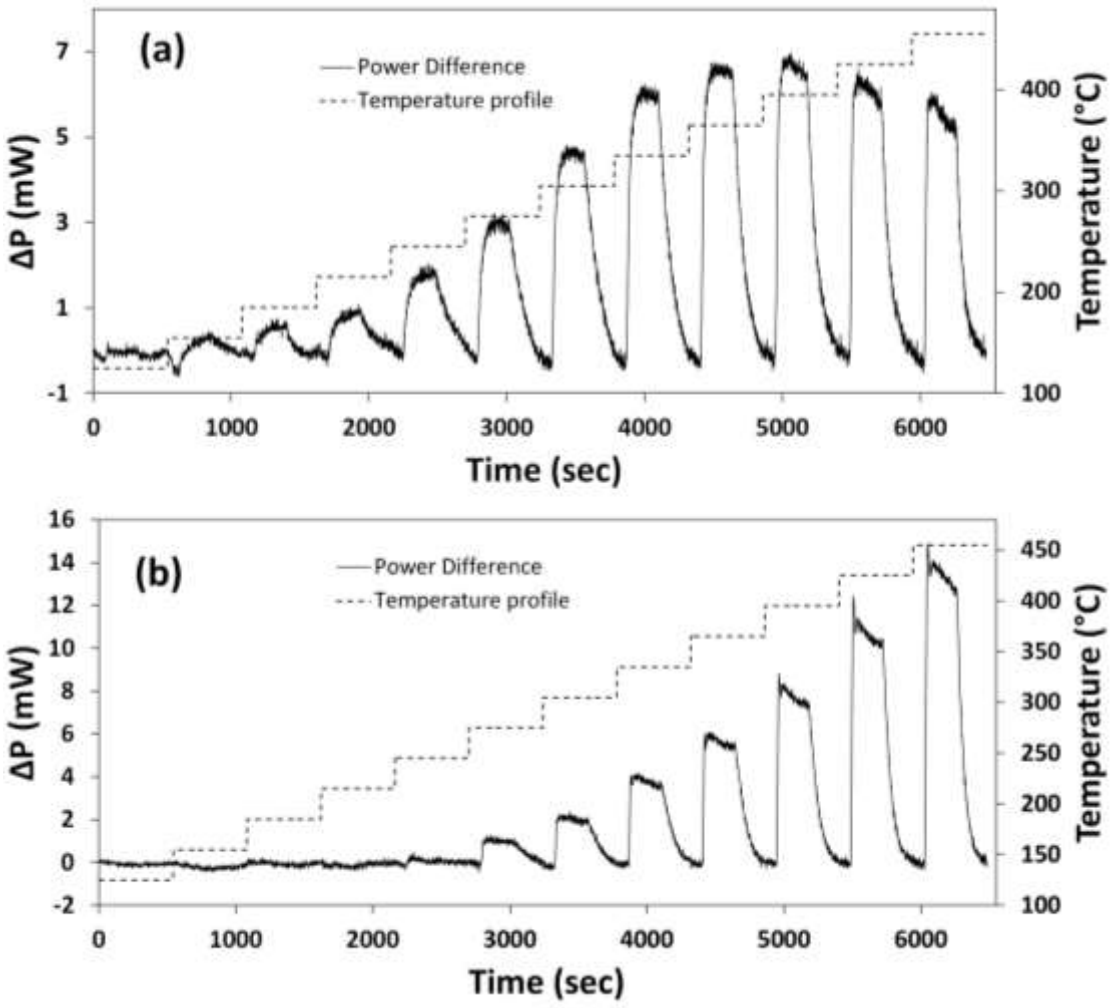

Figure 4.8 Response of thermodynamic sensor using a 12 wt.% loading Pd nanocomposite catalyst to (a) 0. 68 μg/ml TATP and (b) 0.225 μg/ml H_2O_2 at various temperature steps.

When compared to tests performed using pure SnO_2, the Pd:SnO_2 nanocomposite catalysts showed very different behavior (sensor response versus temperature) when exposed to TATP and H_2O_2 as shown in *Figure 4.8(a)*. Unlike pure SnO_2, the nanocomposite catalyst clearly exhibited a positive response to TATP at low temperatures (120 ℃ – 240 ℃) and reached a maximum with amplified response at

395 ℃ without the obvious exothermic reaction. This suggested that a large amount of H_2O had already been generated at low temperature. This change in behavior from that of pure SnO_2 clearly shows the role that palladium played in modification of reaction mechanism. However, as shown in *Figure 4.8(b)*, the catalyst exhibited little or no response to H_2O_2 until a temperature of 275 ℃ was reached, and then kept increasing as temperature was raised to 455 ℃.

The sensor responses as a function of vapor concentration were also performed in both H_2O_2 and TATP to determine the sensitivity and detection limit of our thermodynamic sensor and the results shown in *Figure 4.9(a)* and *4.9(b)*. For comparison purposes between different species, the term "percentage response" was used, which is defined as the power differences (ΔP) at each temperature stage divided by power used to maintain temperature in presence of inert gas at such stage (P_0), which can be expressed as $(P_R - P_0)/P_0 \times 100\%$. The concentration tests were performed at 400 ℃ and the response of the nanocomposite catalyst loaded with 12 wt.% Pd was linear with respect to TATP and H_2O_2 as shown in *Figure 4.9(a)* and *4.9(b)*. Both responses were repeatable when the vapor concentration was reduced to 0.045 μg/ml and 0.14 μg/ml, respectively. The sensor exhibited a response time of less than 5 seconds whereas recovery took significantly longer to reach baseline. The additional time required for recovery was caused by the slow depletion of residual target gas after the supply was cut off.

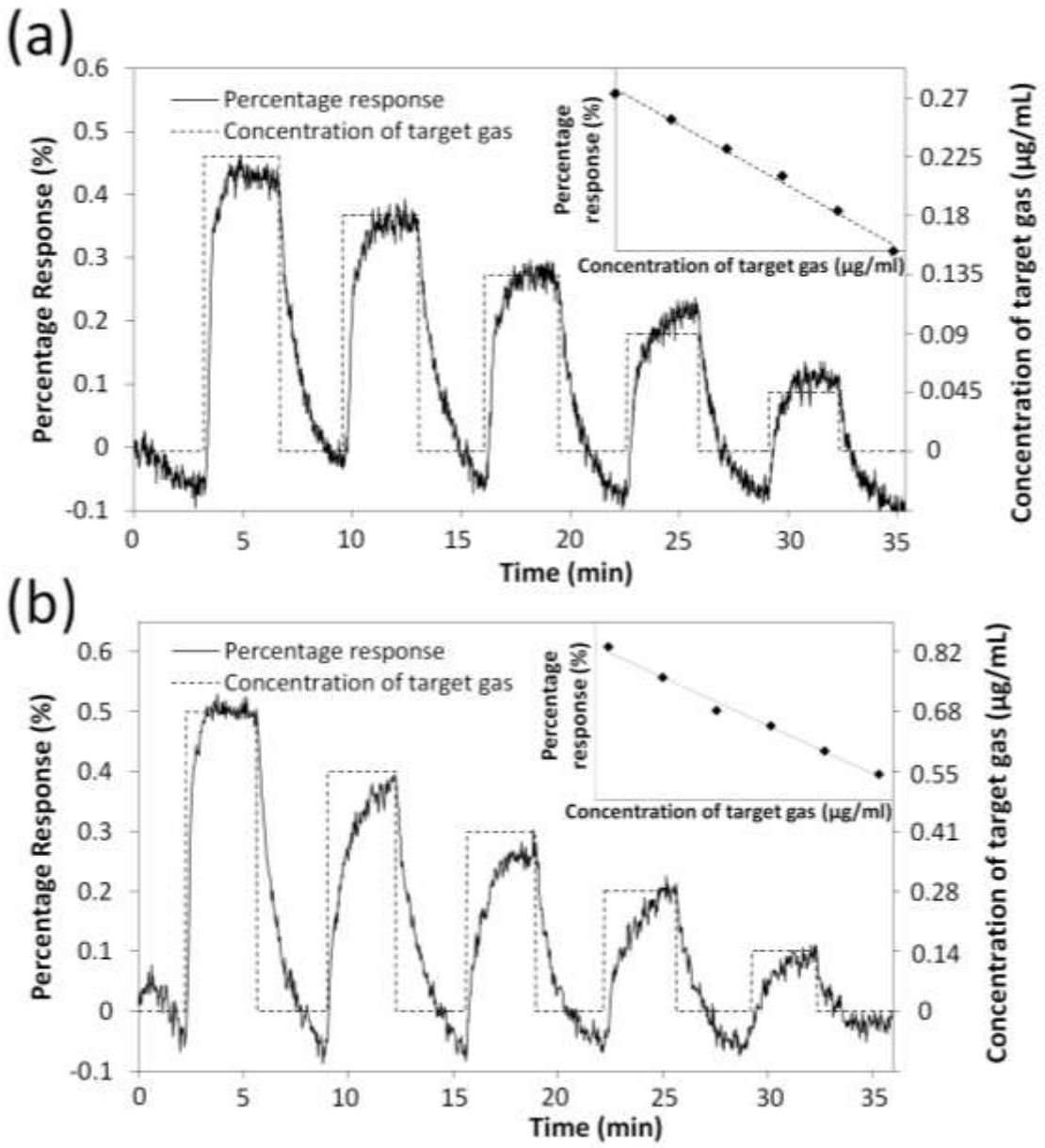

Figure 4.9 Response of a 12 wt.% Pd nanocomposite to (a) H_2O_2 and (b) TATP as a function of concentration in the vapor phase at 400 ℃.

Figure 4.10 shows the magnitude of the heat effect observed for a number of nanocomposite catalysts as a function of palladium loading in the presence of 0.68 µg/ml TATP and 0.225 µg/ml H_2O_2. At palladium loadings less than 8 wt.%, the sensors exhibit a relatively poor response compared to the un-doped SnO_2 catalysts. However, at higher palladium loadings, there was a substantial increase in sensor

response, which abruptly decreased when more than 12 wt.% Pd was incorporated into the catalyst. Higher palladium loadings in the catalyst showed almost no response to TATP and H_2O_2. While there was a substantial improvement in the maximum response to the two target molecules at a 12 wt.% palladium loading, the selectivity between these two target molecules was also significantly improved. A nanocomposite catalyst with a 8 wt.% palladium loading yielded the greatest selectivity (H_2O_2 relative to TATP) while a 12 wt.% palladium loading yielded the greatest sensitivity as shown in *Figure 4.10*.

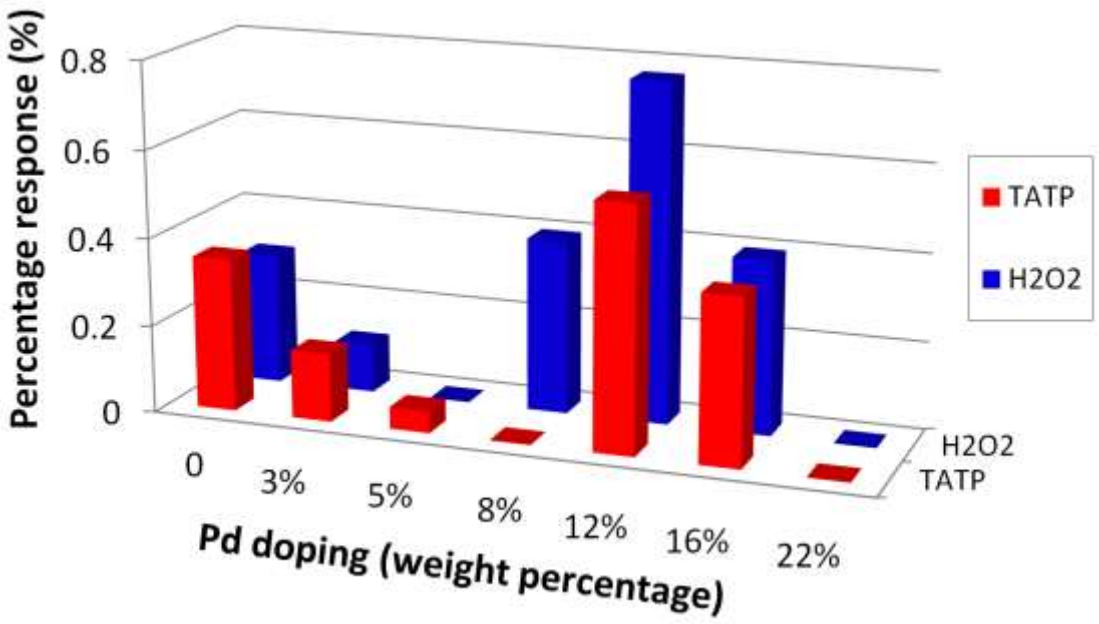

Figure 4.10 Summary of sensitivity and selectivity of Pd:SnO_2 nanocomposite catalyst with various Pd loadings to H_2O_2 and TATP at 400 ℃.

4. Discussion

4.1 Effect of palladium doping amount

The role that palladium additions play when added to a metal oxide matrix such as SnO_2 has been addressed to some extent in the literature [26-35]. However, the exact nature depended on variables including loading method [26, 27], loading

concentration [27, 28], working temperature [29] and species of analytic gases [30-33], each of which played important roles in identifying the specific mechanism. In the current study, sensors using stoichiometric SnO_2 catalysts in the absence of Pd particles exhibited higher sensitivity to oxidizing vapors such as H_2O_2 and TATP compared to sensors using sub-stoichiometric SnO_{2-x}. At low Pd loadings, Pd atoms diffused uniformly into SnO_2 matrix and formed two possible bond types: (1) a strong Pd-Sn alloy metallic bond which was suggested by Tsud, et al [34] and (2) a Pd-O and O-Pd-O ionic bond which was confirmed in XPS. The first type of bond reduced the number of active SnO_2 molecules per unit surface area while the second type of bond essentially gettered oxygen atoms from the stoichiometric SnO_2 leaving a non-stoichiometric SnO_2. This can be a possible cause for the reduction in sensor response for palladium loadings in the range 0 - 8 wt.%. Meanwhile, both O-Pd-O bonds and Pd-O bonds were present in this loading range, as confirmed by XPS but the sensitivity of this catalyst decreased as shown in *Figure 4.10*. This suggests that neither O-Pd-O nor Pd-O independently functioned in a catalytic role.

As the Pd loading was increased, metastable oxygen molecules in the catalyst were released during annealing and diffused throughout the film. However, this oxygen was insufficient for Pd atoms to form O-Pd-O bonds, resulting in the disappearance of the PdO_2 peak as indicated by XPS and shown in *Figure 4.6(b)*. Instead, relatively small Pd metallic clusters encapsulated in a PdO-SnO_2 matrix were formed, resulting in an increase in the Pd peak [34]. In addition, the Sn 3d peak intensity remained constant, whose presence corresponds to stoichiometric SnO_2. This observation could occur by sharing oxygen atoms associated with PdO as indicated by

the XPS spectra in *Figure 4.6(a)*. Nanocomposite catalysts fabricated with 12 wt.% Pd and 88wt.% SnO_2 lead to a maximum in response, regardless of Pd loading in the Pd-SnO_2 nanocomposite. As the Pd loading was increased beyond this level, the size of Pd clusters increased, resulting in a relatively large Pd metallic XPS peak. As a result, the Pd clusters displaced the SnO_2 and caused an additional decrease in amount of SnO_2 and thus, a decrease in sensor response. Also, those sensors with palladium loadings greater than 22% showed no response to peroxides, indicating that neither the palladium nor the Pd^{2+} could function as catalysts.

In conclusion, the experiments suggest that the palladium itself, regardless of its oxidation state, did not affect the sensitivity of the Pd:SnO_2 catalyst but instead, appeared to amplify the signal by varying the oxidation state of SnO_2. Sensors with palladium loadings of 12 wt.% exhibited the maximum sensitivity (sensor response) to both TATP and H_2O_2.

4.2 Protocol of TATP identification

As indicated in *Figure 4.10*, a SnO_2 catalyst with a 12 wt.% palladium loading provided the greatest response to both TATP and H_2O_2 at a temperature of 395 ℃. Thus, sensors with a 12 wt.% Pd loading were selected for long term exposure tests and were maintained at 400 ℃ for prolonged periods as an early warning indicator; i.e. once a positive signal was received for an unknown vapor, measures could be taken to further identify the species of the suspect vapor. The sensor was then scanned at various temperature setpoints ranging from 150 ℃ to 450 ℃ to collect a characteristic signature as a function of temperature. H_2O_2 and TATP have significantly different positive trigger points and their peak response temperatures can be used as a unique

signature to distinguish TATP from H_2O_2. The Pd:SnO_2 nanocomposites with 5 wt.% and 8 wt.% palladium loadings were also employed. The 5 wt.% palladium catalysts only responded to TATP and showed no response to H_2O_2 while the 8 wt.% palladium catalysts gave opposite responses, as shown in *Figure 4.10*. These two sets of sensors provided a certain redundancy in response, which will help mitigate false positives.

5. **Conclusion**

Combinatorial chemistry techniques were used to screen catalyst candidates for optimal sensitivity and selectivity in the system Pd:SnO_2. The resulting nanocomposite catalysts consisted of Pd nano-particles uniformly dispersed in a SnO_2 matrix, the composition and morphology of which was verified by SEM and TEM. In the Pd:SnO_2 nanocomposite catalyst optimized for sensitivity and selectivity, tin was present largely as Sn^{4+} while palladium was present in both the Pd^{2+} and Pd^{4+}oxidation states. Compared to pure SnO_2 catalyst, incremental Pd additions to the nanocomposite modified the catalytic decomposition of TATP, resulting in several unique signatures or sensor responses. For example, the sensor response to TATP using a nanocomposite with 12wt.% palladium loading exhibited a change in sign and enhanced responses. Finally, $PdSnO_2$ nanocomposite catalysts with an 8 wt.% palladium loading yielded the greatest selectivity between TATP and H_2O_2 while catalysts with a 12 wt.% palladium loading provided maximum sensitivity.

REFERENCES

[1] F. Dubnikova, R. Kosloff, Y. Xeiri and Z. Karpas, "Novel approach to the detection of triacetone triperoxide (TATP), its structure and its complexes with ions," *Journal of Physical Chemistry A*, vol. 106, pp. 4951-4956, 2002.

[2] I. Cotte-Rodriguez, H. Chen and R. G. Cooks, "Rapid trace detection of triacetone triperoxide (TATP) of complexation detections of desorption electrospray ionization," *Chemical Communications*, vol. 42, pp. 953-955, 2006.

[3] G. A. Buttigieg, A. K. Knight, S. Denson, C. Pommier and M. B. Denton, "Characterization of the explosive triacetone triperoxide and detection by ion mobility spectrometry," *Forensic Science International*, vol. 135, pp. 53-59, 2003.

[4] R. Rasanen, M. Nousianinen, K. Parakorpi, M. Sillanpaa, L. Polari, O. Anttalainen and M. Utrianinen, "Determination of gas phase triacetone triperoxide with aspiration ion mobility spectrometry and gas chromatography-mass spectrometry," *Analytica Chimica Acta*, vol. 623, pp. 59-65, 2008.

[5] J. Wilkinson, C. T. Konek, J. S. Moran, E. M. Witko and T. M. Korter, "Terahertz absorption spectrum of triacetone triperoxide (TATP)," *Chemical*

Physics Letters, Vols. 172-174, p. 478, 2009.

[6] A. Stambouli, A. El Bouri, T. Bouayoun and M. A. Bellimam, "Headspace GC/MS detection of TATP traces in post-explosion debris," *Forensic Science International,* vol. 146S, pp. 191-194, 2004.

[7] C. Mullen, A. Irwin, B. V. Pond, D. L. Huestis, M. J. Coggiola and H. Oser, "Detection of explosives and explosives-related compounds by single photon laser ionization time-of-flight mass spectrometry," *Analytical Chemistry,* vol. 78, p. 3807, 2006.

[8] C. Shen, J. Li, H. Han, H. Wang, H. Jiang and Y. Chu, "Triacetone triperoxide using low reduced-field proton transfer reaction mass spectrometer," *International Journal of Mass Spectrometry,* vol. 285, pp. 100-103, 2009.

[9] R. S. Ladbeck and U. Karst, "Determination of triacetone triperoxide in ambient air," *Analytical Chemistry,* vol. 482, pp. 183-188, 2003.

[10] N. Barsan, D. Koziej and U. Weimar, "Metal oxide-based gas sensor research: How to," *Sensors and Acutators B,* vol. 121, pp. 18-35, 2007.

[11] N. L. Hung, H. Kim, S. K. Hong and D. Kim, "Enhancement of CO gas sensing properties of ZnO thin films deposited on self-assembled Au nanodots," *Sensors and Actuators B,* vol. 151, pp. 127-132, 2010.

[12] G. Eranna, B. C. Joshi, D. P. Runthala and R. P. Gupta, "Oxide materials for

development of integrated gas sensors: A comprehensive review," *Critical Review of Solid State and Materials Sciences,* vol. 29, pp. 111-188, 2004.

[13] W. H. Zhang, W. D. Zhang and L. Y. Chen, "Highly sensitive detection of explosive Triacetone triperoxide by an In_2O_3 sensor," *Nanotechnoloy,* vol. 21, p. 315502, 2010.

[14] I. Eisele, T. Doll and M. Burgmair, "Low Power gas detection with FET sensors," *Sensors and Actuators B,* vol. 78, pp. 19-25, 2001.

[15] K. Schierbaum, U. Weimar and W. Gopel, "Conductance, work function and catalytic activity of SnO_2-based gas sensors," *Sensors and Actuators B,* vol. 3, pp. 205-214, 1991.

[16] W. Y. Yang, W. G. Kim and S. W. Rhee, "Radio frequency sputter deposition of single phase cuprous oxide using Cu_2O as a target material and its resistive switching properties," *Thin Solid Films,* vol. 517, pp. 967-971, 2008.

[17] C. I. Pearce, R. A. Pattrick, D. J. Vaughan, C. M. Henderson and G. van der Laan, "Copper oxidation state in chalcopyrite: Mixed Cu d^9 and d^{10} characteristics," *Geochimica,* vol. 70, pp. 4635-4642, 2006.

[18] M. Amani, Y. Chu, K. L. Waterman, C. M. Hurley, M. J. Platek and O. J. Gregory, "Detection of triacetone triperoxide (TATP) using a thermodynamic based gas sensor," *Sensors and Actuators B,* vol. 162, pp. 7-13, 2012.

[19] E. Vereshchaginam, R. A. Wolters and J. G. Gardeniers, "Measurement of reaction heats using a polysilicon based microcalorimetric sensor," *Sensors and Actuators A,* vol. 169, pp. 308-316, 2011.

[20] T. Zhang, L. Liu, Q. Qi, S. Li and G. Lu, "Development of microstructure In/Pd-doped SnO_2 sensor for low level CO detection," *Sensors and Actuators B,* vol. 139, pp. 287-291, 2009.

[21] V. Jimenez, J. Espinos and A. Gonzalez-Elipe, "Effect of texture and annealing treatments in SnO_2 and Pd/SnO_2 gas sensor materials," *Sensors and Actuators B,* vol. 61, pp. 23-32, 1999.

[22] T. Skala, K. Veltruska, M. Moroseac, I. Matolinova, A. Cirera and V. Matolin, "Redox process of Pd-SnO_2 system," *Surface Science 566-568(2004)1217-1221,* Vols. 566-568, pp. 1217-1221, 2004.

[23] R. Tan, Y. Guo, J. Zhao, Y. Li, T. Xu and W. Song, "Synthesis, characterization and gas-sensing properties of Pd-doped SnO_2 nano particles," *Transactions of Nonferrous Metals Society of China,* vol. 21, pp. 1568-1573, 2011.

[24] Y. Shen, T. Yamazaki, Z. Liu, D. Meng, T. Kikuta, N. Nakatani, M. Saito and M. Mori, "Microstructure and H_2 gas sensing properties of undoped and Pd-doped SnO_2 nanowires," *Sensors and Actuators B,* vol. 135, pp. 524-529, 2009.

[25] M. Amani, O.J. Gregory. “Grain growth and morphology of In_2O_3:Pd nanocomposite films”, Thin Solid Films, 542(2013)180-185

[26] C. B. Lim and S. Oh, "Microstructure evolution and gas sensitivities of Pd-doped SnO_2-based sensor prepared by three different catalyst-addition process," *Sensors and Actuators B,* vol. 30, pp. 223-231, 1996.

[27] S. Matsushima, T. Maekawa, J. Tamaki, N. Miura and N. Yamazoe, "New methods for supporting palladium on a tin oxide gas sensor," *Sensors and Actuators B,* vol. 9, pp. 71-78, 1992.

[28] M. Yuasa, T. Masaki, T. Kida, K. Shimanoe and N. Yamazoe, "Nano-sized PdO loaded SnO_2 nanoparticles by reverse micelle method for highly sensitive CO gas sensor," *Sensors and Actuators B,* vol. 136, pp. 99-104, 2009.

[29] L. Liu, T. Zhang, S. Li, L. Wang and T. Tian, "Preparation, characterization, and gas-sensing properties of Pd-doped In_2O_3 nanofibers," *Materials Letters,* vol. 63, pp. 1975-1977, 2009.

[30] N. Yamazoe, K. Kurokawa and T. Seiyama, "Effects of additives on semiconductor gas sensor," *Sensors and Actuators,* vol. 4, pp. 283-289, 1983.

[31] G. Tournier, C. Pijolat, R. Lalauze and B. Patissier, "Selective detection of CO and CH_4 with gas sensors using SnO_2 doped with palladium," *Sensors and Actuators B,* Vols. 26-27, pp. 24-28, 1995.

[32] Y. C. Lee, H. Huang, O. K. Tan and M. S. Tse, "Semiconductor gas sensor based on Pd doped SnO_2 nanorod thin films," *Sensors and Actuators B,* vol. 132, pp. 239-242, 2008.

[33] Y. Zhang, Q. Xiang, J. Xu, P. Xu, Q. Pan and F. Li, "Self-assemblies of Pd nanoparticles on the surfaces of single crystal ZnO nanowires for chemical sensors with enhanced performances," *Journal of Material Chemistry,* vol. 19, pp. 4701-4706, 2009.

[34] N. Tsud, V. Johanek, I. Stara, K. Veltruska and V. Matolin, "XPS, ISS and TPD of Pd-Sn interactions on Pd-SnO_x systems," *Thin Solid Films,* vol. 391, pp. 204-208, 2001.

[35] J. Choi, I. Hwang, S. Kim, J. Park, S. Park, U. Jeong, Y. Kang and J. Lee, "Design of selective gas sensor using electrospun Pd doped SnO_2 hollow nanofibers," *Sensors and Actuators B,* vol. 150, pp. 191-199, 2010.

CHAPTER 5

"Detection of Explosives Using Orthogonal Gas Sensors"

by

Yun Chu[1], Daniel Mallin[2], Matin Amani[3], and Otto J. Gregory[4]

IEEE Sensors, Baltimore (2013)12-15

---

[1] PhD Candidate, Department of Chemical Engineering, The University of Rhode Island, Kingston, RI 02881. Email: yun.z.chu@gmail.com

[2] MS Candidate, Department of Electrical, Computer and Biomedical Engineering, The University of Rhode Island, Kingston, RI 02881. Email: daniel.p.mallin@gmail.com

[3] Research Engineer, U.S. Army Research Laboratory, Adelphi, MD 20783. Email: matin.amani@gmail.com

[4] Distinguished Professor, Department of Chemical Engineering, The University of Rhode Island, Kingston, RI 02881. Email: gregory@egr.uri.edu

1. Introduction

The detection of explosives is not only critical for the safety of military personnel but actual for the travelling public, as well as evidenced by numerous terrorist activities both at home and abroad. Detection can be a daunting task, since explosives are comprised of a wide range of compounds including both nitrogen and non-nitrogen based energetic materials with different functional groups (e.g. $–NO_2$, $-ONO_2$, $-NH_2$, -[O-O]-) [1, 2]. Most explosives have extremely low vapor pressures [2-5], which increases the difficulty of vapor phase detection. Conventional analytical instrumentation (e.g. infra-red spectroscopy, fluorescence spectroscopy, mass spectroscopy, Terahertz spectroscopy and Raman Spectroscopy [6-13]) have excellent reliability and selectivity to trace levels of explosives, especially to compounds containing nitro groups. However, these techniques suffer from limitations such as complicated sample preparation and high maintenance costs. They also require skilled operators and are not capable of in situ monitoring. As a result, a simple, low cost, portable sensor or so called electronic "nose" with continuous monitoring capability, high selectivity and sensitivity is needed for explosive detection.

Sensors that rely on measuring the conductivity changes in a semiconducting metal oxide, also known as conductometric sensors, have been widely exploited due to their excellent sensitivity under atmospheric conditions. Metal oxides such as SnO, SnO_2, In_2O_3, WO_3, TiO_2 and ZrO_2, have been used to detect simple gas molecules at trace levels (H_2O, CO, O_2, O_3, H_2, SO_2, NO_2) and even complex explosive compounds [14-21]. The change in resistivity of the metal oxide when exposed to target molecules is due to adsorption or reaction processes when target gases interact with the surface

of metal oxide. Here, the free charge carriers are transferred from the semiconductor to the target gas or vice versa. Gases of the same type, either acceptor gases (which tend to accept free electrons) or donor gases (which tend to lose free electrons), will cause similar changes in resistivity, which makes it difficult to determine the nature of the interactions at the gas/solid interface. All of this translates into poor selectivity, which is a major drawback that impedes the application of conductometric sensors [19, 22-25].

In a previous study, we demonstrated a small footprint thermodynamic based gas sensor capable of detecting explosives at the part per million level. It measures the heat effect due to the catalytic decomposition of target molecules. The sensor has relatively high selectivity down to the part per million level among peroxide based compounds [26]. To further improve its sensitivity without sacrificing selectivity to threat chemical compounds, this thermodynamic sensing platform was combined with a conductometric platform, in such a way that the same catalyst was simultaneously interrogated by two techniques. Combining these two complimentary sensing techniques provides a certain redundancy in sensor response that mitigates the detection of false positives and negatives. One major challenge was that most catalysts with stoichiometric amount of oxygen exhibited maximum sensitivity in terms of the thermodynamic signal (response from thermodynamic platform) while the conductometric signal (response from the conductometric platform) requires a catalyst with non-stoichiometric amount of oxygen. Thus, a hybrid catalyst with multiple oxidation states was developed as part of the study to fulfill this requirement. In this

paper, several metal oxide catalysts were employed to detect explosives using this new platform and confirm this approach as being a viable one.

2. Experimental

2.1 Fabrication of the orthogonal sensor

Photolithography techniques were used to form nickel microheaters on individual alumina substrates with dimension of 7.5 mm by 16.8 mm by 0.5 mm, as shown in *Figure 5.1*. Nickel microheater have a nominal thickness of 4.5 μm and were sputtered in a MRC 822 sputtering system in $9*10^{-3}$ torr argon. Following the sputtering process, the microheaters were nitrogen annealed at 900 ℃ to improve electrical stability of the as-deposited films. A 1 μm alumina film was sputtered over the microheater and a 150 μm high purity alumina coating was applied to the working region of sensor, as indicated in *Figure 5.1 c(4)* and *c(3)*, respectively. Both alumina layers function as insulation layers to prevent the nickel micro-heaters from direct exposure to the gas molecules and prevent electrical shorts to the marginally conductive oxide catalyst.

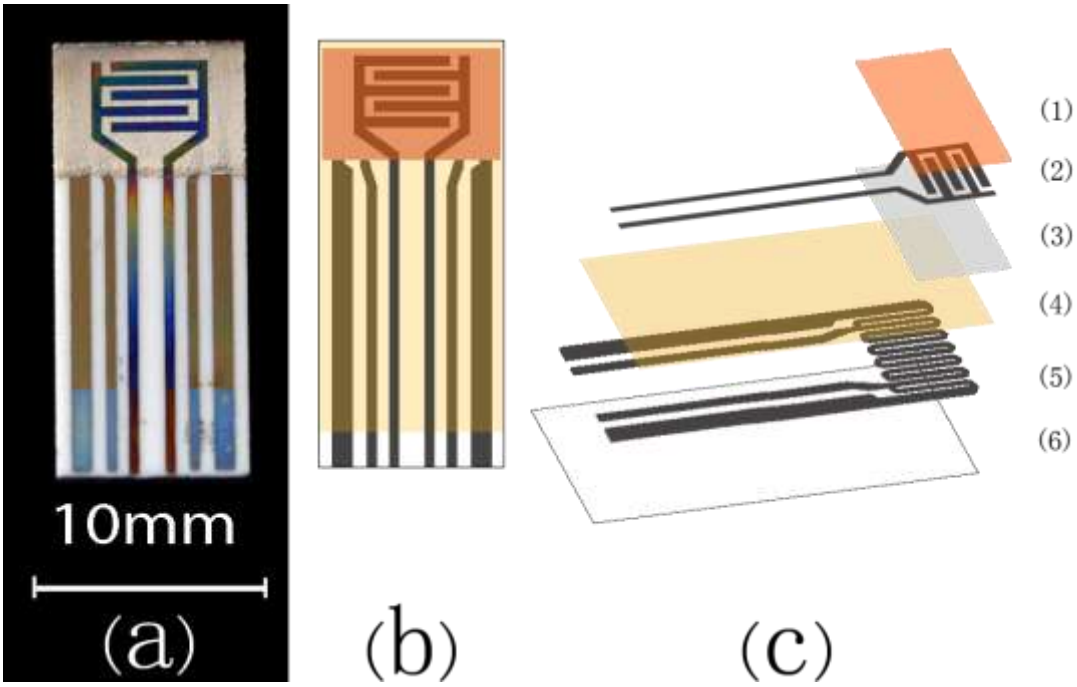

Figure 5.1 Schematic of orthogonal sensor showing an actual picture (a), the top view (b) and expanded views (c) of the metal oxide catalyst layer (1), nickel electrodes (2), alumina coatings (3-4), nickel microheater (5) and alumina substrate (6).

Nickel electrodes were then deposited over the metal oxide catalysts to measure the change in electrical resistivity of the metal oxides when exposed to the target gas. SnO_2 and ZnO were subsequently deposited as the metal oxides using a MRC 8667 sputtering system in pure argon, which produced a nonstoichiometric oxide (oxygen deficient). Both catalysts were then annealed at 500℃ in nitrogen for 5 hours, densifying the film, eliminating point defects and releasing trapped argon atoms in the film. This was followed by a second heat treatment in a nitrogen/oxygen atmosphere (volume ratio of 95:5) for 5 minutes using same annealing temperature. The second heat treatment ensures that the surface of catalyst film was stoichiometric, which is in direct contact with target gas molecules. Underneath the stoichiometric oxide was a much thicker nonstoichiometric oxide that was tailored for the conductivity

measurement. The oxidation states of the metal oxide as a function of depth were characterized using X-ray photoelectron spectroscopy (XPS) to establish depth profiles and confirm the nature of the oxide layer.

2.2 Sensing procedure and data acquisition

A schematic of test apparatus is shown in *Figure 5.2*. Target molecules were delivered to the sensor in the reaction chamber by passing a carrier gas (dry air) over TATP crystals embedded in filter paper placed in target source chamber. The flow rate of carrier gas (dry air) and target gas was precisely metered into the reaction chamber using two mass flow controllers and a digital flow meter, which provided a constant flow of target gas and reference gas to the sensor. The desired concentration of explosive vapor was achieved by mixing the target gas and reference gas at specific flow rate ratios.

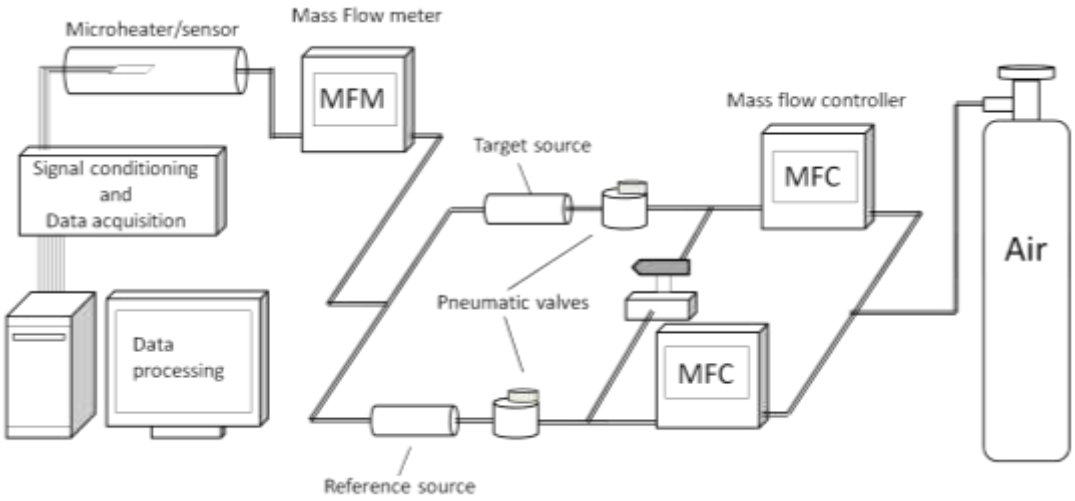

Figure 5.2 Apparatus used for TATP, 2,6-DNT and ammonia nitrate detection using orthogonal sensor. Reference source were constantly kept empty to establish a baseline for the experiment.

Thermodynamic responses and resistivity changes were measured using a dynamic testing protocol. The catalyst-coated microheater was heated to a series of

predetermined temperature setpoints by controlling the electrical resistance of the microheater and correlating it to a calibration curve based on the temperature coefficient of resistivity (TCR) of the nickel microheaters. Electrical power was used to maintain the temperature while switching from an inert gas to target gas. The change in power was recorded to determine the heat effect associated with the interaction of the target molecules with the catalyst. The thermodynamic response was then analyzed by compiling the power differences at different temperature setpoints. Conductivity changes of the metal oxides were measured simultaneously using a four-point probe method; i.e. by supplying constant current through two probes to metal oxide catalyst while recording the applied voltage. The gas delivery system and data acquisition were computer controlled using LabView software.

The thermodynamic and conductometric responses were analyzed by compiling the power and resistivity signals at different temperature setpoints. After reaching the desired temperature, the sensor was allowed to equilibrate for 360 seconds under constant reference gas flow. The target gas was then introduced into the test chamber for 300 seconds, and switched back to the reference gas for another 240 seconds to determine the sensor's ability to recover before the microheater was ramped to the next temperature setpoint. The power difference required to maintain the sensor at a particular temperature and resistivity change of semiconductor in presence of target gas were recorded for each step. Prior to quantifying the sensor response, the base line (reference signal) and signal drift were estimated and subtracted from the sensor response. Typically, all responses smaller than ±5% were considered background or noise, which were attributed to small variations in the target and inert gas flow rates,

and stability of the nickel microheaters. Sensor responses to explosive vapors as a function of target gas concentration were also determined. The sensitivity, detection limit, response time and recovery time for ammonium nitrate (AN), 2,6-dinitrotoluene (2,6-DNT) and triacetone triperoxide (TATP) were evaluated for the conductometric platform and thermodynamic platform in the orthogonal sensor.

3. Results and discussion

3.1 Catalyst characterization

Oxidation states of metallic species in the SnO_2 and ZnO catalyst as a function of depth were characterized by XPS as shown in *Figure 5.3.* Position 1, 2 and 3 in both figures refer to the as-annealed surface 100Å and 600Å below the surface of the catalyst, respectively. Energy states associated with the Sn $3d_{5/2}$ and Sn $3d_{3/2}$ electrons show only slight changes as a function of depth with the exception that both 3d peaks taken at position 1 appear sharper, as shown in *Figure 5.3(b).* When sampled from position 1 to position 3, as shown in *Figure 5.3(c),* a phase transition was observed, during which the Sn 4d peak at 27.2 eV (+4 state) decreased and a shoulder associated with the Sn 4d peak at 26.6 eV (+2 state) increased and eventually formed a new peak. This indicated that a transition from stoichiometric SnO_2 at surface of catalyst to a nonstoichiometric SnO_{2-X} had occurred below the surface. From *Figure 5.3(d),* Zn 2p doublets can be observed, indicating that multiple oxidation states exist at the surface of ZnO catalyst most likely due to the oxygen introduced during annealing processes. Also the Zn $2p_{3/2}$ peaks at positions 2 and 3 shifted to lower binding energies and appear sharper when compared to the peak at position 1, indicating that a uniform ZnO_{1-Y} layer had formed below the surface. This assumption

was confirmed in *Figure 5.3(e)* by the disappearance of ZnO secondary peaks corresponding to the 3s and 3p states and an increase in intensity of the 3d peak as a function of position, which was verified as a transition in oxidation state.

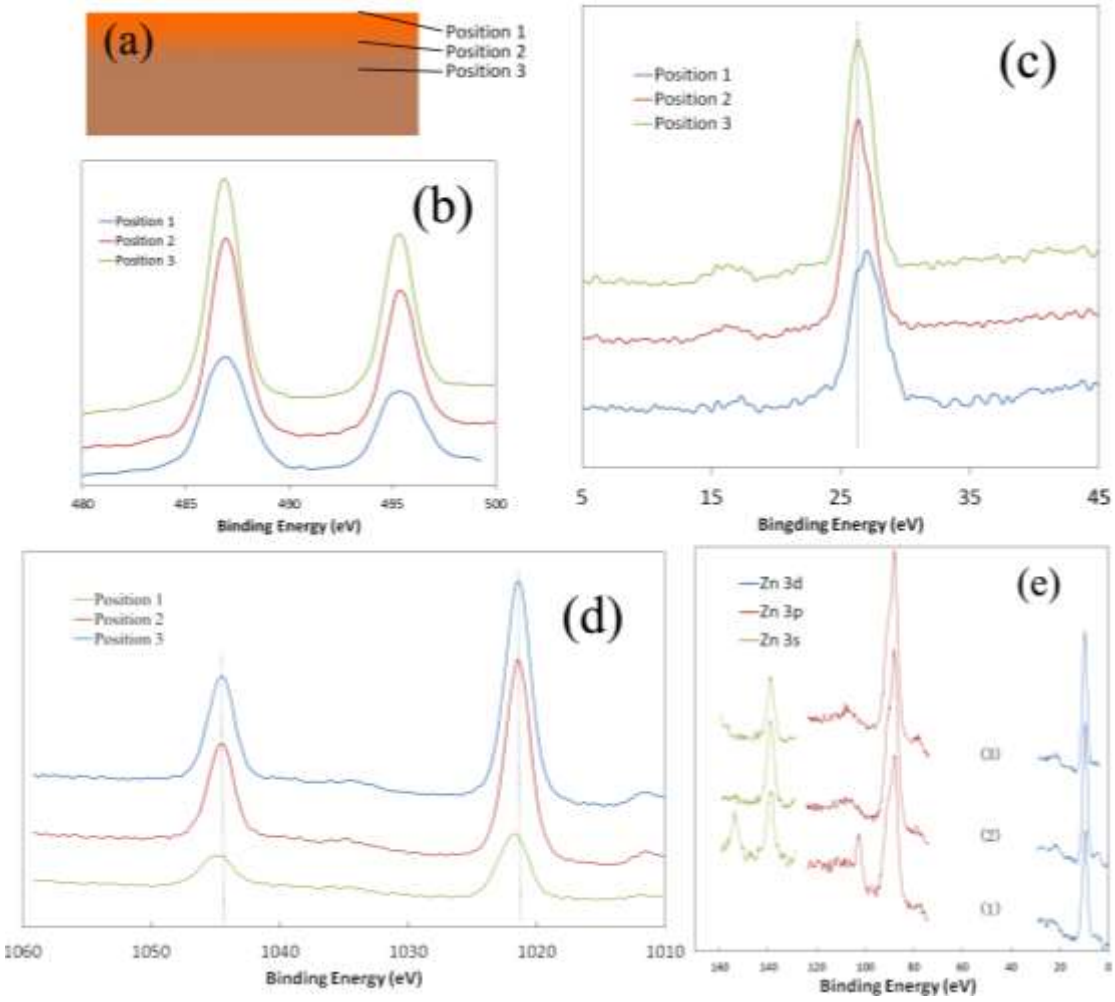

Figure 5.3 X-ray photoelectron spectra (XPS) results of SnO_2 catalyst. *3(a)* indicates the sampling position in a cross-section diagram of catalyst; Sn $3d_{5/2}$ and Sn $3d_{3/2}$ states were shown in *3(b)* and 4d states in *3(c)*. XPS results of ZnO catalyst. *3(d)* indicates the Zn 2p states and 3s, 3p and 3d states in *3(e)*.

3.2 Sensor characteristics

Figure 5.4 shows a typical response from orthogonal sensors using SnO_2 and ZnO as catalysts in presence of 2, 6-DNT. Responses using SnO_2 catalyst are presented in

Figure 5.4(a), and responses using ZnO catalyst were initially collected from separate platforms, each individually tuned for optimal thermodynamic and conductometric response. Each sensor was pre-stabilized at 410 ℃ for 15 minutes before recording data. DNT was then introduced into the test chamber after 1 minute for a period of 360 seconds as shown along the horizontal axis in *Figure 5.4(a)* and *5.4(b)*. The sensor employing SnO_2 catalyst exhibited the fastest thermodynamic response time (less than 5 seconds) whereas the conductometric response took significantly longer (60 - 80 seconds) to reach equilibrium and did not show a sharp transition after introduction of target gas. However, both thermodynamic and conductometric signals completely recovered to the baseline values within 5 minutes. Both the thermodynamic and conductometric signals using a ZnO catalyst demonstrated a rapid response time (less than 10 seconds). However, both responses took a longer time to reach equilibrium and recover, compared to those produced with a SnO_2 catalyst.

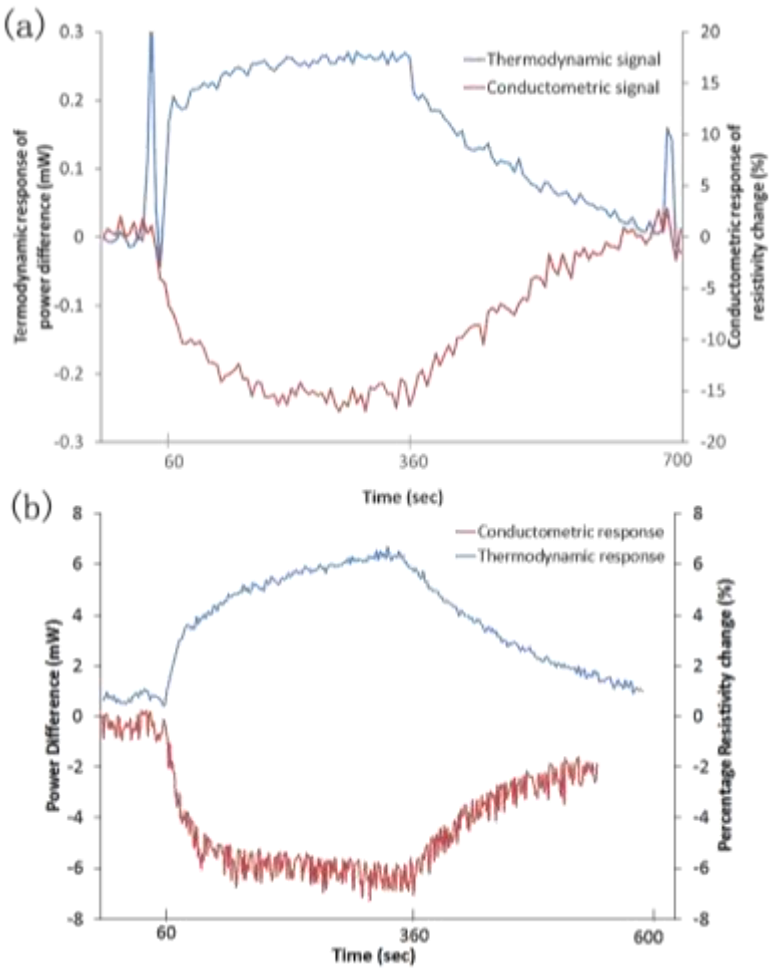

Figure 5.4 Thermodynamic response (blue) and conductometric response (red) to 2, 6-DNT at 410 ℃ taken simultaneously with SnO_2 (a) and ZnO (b) orthogonal sensor.

The difference in response times and recovery times between the two sensing platforms was attributed to their detection mechanisms. The thermodynamic platform measures the heat effect associated with the catalytic decomposition of the target gas, which was initiated instantly as the target gas molecules interact with the surface of catalyst. When additional target gas molecules are introduced, same decomposition occurs immediately. This formed a dynamic equilibrium where decomposition rate was the rate-controlling step. The conductometric platform measures the charge carrier concentration which depended on donating or accepting extra charge carriers as the

target gas molecule was adsorbed onto or desorbed from the surface of catalyst. This process also resulted in a dynamic equilibrium where the adsorption and desorption rate is the rate-controlling step. Since the chemical reaction rate is an order of magnitude faster than physical adsorption rate, the thermodynamic signal exhibits a much faster response time and recovery time compared to that of conductometric signal.

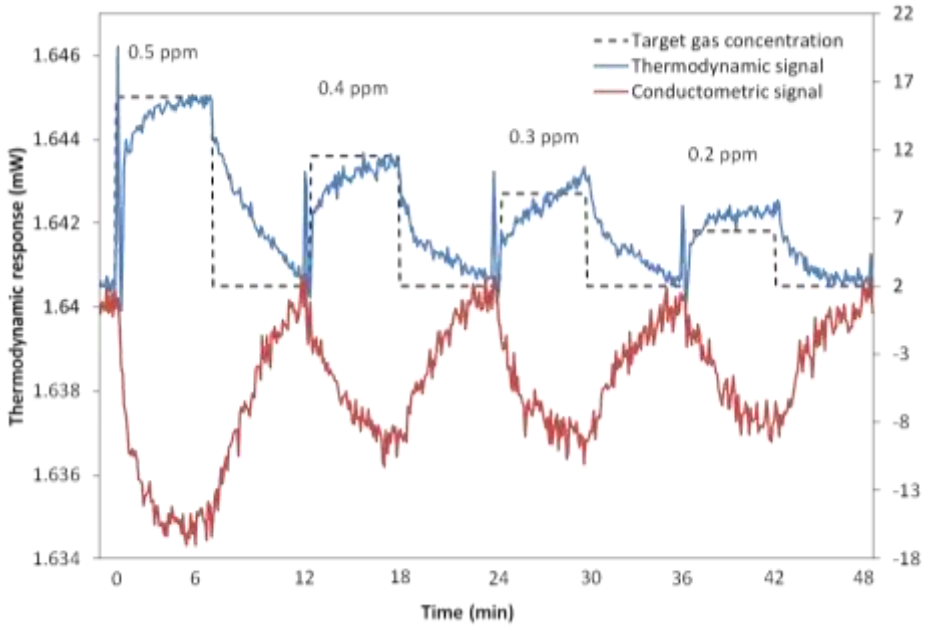

Figure 5.5 Orthogonal response of SnO_2 (where conductometric response is presented in red and thermodynamic response in blue) as a function of 2,6-DNT vapor concentration (black dashed line) at 410 ℃.

The orthogonal sensor response to 2,6-DNT as a function of DNT vapor concentration (at 410 ℃ employing SnO_2) is shown in *Figure 5.5*. Here, the thermodynamic response was linear with respect to DNT vapor concentration whereas the conductometric response remained the same as the DNT vapor concentration decreased. Both responses were repeatable when the vapor concentration was reduced from 0.5 ppm to 0.2 ppm.

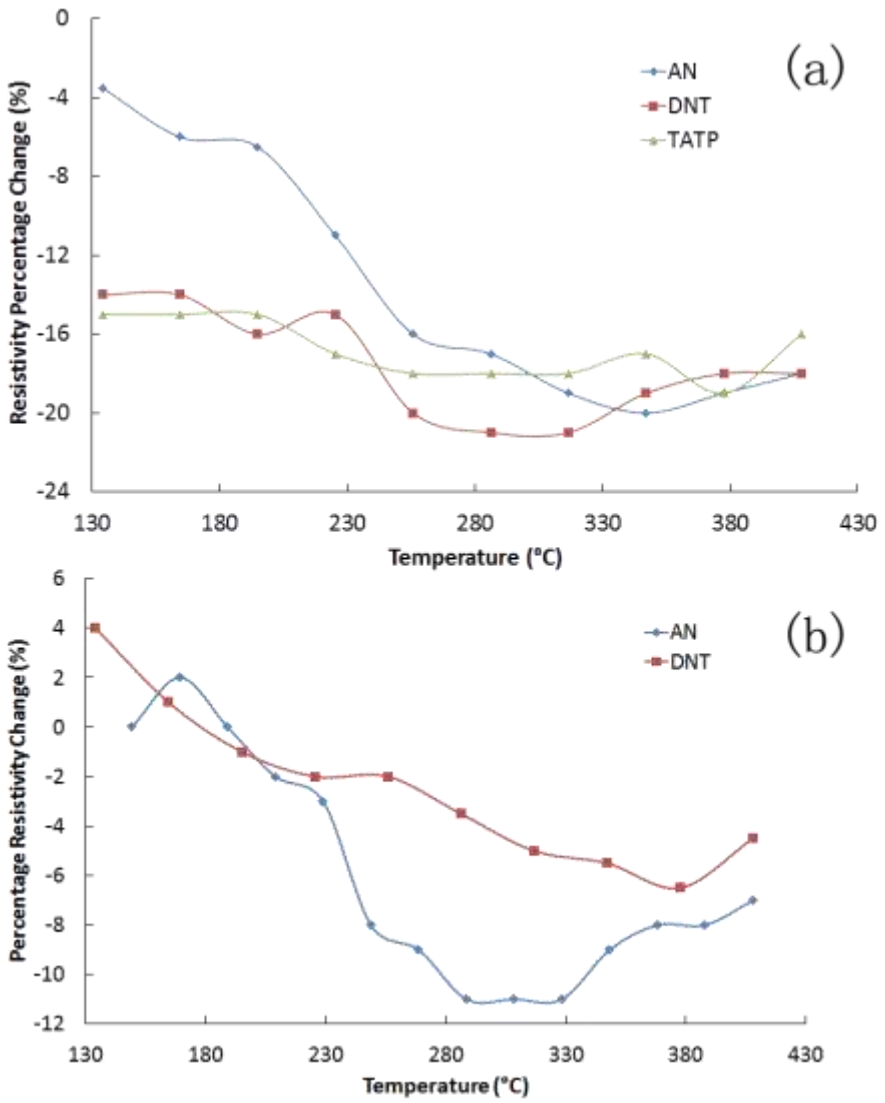

Figure 5.6 Conductometric response of SnO_2 (a) and ZnO (b) to ammonia nitrate (blue), 2,6-DNT (red) and TATP (green) as a function of temperature.

The conductometric response to ammonium nitrate, DNT and TATP vapor as a function of temperature employing SnO_2 and ZnO as catalysts are shown in *Figure 5.6*. The responses of both catalysts to ammonium nitrate was proportional to temperature at low temperature ranges (<250 ℃) and then decreased with temperature as it was raised over 350 ℃. 2, 6-DNT showed similar behavior relative to ammonium nitrate but only exhibited a shallow peak at 280 ℃ with both catalysts. The TATP signal produced from the SnO_2 catalyst changed very little with the temperature,

whereas these sensors employing ZnO catalyst did not show a conductometric response to TATP and therefore, were not included here. These differences in sensor response could be caused by the differences in vapor pressure of target molecules and differences in the functional groups and molecular structures between the target molecules. However, the exact mechanism remains unknown due to the complexity of the processes. As a result, all three compounds (TATP, DNT and ammonium nitrate) exhibited unique signatures (orthogonal responses), which could be used to further characterize their presence and mitigate false positives and negatives.

A series of heat treatment protocols were used to prepare the SnO_2 catalysts for the orthogonal sensor platform and exhibited reliability and reproducibility. However, the optimized heat treatment when using the ZnO catalyst in the orthogonal sensor platform is still under investigation.

4. Conclusion

A gas sensor incorporating a conductometric platform with an existing thermodynamic platform was developed for the trace detection of explosives. This gas sensor could reliably detect nitrogen and non-nitrogen based explosives at the sub ppm level. Specially, a detection limit of 1.5 ppm was established for TATP, a detection limit of 0.01 ppm was established for ammonium nitrate and a detection limit of 0.2 ppm was established for 2,6-DNT using our orthogonal gas sensor. A specially prepared catalyst with both non-stoichiometric and stoichiometric attributes to make detection in the orthogonal platform feasible was confirmed with XPS. Both the thermodynamic and conductometric responses were linear with respect to the concentration of target molecules in the vapor phase. Unique signatures for both the

thermodynamic and conductometric platforms were observed for each explosive, providing a built in redundancy in the signals could be used to further mitigate false positives and negatives could be mitigated.

REFERENCES

[1] K. G. Furton and L. J. Myers, "The scientific foundation and efficacy of the use of canines as chemical detectors for explosives," *Talanta,* vol. 54, pp. 487-500, 2011.

[2] S. Singh, "Sensors-An effective approach for the detection of explosives," *Journal of Harzardous Materials,* vol. 144, pp. 15-28, 2007.

[3] J. C. Oxley, J. L. Smith, K. Shinde and J. Moran, "Determination of the Vapor Density of Triacetone Triperoxide (TATP) Using A Gas Chromatography Headspace Technique," *Propellants, Explosives, Pyrotechnics,* vol. 30, pp. 127-130, 2005.

[4] P. A. Pella, "Measurement of the Vapor Pressure of TNT, 2,4-DNT, 2,6-DNT and EGDN," *Journal of Chemical Thermodynamics, 1977, 9(4), 301,* vol. 9, p. 301, 1977.

[5] B. C. Dioone, D. P. Roundbehler, E. K. Achter, J. R. Hobbs and D. H. Fine, "Vapor Pressure of Explosives," *Journal of Energetic Materials,* vol. 4, p. 447, 1986.

[6] M. W. Todd, R. A. Provencal, T. G. Owano, B. A. Paldus, A. Kachanov, K. L. Vodopyanov, M. Hunter, S. L. Coy, J. I. Steinfeld and J. T. Arnold, "Application of mid-infrared cavity-ringdown spectroscopy to trace explosives

vapor detection using a broadly tunable (6-8 μm) optical parametric oscillator," *Applied Physics B,* vol. 75, pp. 367-376, 2002.

[7] K. J. Albert and D. R. Walt, "High speed fluorescence detection of explosive like," *Analytical Chemistry,* vol. 72, p. 1947–1955, 2000.

[8] Z. Takats, I. Cotte-Rodriguez, N. Talaty, H. Chen and R. G. Cooks, "Direct, trace level detection of explosives on ambient surfaces by desorption electrospray ionization mass spectrometry," *Chemical Communications,* vol. 41, pp. 1950-1952, 2005.

[9] Y. Zhang, X. Ma, S. Zhang, C. Yang, O. Zheng and X. Zhang, "Direct detection of explosives on solid surfaces by low temperature plasma desorption mass spectrometry," *Analyst,* vol. 134, pp. 176-181, 2009.

[10] M. C. Kemp, "Explosive Detection by Terahertz Spectroscopy- A Bridge Too Far?," *Terahertz Science and Technology, IEEE,* vol. 1, pp. 282-292, 2011.

[11] M. R. Leahy-Hoppa, M. J. Fitch and R. Osiander, "Terahertz spectroscopy techniques for explosives detection," *Analytical and Bioanalytical Chemistry,* vol. 395, pp. 247-257, 2009.

[12] I. E. Hayward, T. E. Kirkbride, D. N. Batchelder and R. J. Lacey, "Use of a Fiber Optic Probe for the Detection and Identification of Explosive Materials by Raman Spectroscopy," *Journal of Forensic Sciences,* vol. 40, pp. 883-334,

1995.

[13] M. Gaft and L. Nagli, "UV gated Raman spectroscopy for standoff detection of explosives," *Optical Materials,* vol. 30, pp. 1739-1746, 2008.

[14] J. S. Caygill, F. Davis and S. P. Higson, "Current trends in explosive detection techniques," *Talanta,* vol. 88, pp. 14-29, 2012.

[15] W. K. Choi, S. K. Song, J. S. Cho, Y. S. Yoon, D. Choi, H. J. Jung and S. K. Koh, "H_2 gas-sensing characteristics of SnOx sensors fabricated by a reactive ion-assisted deposition with/without an activator layer," *Sensors and Actuators B,* vol. 40, pp. 21-27, 1997.

[16] N. Barsan, D. Koziej and U. Weimar, "Metal oxide-based gas sensor research: How to," *Sensors and Acutators B,* vol. 121, pp. 18-35, 2007.

[17] T. Seiyama, A. Kato, K. Fujishi and M. Nagatani, "A New detector for gaseous components using semiconductive thin films," *Analytical Chemistry,* vol. 34, pp. 1502-1503, 1962.

[18] J. Barkauskas, "Investigation of conductometric humidity sensors," *Talanta,* vol. 44, pp. 1107-1112, 1997.

[19] G. Korotcenkov and B. K. Cho, "Ozone measuring: what can limit application of SnO2-based conductometric gas sensor?," *Sensors and Actuators B,* vol. 161, pp. 28-44, 2012.

[20] S. S. Symanski and S. Bruckenstein, "Conductometric sensor for parts per billion sulfur dioxide determination," *Analytical Chemistry*, vol. 58, pp. 1771-1777, 1986.

[21] A. Dutta and S. Basu, "Modified metal-insulator-metal (M-I-M) hydrogen gas sensors based on zinc oxide," *Journal of Materials Science: Materials in Electronics*, vol. 6, pp. 415-418, 1995.

[22] P. Massok, M. Loesch and D. Bertrand, "Comparison for the between two Figaro sensors (TGS 813 and TGS 842) for the detection of methane, in terms of selectivity and long-term stability," *Sensors and Actuators B,* vol. 25, pp. 525-528, 1995.

[23] G. Korotcenkov and B. K. Cho, "Instability of metal oxide based conductometric gas sensors and approaches to stability improvement (short survey)," *Sensors and Actuators B,* vol. 156, pp. 527-538, 2011.

[24] A. C. Romain and J. Nicolas, "Long term stability of metal oxide-based gas sensors for E-nose environmental applications: an overview," *Sensors and Actuators B,* vol. 146, pp. 502-506, 2010.

[25] I. Sayago, J. Gutierrez, L. Ares, J. I. Robla, M. C. Horrilo, J. Getino, J. Rino and J. A. Agapito, "Long-term reliability of sensors for detection of nitrogen oxides," *Sensors and Actuators B,* vol. 26, pp. 56-58, 1995.

[26] M. Amani, Y. Chu, K. L. Waterman, C. M. Hurley, M. J. Platek and O. J. Gregory, "Detection of triacetone triperoxide (TATP) using a thermodynamic based gas sensor," *Sensors and Actuators B*, vol. 162, pp. 7-13, 2012.

CHAPTER 6

CONCLUSIONS AND FUTURE WORK

1. Conclusions

As mentioned in Chapter 1, a hypothesis was proposed that *the heat effect of catalytic decomposition of specific explosive molecules can be measured as a function of temperature and can thus be utilized for the identification of explosive species.* To support this hypothesis, four goals were identified as follows:

To fabricate and test a thermodynamic sensor and establish the response profile to using different catalysts as a function of temperature and determine the detection limit and sensing mechanism of sensors.

To determine the interference effect of explosive precursors, e.g. H_2O_2 and acetone which could lead to false positive during the detection TATP.

To optimize catalyst composite to enhance its selectivity and sensitivity.

To develop an orthogonal sensing platform and testing apparatus to minimize false positives.

A thermodynamic gas sensor based on the hypothesized theory was successfully fabricated and associated detection system was developed. Explosive compounds decompose when interacting with metal oxide catalyst which is maintained at constant temperature by a dynamic electric power. Heat effect of decomposition processes can then be determined through measurement of the change in electric power supplied to the sensor. Several metal oxide catalysts were employed in this research.

This thermodynamic sensing system exhibited a promising potential in explosive detection due to its superior sensitivity and response time to trace level TATP. Interference study toward its precursor, hydrogen peroxide and acetone, showed that the sensor had demonstrated the ability to reliably distinguish TATP from acetone, but not from hydrogen peroxide.

In order to improve selectivity and detection limit, palladium-tin oxide combinatorial libraries were fabricated using a co-sputtering technique to screen potential catalysts with optimum composition. Sensors with various palladium loadings exhibited very different responses with respect to selectivity and sensitivity. The addition of 12 wt.% palladium loading into SnO_2 catalysts yielded the maximum improvement to magnitude of the sensor response to both TATP and H_2O_2, while an 8 wt.% palladium loading exhibited the greatest selectivity between the two. This is because different doping level changes the mechanism of interaction between palladium and tin atoms and thus the oxidation state of tin oxide is altered to different states, verified by XPS.

An orthogonal detection system was also introduced to sense various explosives at lower level, and more importantly, to minimize the frequency of false positives. This orthogonal detection system is comprised of two independent sensing platforms, a thermodynamic based sensor and a conductometric based sensor, which take measurement from the same catalyst simultaneously and thus provides a redundancy in response for explosive identification. TATP, DNT and ammonium nitrate were reliably detected and the experiment results indicated a detection limit of ppb level.

2. Future works

The development of explosive technology has benefited the whole world in many ways, but also granted terrorist groups with more choices and opportunities. Different types of homemade explosives or IEDs employing new materials that can be transparent to current security measures are intended to be fabricated by terrorists. Therefore, there's always a challenge and a demand to improve current detection techniques. Regarding to future developments, our research will focus on several different directions, including study of effect of humidity interference, advanced gas delivery system and miniaturization of sensing platforms.

2.1 Study of humidity interference

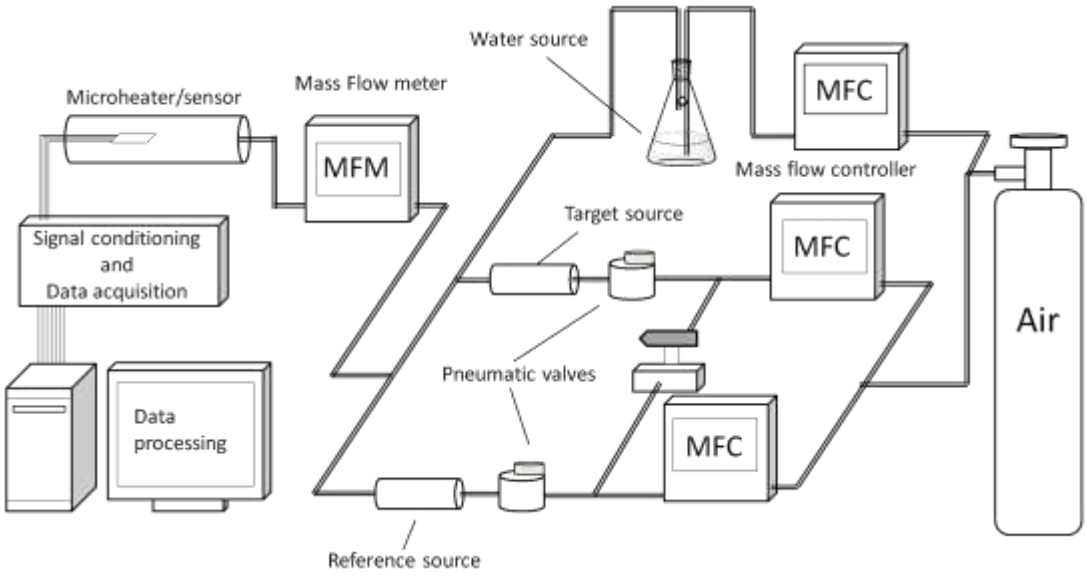

Figure 6.1 Schematic of gas sensing system for humidity study.

Researchers have shown that humidity plays an important role in sensing mechanisms of many gas detection techniques [1-3]. To guarantee an accurate and reliable detection, the effect of humidity toward sensor response needs to be studied. We are planning to incorporate our current orthogonal system with a humidity sensor,

which can record humid level along with explosive detection. By adjusting the flow rate accordingly, mixed gas at different humid levels can be achieved (*Figure 6.1*). The results will then be analyzed and the influence of humidity at different levels will be evaluated. The ultimate goal of this study is to establish a model to eliminate the humidity factor and guarantee reliability of our sensor.

2.2 Gas sampling and delivery system

Currently during bench scale experiments, a liquid gas cylinder is used to build up a stable pressure gradient along the pipeline to supply a steady stream of dry air in our experiments. However, since this research is aiming for universal deployment in public, or building a portable device, more advanced delivery system is needed. In addition, inline preconcentration of target gas can greatly help the sensor to achieve lower the detection limit and thus should be considered when designing new gas inlet system.

For most of the statically deployed gas sensing devices, i.e. carbon monoxide alarm and smoke detector, their detection relies on the diffusion of target substances in air. The advantage of this approach, obviously, is that no extra power is needed for gas delivery; however, the diffusion process varies upon many parameters including parameters of target molecules (molecular weight, diffusion coefficient and stability), concentration of target vapor, temperature, geometry of the monitored space, and any other mechanical turbulence. Therefore, the detection time can be very difficult to predict when monitoring is needed in a large open space, unless it can be intensively deployed to form a network, or installed at the only route that everyone passes, i.e. on to the security door at airport. Another way of deployment is to incorporate the sensor

with ventilation system, creating a passive alarm scheme. The device will react to any interested species in presence of anywhere of the entire area, but is not capable of accurate locating of the suspicious individual or subject. A combination of closely deployed sensor, which provides inline scanning, together with the passive sensor that works as an alternative insurance would be ideal for real-life application.

As for a handheld sensing device, diffusion-controlled and micro motor-controlled gas delivery system can both be considered. An external probe can be used in diffusion-controlled device to accelerate the detection rate. Temperature range over which the sensor scans should be carefully evaluated for security causes.

Engineering processes often use a reflux system for preconcentration, which unfortunately is not applicable in our case due to size and cost considerations. Most of the existing researches on preconcentration processes require independent sampling step and are not capable of real-time detection [4]. Two possible approaches that can be used for continuous detection are online sorbent trap system and membrane extraction system. The first one utilizes a specially prepared material (i.e. thin film with micro-channels [5]) that captures only target molecules. By periodically heating the sorbent trap, the captured molecules will all be released at once forming a highly concentrated vapor phase. Cryogenic trap is a very similar technique to sorbent trap only in that it employs low temperature to capture target molecules, making this approach unfeasible with high humidity environments [6]. The membrane extraction technique has been widely researched for gas separation [7, 8]. This technique is particularly attractive for continuous monitoring applications due to its improved selectivity and the enrichment power of the membranes, minimized solvent use, and

the automation potential. The sample can continuously flow through or over the membrane, and the analytes can selectively permeate through the membrane while the bulk matrix of air and other interference are eliminated.

2.3 Development of alternative platforms

A microelectromechanical system (MEMS) that consists of all the elements of an orthogonal sensor was developed. A prototype had been built with dimension of 2.8 mm * 1.8 mm *0.7 mm, which was 43 times smaller in volume than orthogonal sensor (shown in *Figure 6.2*). The MEMS platform also exhibited superior energy conservation capability and heat reservation capability. However, limited by its size, the MEMS platform had not reach the requirement of actual testing. Improvements on designing or alternative connecting parts are needed to continue this work.

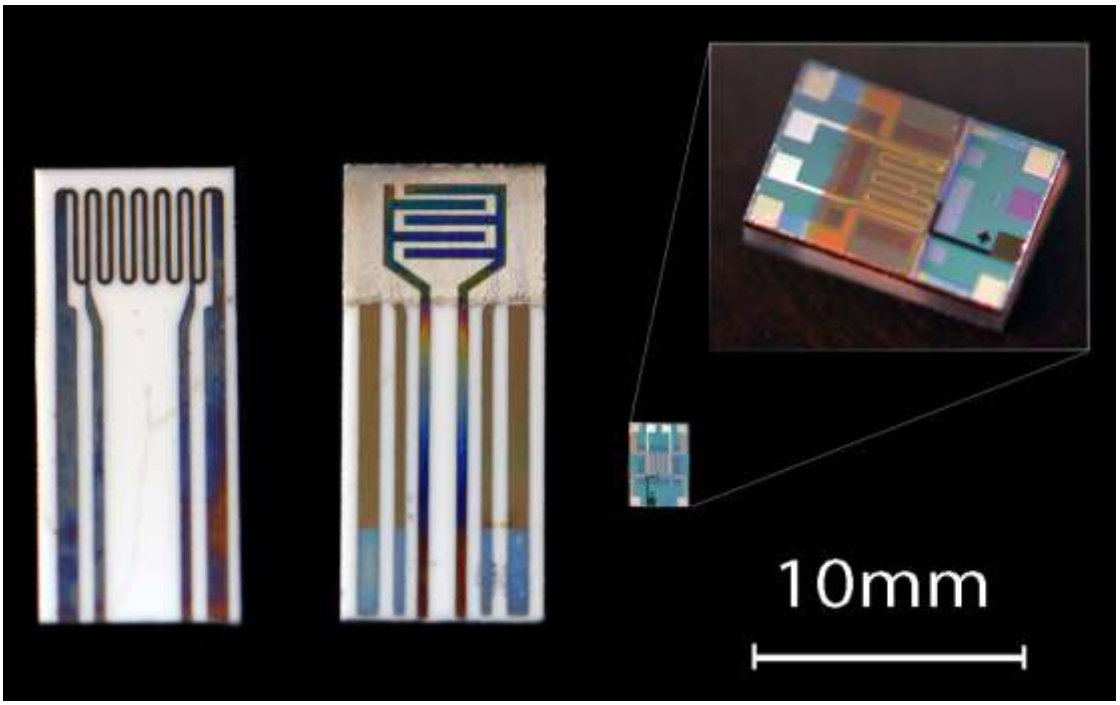

Figure 6.2 Actual picture of a thermodynamic sensor (left), an orthogonal sensor (center) and an MEMS device (right).

2.3.1 Introduction of MEMS

Microelectromechanical systems, also known as MEMS, are microscopic devices such as actuators, transducers etc. that combine electronics with mechanical operations using integrated processing technology [9]. These sub-micron to millimeter scale devices have application in micro sensor elements, micro actuator elements and micro energy systems [10]. Unlike many conventional sensors, MEMS based sensors yield many advantages which make it an ideal platform for repeatability and mass production. Due to the relatively small scale, integrated circuit fabrication techniques allow hundreds or thousands of identical devices to be built simultaneously on a single silicon wafer. Compared to building up a device from individual components, the simplicity of fabrication greatly reduces the cost and improves the reliability. Meanwhile, MEMS can be packaged into arrays and integrated with electronics that require much less power, which often find applications where weight, power and space are critical.

For sensor application, one of the most important advantages of MEMS is that they improve sensitivity and reduce the response time. With each component placed close together, the deployment for connecting lines and routes can be avoided. As a result, electrical signals will receive much less interferences from junctions between elements and connecting lines and thus can be more sensitive. With smaller scale, much less heat consumption is required for MEMS devices, which would greatly benefit sensors that measures heat activities. Silicon which usually is employed as the body material of MEMS device, has relatively smaller heat capacity (19.79 J/mol·K) but higher thermal conductivity (149 W/m·K), and thus can reach designated

temperature in a shorter period of time, compared with other materials, i.e. aluminum oxide. As a result, faster response time can be expected.

In this work, the orthogonal sensor introduced in Chapter 5 was re-designed and implemented on a MEMS platform. The designing principle and fabrication processes are discussed blow.

2.3.2 Principle of etchant selection and fabrication process

The main purpose of transferring the sensor platform to MEMS based platform was to produce a smaller footprint and less heat consumption. In addition to the thermodynamic sensor and conductometric sensor, a K-type thermocouple was incorporated into the MEMS system to monitor temperature activity. A schematic of the MEMS sensor is shown in *Figure 6.3*. The fabricated dimension of MEMS platform was 2.8mm * 1.8mm * 0.7mm. One of the most important processes involved in the fabrication was etching processes, which in this study was used to create a suspended plane (1 mm * 1 mm * 5 μm) which was supported by tiny bridges (0.1 mm * 0.1 mm * 5 μm) to reduce heat sink.

Etching in micromachining is a process in which layers are chemically removed from wafer during manufacturing. Etching pattern can be controlled by masking layers applied through photolithography process. Isotropic etching refers to process in which etchant erode the substrate material equally in all direction, while anisotropic etching is controlled in limited directions to certain materials, which could avoid formation of cavities under masking layer. Anisotropic etching is thus favored in every step of this study. For this purpose, (100) oriented silicon wafer was selected as the substrate

material for this MEMS platform. Three types of etchant were employed for different etching purposes (etching of Si and etching of SiO_2).

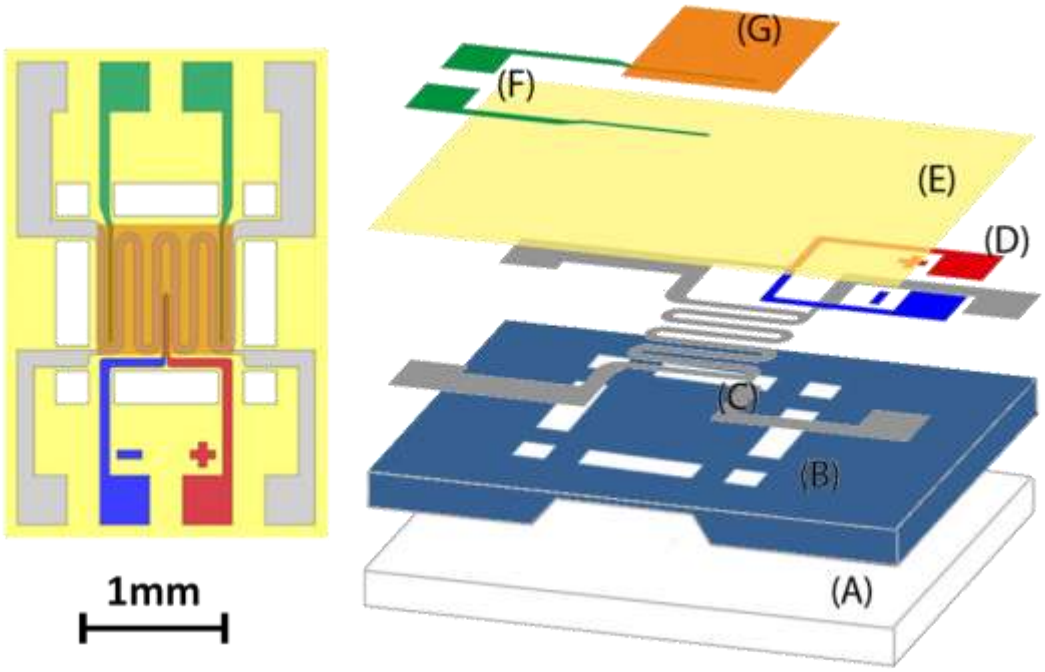

Figure 6.3 Schematics showing top view (left) and expanded view (right) of orthogonal sensor on a MEMS platform. Elements including (A) pyrex substrate, (B) silicon wafer, (C) nickel microheater, (D) type K thermocouple, (E) silicon oxide layer, (F) platinum electrodes and (G) metal oxide catalysts.

A potassium hydroxide (KOH) solution and a tetramethylammonium hydroxide (TMAH, $(CH_3)_4NOH$) solution were employed respectively as two types of Si etching processes. Related reaction equations are shown as follows.

$$2OH^- + H_2O + Si \Rightarrow SiO_3^{2-} + 2H_2 \uparrow$$

$$2OH^- + SiO_2 \Rightarrow SiO_3^{2-} + H_2O$$

To (100) oriented silicon, KOH and TMAH were both reported to have much higher etching rate of (100) plane and (110) plane than (111) plane, and slow etching rate to SiO_2 [11-14]. Etching rate was determined by temperature and concentration of etchant solvent [13, 14]. Etching a (100) silicon surface through a rectangular hole

would create a cave with flat (100) oriented bottom and flat (111) oriented sidewall (demonstrated in *Figure 6.4*). The angle of sidewall to bottom is calculated to be 54.7 °. The undercut (δ) can be calculated through etching periode (T) and etching rate of (111) plane (R_{111}), which can be expressed as $\delta = \int \sqrt{6} \cdot dT \cdot dR_{111}$. Since R_{111} decrease as concentration of etchant decrease, δ can be calculated through etch depth (D) instead, which can be expressed as $\delta = \frac{\sqrt{6} \cdot D}{R_{100}/R_{111}}$, where R_{100}/R_{111} is a constant.

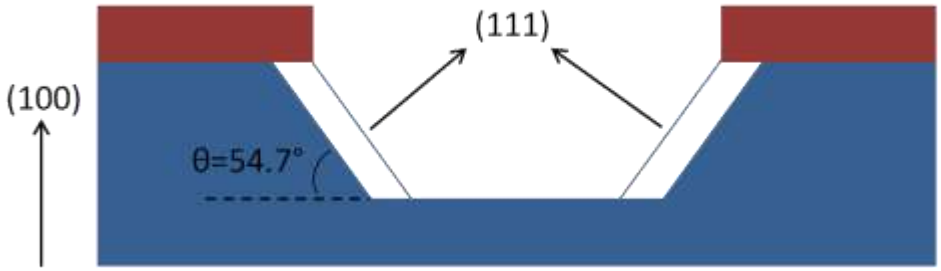

Figure 6.4 Schematic of cross section of (100) oriented silicon wafer being etched by KOH.

Literature reported that TMAH has two to three times higher (111)/(100) etch ratio than that of KOH [14]. Also, etch rate of SiO_2 is an order of magnitude lower in TMAH than in KOH. As a result, KOH was used for bulk silicon removal and TMAH was used for areas requiring precise control.

A buffered oxide etchant (BOE) prepared with hydrofluoric acid (HF) and ammonium fluoride (NH_4F) was used for SiO_2 etching. Since formation of extra hydrogen ions is impeded by NH_4F, this BOE solution has very limited etch rate toward silicon. Reaction equation is as follows.

$$4H^+ + 4F^- + SiO_2 \Rightarrow SiF_4 + 2H_2O$$

A 1.5 μm SiO_2 film was thermally grown on both sides of the (100) oriented silicon wafer through a heat treatment process at 1000 ℃ for 48 hours. Part of the SiO_2

and Si was then removed via a BOE etching and a KOH etching, as demonstrated in *Figure 6.5(1)*. The remaining thickness of Si was estimated to be less than 10 μm. A pyrex wafer was then anodically bonded to the Si wafer as the substrate material, forming a cavity in between the two wafers. Nickel microheaters and type K thermocouple was then deposited onto this reinforced wafer, followed by a SiO_2 insulation layer on top as shown in *Figure 6.5(2)*. Ultra-thin (<100Å) tantalum film were applied between each layer to improve adhesion. Platinum electrodes and catalyst layer were then sputtered over the SiO_2 insulation layer. Deposition parameters were provided in *Table 3.1* and *Table 4.1*. Excess SiO_2 and Si material were removed using BOE and TMAH solutions, leaving only critical bridge as support of electrical components. The areas marked in white color in *Figure 6.3(1)* are the regions removed during second etching. The cross sections of these processes are shown in *Figure 6.5(3)* and *(4)*.

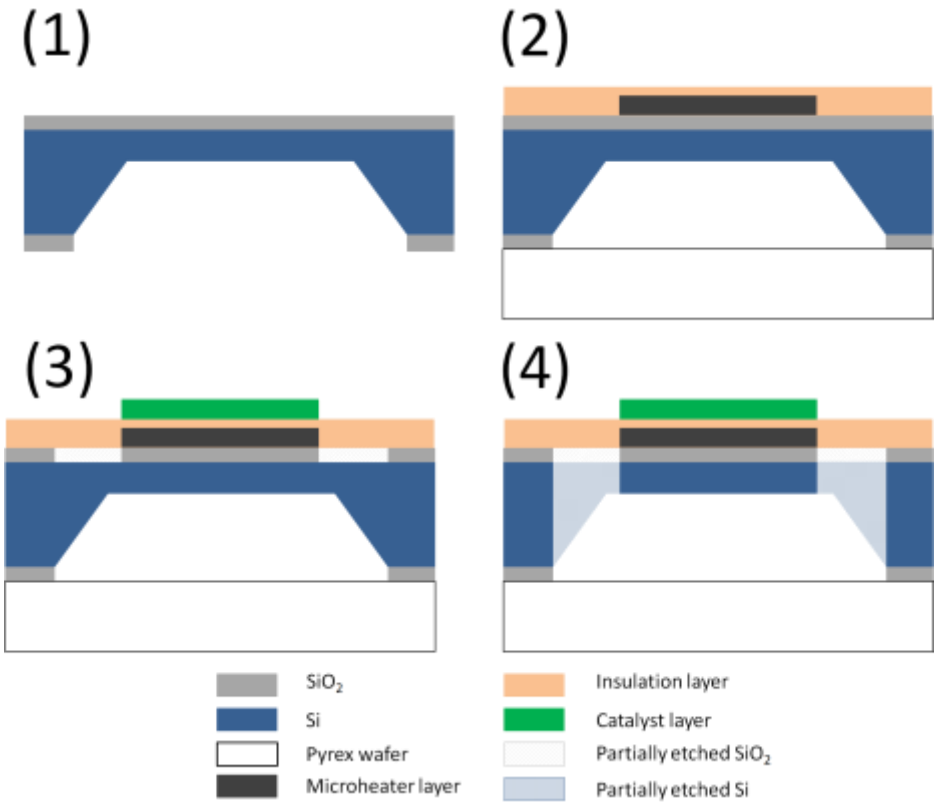

Figure 6.5 Schematic of cross section of MEMS wafer demonstrating the fabrication process from (1) to (4).

2.3.3 Evaluation of energy consumption and temperature distribution

Energy required to heat single sensor on an original orthogonal platform and on a MEMES platform from 25℃ to 450℃ is calculated to be 81.96 J and 1.334 J, respectively, according to their specific heat capacity [6] and geometric dimensions. Detailed calculations were presented in Appendix A. Apparently Energy consumption of MEMS platforms is an order of magnitude lower than that of original platform.

Thermal image of two sensor platform works at 450℃ were shown in *Figure 6.6* and *Figure 6.7.* Simplification and assumptions were used during calculation, which were presented in Appendix B.

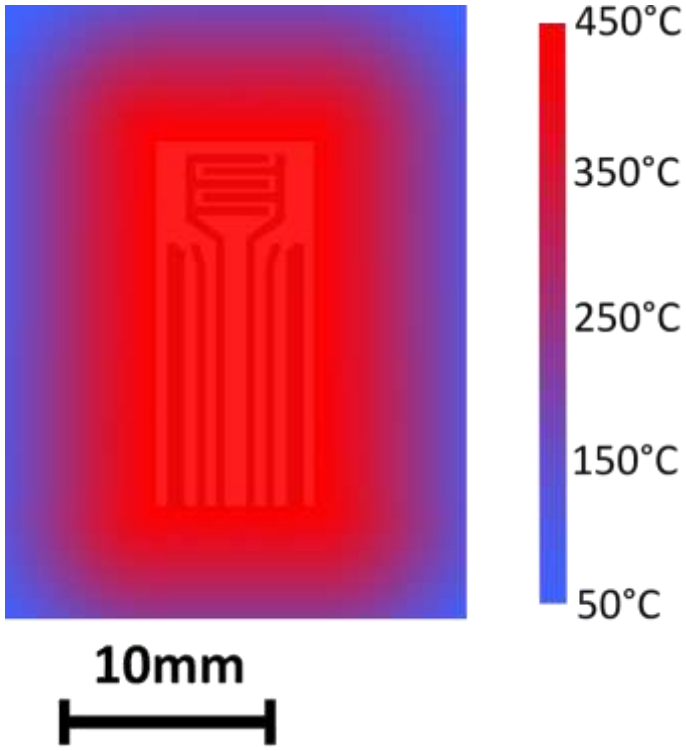

Figure 6.6 Schematic of temperature distribution of a solid state sensor maintained at 450 ℃ in air.

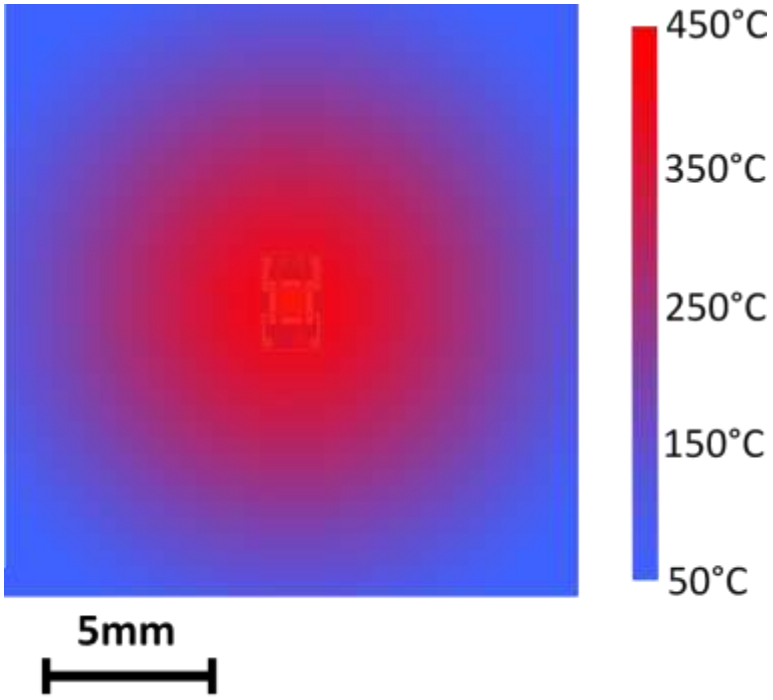

Figure 6.7 Schematic of temperature distribution of a MEMS sensor maintained at 450 ℃ in air.

According to results, temperature of sensor on solid state platform was cooled from 450 ℃ to 449.75 ℃ within 1 mm, while with special design, temperature of MEMS based sensor was able to cool from 450 ℃ to 448.763 ℃ within 0.1 mm. Considering the thermal conductivity of Si is twice as that of Al_2O_3, the designing was a success to reduce heat transfer. The MEMS platform was planned to be connected directly to a printed circuit board (PCB). However, the temperature at the edge of MEMS platform was still far beyond the limit of PCB (140 ℃). Alternative methods were still under investigation.

REFERENCES

[1] M. Makinen, M. Silanpaa, A. K. Viitanen, A. Knap, J. M. Makela and J. Puton, "The effect of humidity on sensitivity of amine detection in ion mobility spectrometry," *Talanta,* vol. 84, pp. 116-121, 2011.

[2] H. E. Endress, R. Hartinger, M. Schwaiger, G. Gmelch and M. Roth, "A capacitive CO2 sensor system with suppression of the humidity interference," *Sensors and Actuators B,* vol. 57, pp. 83-87, 1999.

[3] A. Marsal, A. Cornet and J. R. Morante, "Study of the CO and humidity interference in La doped tin oxide CO2 gas sensor," *Sensors and Actuators B,* vol. 94, pp. 324-329, 2003.

[4] M. R. Ras, F. Borrull and R. M. Marce, "Sampling and preconcentration techniques for determination of volatile organic compounds in air samples," *TrAC Trends in Analytical Chemistry,* vol. 28, pp. 347-361, 2009.

[5] R. R. Lima, R. A. Carvalho, A. P. Nascimento Fiho, M. L. Silva and N. R. Demarquette, "Production and deposition of adsorbent films by plasma polymerization on low cost micromachined non-planar microchannels for preconcentration of organic compound in air," *Sensors and Actuators B,* vol. 108, pp. 435-444, 2005.

[6] C. Thammakhet, P. Thavarungkul, R. Brukh, S. Mitra and P. Kanatharana, "Microtrap modulated flame ionization detector for on-line monitoring of

methane," *Journal of Chromatography A,* vol. 2005, pp. 243-248, 1072.

[7] H. Cong, M. Radosz, B. F. Towler and Y. Shen, "Polymer–inorganic nanocomposite membranes for gas separation," *Separation and Purification Technology,* vol. 55, pp. 281-291, 2007.

[8] M. A. Aroon, A. F. Ismail, T. Matsuura and M. M. Montazer-Rahmati, "Performance studies of mixed matrix membranes for gas separation: A review," *Separation and Purification Technology,* vol. 75, pp. 229-242, 2010.

[9] M. Goel, "Recent developments in electroceramics: MEMS application for energy and environment," *Ceramics International,* vol.30, pp. 1147-1154, 2004.

[10] T.A. Ameel, R.O. Warrington, R.S. Wegeng and M.K. Drost, "Miniaturization technologies applied to energy systems," *Energy Conversion and Management,* vol. 38, pp. 969-982, 1997.

[11] I. Zubel, I. Barycka, K. Kotowska and M. Kramkowska, "Silicon anisotropic etching in alkaline solutions IV: The effect of organic and inorganic agents on silicon anisotropic etching process," *Sensors and Actuators A,* vol. 87, pp. 163-171, 2001.

[12] R. Holly and K. Hingerl, "Fbrication of silicon vertical taper structures using KOH anisotropic etching," *Microelectronic Engineering,* vol. 83, pp. 1430-1433, 2006.

[13] K. Sato, M. Shikida, Y. Matsushima, T. Yamashiro, K. Asaumi, Y. Iriye and M. Yamamoto, "Characterization of orientation-dependent etching properties of single-crystal silicon: effects of KOH concentration," *Sensors and Actuators A*, vol. 64, pp. 87-93, 1998.

[14] Y. Fan, P. Han, P. Liang, Y. Xing, Z. Ye and S. Hu, "Differences in etching characteristics of TMAH and KOH on preparing inverted pyramids for silicon solar cells," *Applied Surface Science*, vol. 264, pp. 761-766, 2013.

Appendix A

Calculations of energy consumption

1. Solid state orthogonal platform.

In this calculation, solid state platform was simplified to a uniform aluminum oxide plate. Thin film layers deposited on top were ignored. Related material properties were provided by Engineeringtoolbox.com.

Dimension: 16.8 mm * 7.5 mm * 0.5 mm.

Amounts of chemical substance (*n*):

$$n = \rho \cdot V/M,$$

Where ρ is density of alumina (3.9 g/cm^3); V is volume of alumina (0.063 cm^3); M is molar mass of alumina (102 g/mol).

Energy (Q) required to heat sensor to certain temperature can then be calculated:

$$Q = C_p \cdot (T_1 - T_0) \cdot n$$

Where C_p is the specific heat capacity of alumina (79.04 J/mol·K), T_1 is the target temperature (450 ℃), T_2 is the starting temperature (25 ℃). Q was calculated to be 81.96 J.

2. MEMS platform

In this calculation, MEMS platform was simplified to two parts: a uniform silicon wafer treated via etching process and a pyrex wafer.

Dimension of Si wafer can be expressed as original size of wafer before etching subtracted by the removed parts: 2.8mm * 1.8 mm * 0.2 mm – 1.6 mm * 1.6 mm * 0.2 mm.

Dimension of pyrex wafer: 2.8 mm * 1.8 mm * 0.5mm.

Same equations were used to calculate Q of silicon.

$$n = \rho \cdot V/M,\ Q = C_p \cdot (T_1 - T_0) \cdot n$$

Where for Si, ρ = 2.329 g/cm^3; V = 0.493*10^{-3} cm^3; M = 28 g/mol; C_p = 19.79 J/mol·K.

For Q of pyrex glass, an alternative equation was used:

$$m = \rho \cdot V,\ Q = C_p' \cdot (T_1 - T_0) \cdot m$$

Where m is mass of pyrex wafer, ρ = 2.23 g/cm^3; V = 1.24*10^{-3} cm^3; C_p' = 0.84 J/g·K.

Q of Si was calculated to be 0.347 J and Q of pyrex was 0.987 J.

Total Q of MEMS = 1.334 J.

Appendix B

Calculations of thermal graphs

1. Solid state orthogonal platform.

In this calculation, solid state platform was simplified to a uniform isotropic thermal media. Heat loss at junction and that due to convection and radiation were ignored. Related material properties were provided by Engineeringtoolbox.com. Dimensions of analyzed area were provided in *Figure B1*.

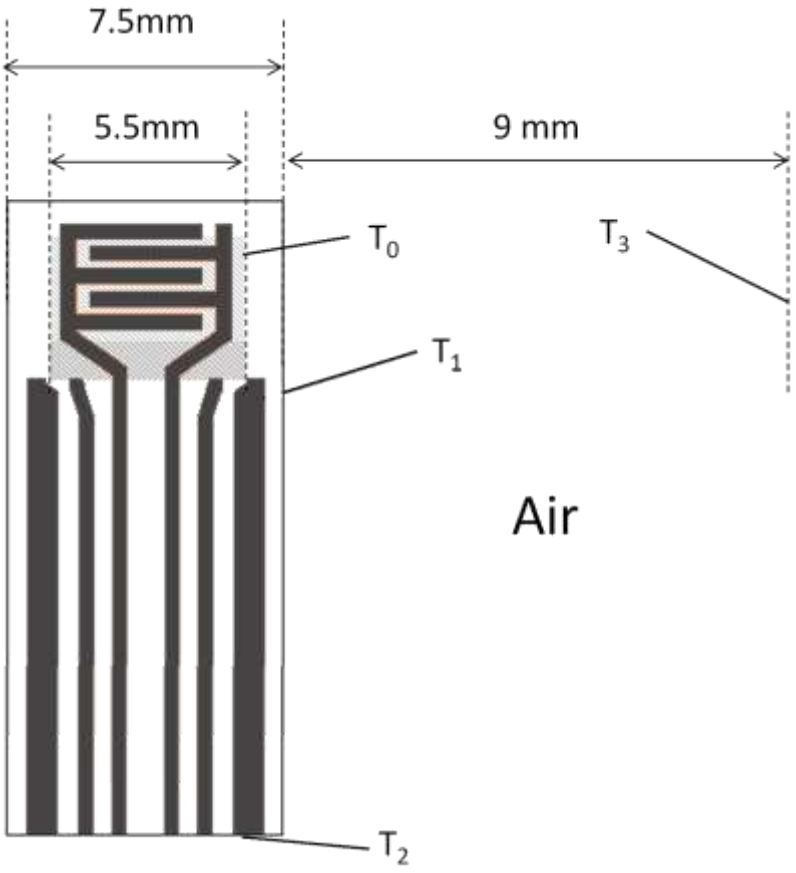

Figure B 1 Schematic showing dimensions and properties of solid state sensor for calculation purpose.

Region marked with diagonals is heating region in which temperature was kept 450 ° (T_0). Temperature indicated 50 ℃ 9mm apart from edge of sensor (T_3).

Temperature on the right edge (T_1) and bottom edge (T_2) of sensor were unknown. Since distance from heating region to top, left and right edge all equal to 1mm, it was obvious that temperature on these three edges share the same T_1. Fourier's law was applied and following equations was obtained.

$$\kappa_1 \cdot \frac{(T_0 - T_1)}{1\ mm} = \kappa_2 \cdot \frac{(T_1 - T_3)}{9\ mm}$$

In which κ_1 and κ_2 are the thermal conductivity of aluminum oxide (30 W/m·K) and air (which was simplified to a constant of 0.04 W/ m·K and does not change along temperature). T_1 was calculated to be 449.97 ℃. T_2, which was calculated in the same way, equals to 449.75 ℃.

A temperature profile as a function of distance (x) from heating region toward right direction can be obtained as follows.

$$\mathrm{T}(x) = \begin{cases} 450 - 0.03 \cdot x & (0 < x < 1\ mm) \\ 494.17 - 44.42x & (1\ mm < x < 10\ mm) \end{cases} \quad ℃$$

2. MEMS platform

In this calculation, MEMS platform was simplified to two parts: silicon wafer as an isotropic thermal media with special geometry and pyrex glass as a uniform media. Heat loss at junction and that due to convection and radiation were ignored. Related properties were provided by Engineeringtoolbox.com. Dimensions of analyzed area were provided in *Figure B2(a)*and *(b)*.

Boundary temperature (T_0) at heating region is 450 ℃. There were 8 bridges with dimension of 0.05 mm * 0.1 mm * 10 μm connecting heating region and body of MEMS. Same estimation of 50 ℃ was used for air temperature (T_3) 9mm apart from

sensor. Temperatures at the other end of bridge (T_1) and on the edge of sensor (T_2) were unknown. Thickness of pyrex wafer was 0.5 mm.

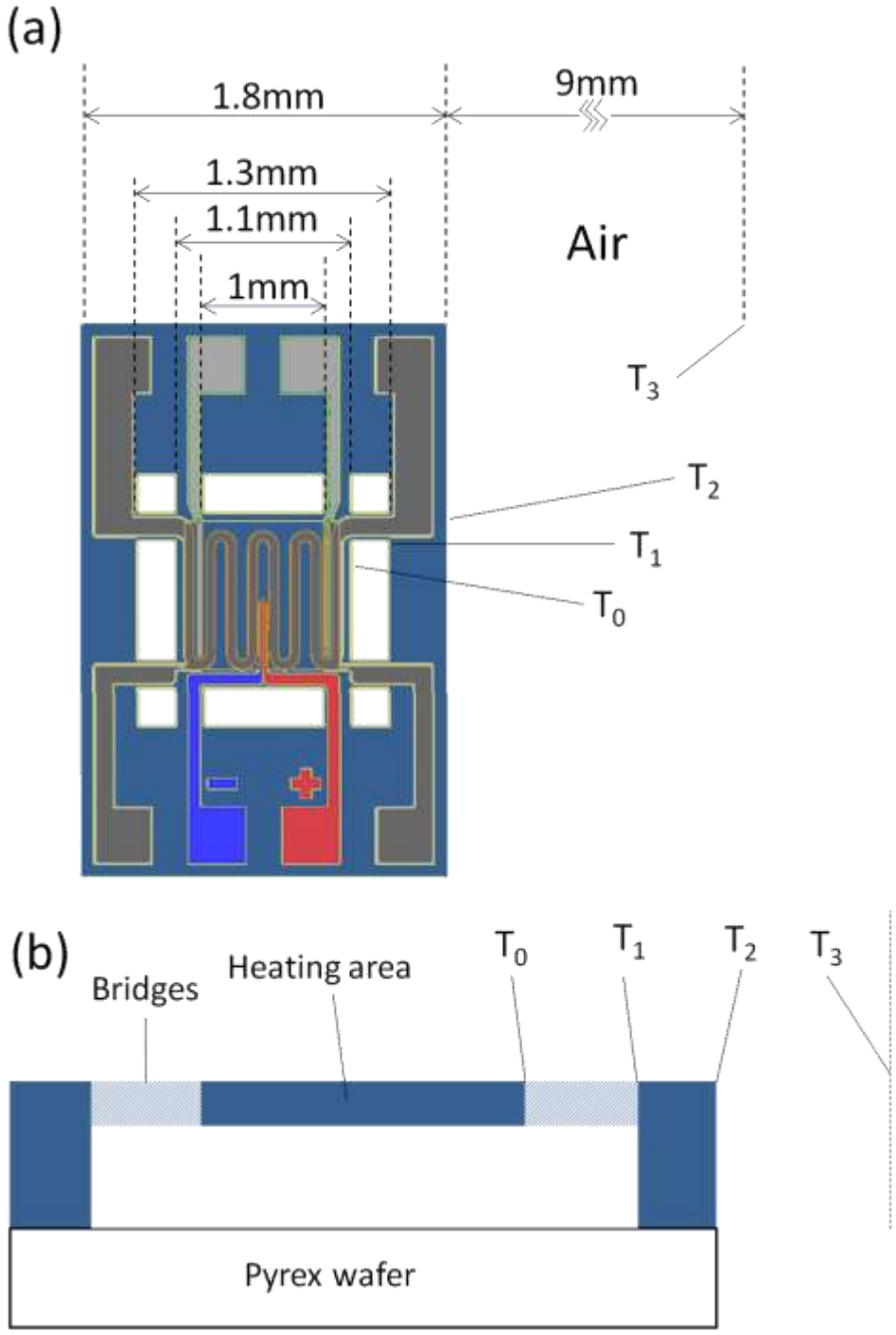

Figure B 2 Schematic of (a) top view and (b) cross section of MEMS sensor demonstrating dimension and properties for calculation purpose.

Fourier's law was used to obtain temperature profile.

$$\kappa_1 \cdot \frac{(T_0 - T_1)}{0.1\ mm} \cdot 0.05\ mm \times 10\ \mu m \times 8 = \kappa_1 \cdot \frac{(T_1 - T_2)}{0.25\ mm} \cdot 1.3\ mm \times 200\ \mu m \times 4$$

$$\kappa_1 \cdot \frac{(T_1 - T_2)}{0.25\ mm} + \kappa_2 \cdot \frac{(T_1 - T_2)}{0.25\ mm} = \kappa_3 \cdot \frac{(T_2 - T_3)}{9\ mm}$$

In which κ_1, κ_2 and κ_3 are the thermal conductivity of silicon (149 W/m·K), pyrex glass (1.005 W/m·K) and air (which was simplified to a constant of 0.04 W/ m·K and does not change along temperature). T_1 was calculated to be 448.763 ℃ and T_2 was 448.76 ℃.

A temperature profile as a function of distance (x) from heating region toward right direction can be obtained as follows.

$$\mathrm{T}(x) = \begin{cases} 450 - 12.37 \cdot x & (0 < x < 0.1\ mm) \\ 448.775 - 0.012 \cdot x & (0.1\ mm < x < 0.35 mm) \\ 464.267 - 44.31 \cdot x & (0.35\ mm < x < 9.35\ mm) \end{cases} \quad ℃$$

BIBLIOGRAPHY

Afzal A., Iqbal N., Mujahid A. and Schirhagl R., "Advanced vapor recognition materials for selective and fast responsive surface acoustic wave sensors: A review," Analytica Chimica Acta, vol. 787, pp. 36-49, 2013.

Agrawal J. P. and Hodgson R. D., Organic Chemistry of Explosives, Chichester, UK: John Wiley & Sons, Ltd, 2007.

Albert K. J., Lewis N. S., Schauer C. L., Sotzing G. A., Stitzel S. E., Vaid T. P. and Walt D. R., "Cross reactive chemical sensor arrays," Chemical Reviews, vol. 100, pp. 2595-2626, 2000.

Albert K. J. and Walt D. R., "High speed fluorescence detection of explosive like," Analytical Chemistry, vol. 72, p. 1947–1955, 2000.

Amani M., Gregory O.J., “Grain growth and morphology of In_2O_3:Pd nanocomposite films”, Thin Solid Films, 542(2013)180-185

Amani M., Chu Y., Waterman K.L., Hurley C.M., Platek J.M., Gregory O.J., “Detection of Triacetone Triperoxide (TATP) using a thermodynamic based gas sensor”, Sensors and Actuators B, 162(2012)7-13

Ameel T.A., Warrington R.O., Wegeng R.S. and Drost M.K., "Miniaturization technologies applied to energy systems," *Energy Conversion and Management*, vol. 38, pp. 969-982, 1997

Aroon M. A., Ismail A. F., Matsuura T. and Montazer-Rahmati M. M.,

"Performance studies of mixed matrix membranes for gas separation: A review," Separation and Purification Technology, vol. 75, pp. 229-242, 2010.

Arshak K., Moore E., Lyons G. M., Harris J. and Clifford S., "A review of gas sensors employed in electronic nose applications," Sensor Review, vol. 24, pp. 181-198, 2004.

Asbury G. R., Klasmeier J. and Hill H. H., "Analysis of explosives using electrospray ionization/ion mobility spectrometry (ESI/IMS)," Talanta, vol. 50, pp. 1291-1298, 2000.

Banas A., Banas K., Bahou M., Moser H. O., Wen L., Yang P., Li Z. J., Li Z.J., Cholewa M., Lim S.K., Lim Ch.H., Cholewa M., Lim S. K. and Lim C. H., "Post-blast detection of traces of explosives by means of Fourier transform infrared spectroscopy," Vibrational Spectroscopy, vol. 51, pp. 168-176, 2009.

Barkauskas J., "Investigation of conductometric humidity sensors," Talanta, vol. 44, pp. 1107-1112, 1997.

Barsan N., Koziej D. and Weimar U., "Metal oxide-based gas sensor research: How to," Sensors and Acutators B, vol. 121, pp. 18-35, 2007.

Benson S., Lennard C., Maynard P. and Roux C., "Forensic applications of isotope ratio mass spectrometry—A review," Forensic Science International, vol. 157, pp. 1-22, 2006.

Berntsen T. G., "Global training centre of mine detection dogs in Bosnia: Breeding and training program," Journal of Veterinary Behavior: Clinical Applications and Research, vol. 4, p. 245–246, 2009.

Blue R., Vobeck Z., Skabara P. J. and Uttamchandani D., "The development of sensors for volatile nitro-containing compounds as models for explosives detection," Sensors and Actuators B: Chemical, vol. 176, pp. 534-542, 2013.

Brudzewski K., Osowski S. and Pawlowski W., "Metal oxide sensor arrays for detection of explosives at sub-parts-per million concentration levels by the differential electronic nose," Sensors and Actuators B, vol. 161, pp. 528-533, 2012.

Bunyan P., Baker C. and Rurner N., "Application of heat conduction calorimetry to high explosives," Thermochimica Acta, vol. 401, pp. 9-16, 2003.

Burger A. and Wehrstedt K. D., "Azodicarboxylates: Explosive properties and DSC measurements," Journal of Loss Prevention in the Process Industries, vol. 23, p. 734–739, 2010.

Burns D. T. and Lewis R. J., "Analysis and characterisation of nitroglycerine based explosives by proton magnetic resonance spectrometry," Analytica Chimica Acta, vol. 300, pp. 221-225, 1995.

Buttigieg G. A., Knight A. K., Denson S., Pommier C. and Denton M. B., "Characterization of the explosive triacetone triperoxide and detection by

ion mobility spectrometry," Forensic Science International, vol. 135, pp. 53-59, 2003.

Buxton T. L. and Harrington P. B., "Rapid multivariate curve resolution applied to identification of explosives by ion mobility spectrometry," Analytica Chimica Acta, vol. 434, pp. 269-282, 2001.

Cagan D. A., Munoz R. A., Tangkuaram T. and Wang J., "Highly sensitive electrochemical detection of trace liquid peroxide explosives at a Prussian-blue 'artificial-peroxidase' modified electrode," Analyst, vol. 131, pp. 1279-1281, 2006.

Capua E., Cao R., Sukenik C. N. and Naaman R., "Detection of triacetone triperoxide (TATP) with an array of sensors based on non-specific interactions," Sensors and Actuators B, vol. 140, p. 122–127, 2009.

Caron T., Cuillemot M., Montmeat P., Veignal F., Perraut F., Prene P. and Serein-Spirau F., "Ultra trace detection of explosives in air: Development of a portable fluorescent detector," Talanta, vol. 81, p. 543–548, 2010.

Carreto-Vazquez V. H., Wojcik A. K., Liu Y., Bukur D. B. and Mannan M. S., "Miniaturized calorimeter for thermal screening of energetic materials," Microelectronics Journal, vol. 41, pp. 874-881, 2010.

Carter J. C., Angel S. M., Lawrence-Snyder M., Scaffidi J., Whipple R. E. and Reynolds J. G., "Standoff Detection of High Explosive Materials at 50 Meters in Ambient Light Conditions Using a Small Raman Instrument,"

Applied Spectroscopy, vol. 59, pp. 120-138, 2005.

Casey V., Cleary J., D'Arcy G. and McMonagle J. B., "Calorimetric combustible gas sensor based on a planar thermopile array: fabrication, characterisation, and gas response," Sensors and Actuators B, vol. 96, p. 114–123, 2003.

Caygill J. S., Davis F. and Higson S. P., "Current trends in explosive detection techniques," Talanta, vol. 88, pp. 14-29, 2012.

Cerioni L. M. and Pusiol D. J., "A new method to obtain frequency offsets in NQR multi-pulse sequences," Hyperfine Interactions, vol. 159, pp. 389-393, 2005.

Charles P. T. and Kusterbeck A. W., "Trace level detection of hexahydro-1,3,5-trinitro-1,3,5-triazine (RDX) by microimmunosensor," Biosensors and Bioelectronics, vol. 14, p. 387–396, 1999.

Charlesworth J. M., Partridge A. C. and Garrard N., "Mechanistic studies on the interactions between poly (pyrrole) and organic vapors," Journal of Physical Chemistry, vol. 97, pp. 5418-5423, 1993.

Chen Y., Liu H., Fitch M. J., Osiander R., Spicer J. B., Shur M. and Zhang X. C., "THz diffuse reflectance spectra of selected explosives and related compounds," Proceedings of SPIE, vol. 5790, pp. 19-24, 2005.

Chen W., Wang Y., Bruckner C., Li C. and Lei Y., "Poly[meso-tetrakis(2-thienyl)porphyrin] for the sensitive electrochemical detection of

explosives," Sensors and Actuators B, vol. 147, p. 191–197, 2010.

Cho J., Anandakathir A., Kumar A., Kumar J. and Kurup P. U., "Sensitive and fast recognition of explosives using fluorescent polymer sensors and pattern recognition analysis," Sensors and Actuators B, vol. 160, p. 1237–1243, 2011.

Choi J., Hwang I., Kim S., Park J., Park S., Jeong U., Kang Y. and Lee J., "Design of selective gas sensor using electrospun Pd doped SnO_2 hollow nanofibers," Sensors and Actuators B, vol. 150, pp. 191-199, 2010.

Choi W. K., Song S. K., Cho J. S., Yoon Y. S., Choi D., Jung H. J. and Koh S. K., "H_2 gas-sensing characteristics of SnO_x sensors fabricated by a reactive ion-assisted deposition with/without an activator layer," Sensors and Actuators B, vol. 40, pp. 21-27, 1997.

Cong H., Radosz M., Towler B. F. and Shen Y., "Polymer–inorganic nanocomposite membranes for gas separation," Separation and Purification Technology, vol. 55, pp. 281-291, 2007.

Chu F. and Yang J., "Study of nitro aromatic explosives sensor based on fluorescence quenching," Optik - International Journal for Light and Electron Optics, vol. 122, pp. 2246-2248, 2011.

Collin O. L., Zimmermann C. M. and Jackson G. P., "Fast gas chromatography negative chemical ionization tandem mass spectrometry of explosive compounds using dynamic collision-induced dissociation," Mass

Spectrometry, vol. 279, pp. 93-99, 2009.

Cotte-Rodriguez I., Chen H. and Cooks R. G., "Rapid trace detection of triacetone triperoxide (TATP) of complexation detections of desorption electrospray ionization," Chemical Communications, vol. 5, pp. 953-955, 2006.

Cook D. J., Decker B. K., Maislin G. and Allen M. G., "Through container THz sensing: applications for explosives screening," Proceedings of SPIE, vol. 5354, pp. 55-62, 2004.

Datskos P. G., Lavrik N. V. and Sepaniak M. J., "Detection of explosive compounds with the use of microcantilevers with nanoporous coatings," Sensor Letters, vol. 1, pp. 25-32, 2003.

Demchenko A. P., Introduction to Fluorescence Sensing, Netherland: Springer Netherlands, 2009.

Diesel G., Brodbelt D. and Pfeiffer D. U., "Reliability of assessment of dogs' behavioural responses by staff working at a welfare charity in the UK," Applied Animal Behaviour Science, vol. 115, p. 171–181, 2008.

Dioone B. C., Roundbehler D. P., Achter E. K., Hobbs J. R. and Fine D. H., "Vapor Pressure of Explosives," Journal of Energetic Materials, vol. 4, p. 447, 1986.

Dubnikova F., Kosloff R., Zeiri Y. and Karpas Z., "Novel approach to the detection of triacetone triperoxide (TATP), its structure and its complexes with ions," Journal of Physical Chemistry A, vol. 106, p. 4951–4956, 2002.

Dutta A. and Basu S., "Modified metal-insulator-metal (M-I-M) hydrogen gas sensors based on zinc oxide," Journal of Materials Science: Materials in Electronics, vol. 6, pp. 415-418, 1995.

Eiceman G. A., Preston D., Tiano G., Rodriguez J. and Parmeter J. E., "Quantitative calibration of vapor levels of TNT, RDX, and PETN using a diffusion generator with gravimetry and ion mobility spectrometry," Talata, vol. 45, pp. 57-74, 1997.

Eisele I., Doll T. and Burgmair M., "Low Power gas detection with FET sensors," Sensors and Actuators B, vol. 78, pp. 19-25, 2001.

Eles P. T. and Michal C. A., "Two-photon excitation in nuclear quadrupole resonance," Chemical Physics Letters, vol. 376, pp. 268-273, 2003.

Eliasson C., Macleod N. A. and Matousek P., "Noninvasive detection of concealed liquid explosives using Raman spectroscopy," Analytical Chemistry, vol. 79, pp. 8185-8189, 2007.

Endress H. E., Hartinger R., Schwaiger M., Gmelch G. and Roth M., "A capacitive CO_2 sensor system with suppression of the humidity interference," Sensors and Actuators B, vol. 57, pp. 83-87, 1999.

Eranna G., Joshi B. C., Runthala D. P. and Gupta R. P., "Oxide materials for development of integrated gas sensors: A comprehensive review," Critical Review of Solid State and Materials Sciences, vol. 29, pp. 111-188, 2004.

Ewing R. G., Atkinson D. A., Eiceman G. A. and Ewing G. J., "A critical review of

ion mobility spectrometry for the detection of explosives and explosive related compounds," Talanta, vol. 54, pp. 515-529, 2001.

Fan Y., Han P., Liang P., Xing Y., Ye Z.and Hu S., "Differences in etching characteristics of TMAH and KOH on preparing inverted pyramids for silicon solar cells," *Applied Surface Science*, vol. 264, pp. 761-766, 2013.

Federici J. F., Schulkin B., Huang F., Gary D., Barat R., Oliveira F. and Zimdars D., "THz imaging and sensing for security applications—explosives, weapons and drugs," Semiconductor Science and Technology, Vols. S266-S280, p. 20, 2005.

Foltynowicz R. J., Allman R. E. and Zuckerman E., "Terahertz absorption measurement for gas-phase 2,4-dinitrotoluene from 0.05 THz to 2.7 THz," Chemical Physics Letters, vol. 431, pp. 34-38, 2006.

Fordham S., High Explosives and Propellants, Fordham, Stanley, UK: Pergamon Press Ltd., 1980.

Furton K. G. and Myers L. J., "The scientific foundation and efficacy of the use of canines as chemical detectors for explosives," Talanta, vol. 54, pp. 487-500, 2011.

Gaft M. and Nagli L., "UV gated Raman spectroscopy for standoff detection of explosives," Optical Materials, vol. 30, pp. 1739-1746, 2008.

Gaggiotti G., Galdikas A., Kaciulis S., Mattogno G. and Setkus A., "Temperature dependencies of sensitivity and surface chemical composition of SnO_x gas

sensors," Sensors and Actuators B, vol. 25, p. 516–519, 1995.

Gardner J. W. and Bartlett P. N., Electronic Noses – Principles and Applications, Oxford, UK: Oxford University Press, 1999.

Garroway A. N., Buess M. L., Miller J. B., Suits B. H., Hibbs A. D., Barrall G. A., Matthews R.and Burnett L. J., "Remote sensing by nuclear quadrupole resonance," IEEE Transactions, Geoscience and Remote Sensing, vol. 39, pp. 1108-1118, 2001.

Garroway A. N., Buess M. L., Yesinowski J. P. and Miller J. B., "Narcotics and explosive detection by ^{14}N pure NQR," Proceedings of SPIE, vol. 2092, pp. 318-327, 1993.

Gazit I. and Terkel J., "Explosives detection by sniffer dogs following strenuous physical activity," Applied Animal Behaviour Science, vol. 81, pp. 149-161, 2003.

Gazit I. and Terkel J., "Domination of olfaction over vision in explosives detection by dogs," Applied Animal Behaviour Science, vol. 82, pp. 65-73, 2003.

Goel M., "Recent developments in electroceramics: MEMS application for energy and environment," *Ceramics International*, vol.30, pp. 1147-1154, 2004.

Grechishkin V. S. and Sinyavskii N. Y., "New technologiesnuclear quadrupole resonance as an explosive and narcotic detection technique," Physics

Uspekhi, vol. 40, pp. 393-406, 1997.

Green E. M., "Explosives Regulation in the USA," Industrial Minerals, vol. 465, p. 78, 2006.

Grevea J. O. A., Greve A., Olsen J., Privorotskaya N., Senesac L., Thundat T., King W. P. and Boisen A., "Micro-calorimetric sensor for vapor phase explosive detection with optimized heat profile," Microelectronic Engineering, vol. 87, p. 696–698, 2010.

Guerrero L. A., "Quick Learning Techniques: Dogs used to detect narcotics and explosives," Journal of Veterinary Behavior: Clinical Applications and Research, vol. 4, p. 253, 2009.

Gupta N. and Dahmani R., "AOTF Raman spectrometer for remote detection of explosives," Spectrochimica Acta A, vol. 56, pp. 1453-1456, 2000.

Habib M. K., "Controlled biological and biomimetic systems for landmine detection," Biosensors and Bioelectronics, vol. 23, pp. 1-18, 2007.

Hall N. J., Smith D. W. and Wynne D. L., "Training domestic dogs (Canis lupus familiaris) on a novel discrete trials odor-detection task," Learning and Motivation, p. In press, 2013.

Harper R. J., Almirall J. R. and Furto K. G., "Identification of dominant odor chemicals emanating from explosives for use in developing optimal training aid combinations and mimics for canine detection," Talanta, vol. 67, pp. 313-327, 2005.

Haverbeke A., Laporte B., Depiereux E., Giffroy J. M. and Diederich C., "Training methods of military dog handlers and their effects on the team's performances," Applied Animal Behaviour Science, vol. 113, pp. 110-122, 2008.

Hayward I. E., Kirkbride T. E., Batchelder D. N. and Lacey R. J., "Use of a Fiber Optic Probe for the Detection and Identification of Explosive Materials by Raman Spectroscopy," Journal of Forensic Sciences, vol. 40, pp. 883-334, 1995.

Heeger A. J., "Semiconducting and metallic polymers: the fourth generation of polymeric materials," Current Applied Physics, vol. 1, pp. 247-267, 2001.

Holmgren E., Ek S. and Colmsjo A., "Extraction of explosives from soil followed by gas chromatography–mass spectrometry analysis with negative chemical ionization," Journal of Chromatography A, vol. 1222, pp. 109-115, 2012.

Holly R. and Hingerl K., "Fbrication of silicon vertical taper structures using KOH anisotropic etching," *Microelectronic Engineering*, vol. 83, pp. 1430-1433, 2006.

Hu Y., Huang P., Guo L., Wang X. and Zhang C., "Terahertz spectroscopic investigations of explosives," Physics Letters A, vol. 359, pp. 728-732, 2006.

Hu Y., Tan O. K., Pan J. S., Huang H. and Cao W., "The effects of annealing

temperature on the sensing properties of low temperature nano-sized $SrTiO_3$ oxygen gas sensor," Sensors and Actuators B, vol. 108, p. 244–249, 2005.

Huang S. D., Kolaitis L. and Lubman D. M., "Detection of explosives using laser desorption in ion mobility spectrometry/mass spectrometry," Applied Spectroscopy, vol. 41, pp. 1371-1376, 1987.

Huang J., Kuo D. and Shew B., "The effects of heat treatment on the gas sensitivity of reactively sputtered SnO_2 films," Surface and Coatings Technology, vol. 79, pp. 263-267, 1996.

Hung N. L., Kim H., Hong S. K. and Kim D., "Enhancement of CO gas sensing properties of ZnO thin films deposited on self-assembled Au nanodots," Sensors and Actuators B, vol. 151, pp. 127-132, 2010.

Hwang S., Kim Y. Y., Lee J. H., Seo D. K., Lee J. Y. and Cho H. K., "Irregular electrical conduction types in tin oxide thin films induced by nanoscale phase separation," Journal of the American Ceramic Society, vol. 95, pp. 324-332, 2012.

Industry Report, Sensors Markets 2016, Freedonia, 2013.

Intelliegence Reform and Terrorism Prevention Act of 2004, Public Law, December 2004, 108-458.

Ippolito S. J., Kandasamy S., Kalantar-zadeh K. and Wlodarski W., "Hydrogen sensing characteristics of WO3 thin film conductometric sensors activated

by Pt and Au catalysts," Sensors and Actuators B, vol. 108, pp. 154-158, 2005.

Izake E. L., "Forensic and homeland security applications of modern portable Raman spectroscopy," Forensic Science International, vol. 202, pp. 1-8, 2010.

Janata J., Josowicz M., Vanysek P. and Michael DeVaney D., "Chemical sensors," Analytical Chemistry, vol. 70, p. 179–208, 1998.

Janni J., Gilbert B. D., Field R. W. and Steinfeld J. I., "Infrared absorption of explosive molecule vapors," Spectrochimica Acta Part A: Molecular and Biomolecular Spectroscopy, vol. 53, pp. 1375-1381, 1997.

Jezierski T., Adamkiewicz E., Walczak M., Porkopczyk M. and Wziatek M., "Factors affecting drugs and explosives detection by dogs in experimental tests," Journal of Veterinary Behavior: Clinical Applications and Research, vol. 8, p. e33, 2013.

Jimenez V., Espinos J. and Gonzalez-Elipe A., "Effect of texture and annealing treatments in SnO2 and Pd/SnO2 gas sensor materials," Sensors and Actuators B, vol. 61, pp. 23-32, 1999.

Kannan G. K., Nimal A. T., Mittal U., Yadava R. D. and Kapoor J. C., "Adsorption studies of carbowax coated surface acoustic wave (SAW) sensor for 2,4-dinitro toluene (DNT) vapour detection," Sensors and Actuators B, vol. 101, pp. 328-334, 2004.

Kanu A. B., Wu C. and Hill H. H. Jr., "Rapid preseparation of interferences for ion mobility spectrometry," Analytica Chimica Acta, vol. 610, pp. 125-134, 2008.

Karasek F. W. and Denney D. W., "Detection of 2,4,6-trinitrotoluene vapours in air by plasma chromatography," Journal of Chromatography, vol. 93, pp. 141-147, 1974.

Kato K., Omoto H., Tomioka T. and Takamatsu A., "Optimum packing density and crystal structure of tin-doped indium oxide thin films for high-temperature annealing processes," Applied Surface Science, vol. 257, p. 9207–9212, 2011.

Kemp M. C., "Explosive Detection by Terahertz Spectroscopy- A Bridge Too Far?," Terahertz Science and Technology, IEEE, vol. 1, pp. 282-292, 2011.

Kemp M. C., Taday P. F., Cole B. E., Cluff J. A., Fitzgerald A. J. and Tribe W. R., "Security applications of terahertz technology," Proceedings of SPIE, vol. 5070, pp. 44-52, 2003.

Khayamian T., Tabrizchi M. and Jafari M. T., "Analysis of 2,4,6-trinitrotoluene, pentaerythritol tetranitrate and cyclo-1,3,5-trimethylene-2,4,6-trinitramine using negative corona discharge ion mobility spectrometry," Talanta, vol. 54, pp. 515-529, 2001.

Khlebarov Z. P., "Surface acoustic wave gas sensor," Sensors and Actuators B, vol. 8, pp. 33-40, 1992.

Kim S. S., Jayakody J. R. and Marino R. A., "Experimental investigations of the strong off resonant comb (SORC) pulse sequence in ^{14}N NQR," Verlag der Zeitschrift für Naturforschung (A), vol. 47, pp. 415-420, 1993.

Korotcenkov G., Boris I., Brinzari V., Han S. H. and Cho B. K., "The role of doping effect on the response of SnO_2-based thin film gas sensors: Analysis based on the results obtained for Co-doped SnO_2 films deposited by spray pyrolysis," Sensors and Actuators B, vol. 182, pp. 112-124, 2013.

Korotcenkov G. and Cho B. K., "Instability of metal oxide based conductometric gas sensors and approaches to stability improvement (short survey)," Sensors and Actuators B, vol. 156, pp. 527-538, 2011.

Korotcenkov G. and Cho B. K., "Ozone measuring: what can limit application of SnO2-based conductometric gas sensor?," Sensors and Actuators B, vol. 161, pp. 28-44, 2012.

Korotcenkov G. and Cho B. K., "Engineering approaches for the improvement of conductometric gas sensor parameters: Part 1. Improvement of sensor sensitivity and selectivity," Sensors and Actuators B, vol. 188, pp. 709-728, 2013.

Kriz D. and Ansell R. J., "Man Made Mimics of Antibodies and their Application in Analytical Chemistry," Molecularly Imprinted Polymers, vol. 23, p. 417–436, 2001.

Ladbeck R. S. and Karst U., "Determination of triacetone triperoxide in ambient air," Analytical Chemistry, vol. 482, pp. 183-188, 2003.

Latosinska J. N., "Nuclear Quadrupole Resonance spectroscopy in studies of biologically active molecular systems - a review," Journal of Pharmaceutical and Biomedical Analysis, vol. 38, pp. 577-587, 2005.

Leahy-Hoppa M. R., Fitch M. J. and Osiander R., "Terahertz spectroscopy techniques for explosives detection," Analytical and Bioanalytical Chemistry, vol. 395, pp. 247-257, 2009.

Lee K. B., Gu M. B. and Moon S. H., "Degradation of 2,4,6-trinitrotoluene by immobilized horseradish peroxidase and electrogenerated peroxide," Water Research, vol. 37, pp. 983-992, 2003.

Lee Y. C., Huang H., Tan O. K. and Tse M. S., "Semiconductor gas sensor based on Pd doped SnO_2 nanorod thin films," Sensors and Actuators B, vol. 132, pp. 239-242, 2008.

Lerchner J., Caspary D. and Wolf G., "Calorimetric detection of volatile organic compounds," Sensors and Actuators B, vol. 70, pp. 57-66, 2000.

Li X., Li Q., Zhou H., Hao H., Wang T., Zhao S., Lu Y.and Huang G., "Rapid, on-site identification of explosives in nanoliter droplets using a UV reflected fiber optic sensor," Analytica Chimica Acta, vol. 751, pp. 112-118, 2012.

Lim C. B. and Oh S., "Microstructure evolution and gas sensitivities of Pd-doped

SnO2-based sensor prepared by three different catalyst-addition process," Sensors and Actuators B, vol. 30, pp. 223-231, 1996.

Lima R. R., Carvalho R. A., Nascimento Fiho A. P., Silva M. L. and Demarquette N. R., "Production and deposition of adsorbent films by plasma polymerization on low cost micromachined non-planar microchannels for preconcentration of organic compound in air," Sensors and Actuators B, vol. 108, pp. 435-444, 2005.

Lin H. and Suslick K. S., "A colorimetric sensor array for detection of triacetone triperoxide vapor," Journal of American Chemistry Society, vol. 132, pp. 15519-15521, 2010.

Liu H., Chen Y., Bastiaans G. J. and Zhang X., "Detection and identification of explosive RDX by THz diffuse reflection spectroscopy," Optics Express, vol. 14, pp. 415-423, 2006.

Liu L., Zhang T., Li S., Wang L.and Tian T., "Preparation, characterization, and gas-sensing properties of Pd-doped In_2O_3 nanofibers," Materials Letters, vol. 63, pp. 1975-1977, 2009.

Liu Y., Ugaz V. M., North S. W., Rogers W. J. and Mannan S., "Development of a miniature calorimeter for identification and detection of explosives and other energetic compounds," Journal of Hazardous Materials, vol. 142, pp. 662-668, 2007.

Lopez-Avila V. and Hill H. H., "Field analytical chemistry," Analytical

Chemistry, vol. 69, pp. 289-306, 1997.

Lubczyk D., Siering C., Lorgen J., Shifrina Z. B., Mullen K. and Waldvogel S. R., "Simple and sensitive online detection of triacetone triperoxide explosive," Sensors and Actuators B, vol. 143, pp. 561-566, 2010.

Ly S. Y., Kim D. H. and Kim M. H., "Square-wave cathodic stripping voltammetric analysis of RDX using mercury-film plated glassy carbon electrode," Talanta, Vols. 919-926, p. 58, 2002.

Makinen M., Silanpaa M., Viitanen A. K., Knap A., Makela J. M. and Puton J., "The effect of humidity on sensitivity of amine detection in ion mobility spectrometry," Talanta, vol. 84, pp. 116-121, 2011.

Marsal A., Cornet A. and Morante J. R., "Study of the CO and humidity interference in La doped tin oxide CO_2 gas sensor," Sensors and Actuators B, vol. 94, pp. 324-329, 2003.

Martin M., Crain M., Walsh K., McGill R. A., Houser E., Stepnowski J. and Stepnows S., "Microfabricated vapor preconcentrator for portable ion mobility spectroscopy," Sensors and Actuators B, vol. 126, pp. 447-454, 2007.

Massok P., Loesch M. and Bertrand D., "Comparison for the between two Figaro sensors (TGS 813 and TGS 842) for the detection of methane, in terms of selectivity and long-term stability," Sensors and Actuators B, vol. 25, pp. 525-528, 1995.

Masunaga K., Hayama K., Onodera T., Hayashi K., Miura N., Matsumoto K. and Toko K., "Detection of aromatic nitro compounds with electrode polarization controlling sensor," Sensors and Actuators B, Vols. 427-434, p. 108, 2005.

Mathis J. A. and McCord B. R., "The analysis of high explosives by liquid chromatography/electrospray ionization mass spectrometry: multiplexed detection of negative ion adducts," Rapid Communications in Mass Spectrometry, vol. 19, pp. 99-104, 2005.

Matin A., Yun C., Waterman K. L., Hurley C. M., Platek M. J. and Gregory O. J., "Detection of triacetone triperoxide (TATP) using a thermodynamic based gas sensor," Sensors and Actuators B, vol. 162, pp. 7-13, 2012.

Matsushima S., Maekawa T., Tamaki J., Miura N.and Yamazoe N., "New methods for supporting palladium on a tin oxide gas sensor," Sensors and Actuators B, vol. 9, pp. 71-78, 1992.

Matyas R., Selesovsky J. and Musil T., "Sensitivity to friction for primary explosives," Journal of Hazardous Materials, Vols. 213-214, pp. 236-241, 2012.

Meaney M. S. and McGuffin V. L., "Luminescence-based methods for sensing and detection of explosives," Analytical and Bioanalytical Chemistry, vol. 391, pp. 2557-2576, 2008.

Michael Ben Alexandera T. F., Alexandera M. B., Friend T. and Haug L.,

"Obedience training effects on search dog performance," Applied Animal Behaviour Science, vol. 132, pp. 152-159, 2011.

Mikhaltsevitch V. T. and Rudakov T. N., "On the NQR detection of nitrogenated substances by multi-pulse sequences," Physica Status Solidi (b), vol. 241, pp. 411-419, 2004.

Miller J. B., "Chapter 7 - Nuclear quadrupole resonance detection of explosives," in Counterterrorist Detection Techniques of Explosives, Oxford, UK, Elsevier, 2007, pp. 157-198.

Millot Y. and Man P. P., "Determination of quadrupole parameters with a composite pulse for spurious signal suppression," Journal of Magnetic Resonance, vol. 150, pp. 10-16, 2001.

Monterola M. P., Smith B. W., Omenetto N. and Winefordner J. D., "Photofragmentation of nitro-based explosives with chemiluminescence detection," Analytical and Bioanalytical Chemistry, vol. 391, pp. 2617-2626, 2008.

Moore D. S. and Scharff R. J., "Portable Raman explosive detection," Analytical and Bioanalytical Chemistry, vol. 393, pp. 1571-1578, 2009.

Mullen C., Irwin A., Pond B. V., Huestis D. L., Coggiola M. J. and Oser H., "Detection of explosives and explosives-related compounds by single photon laser ionization time-of-flight mass spectrometry," Analytical Chemistry, vol. 78, p. 3807–3814, 2006.

Munoz B. C., Steinthal G. and Sunshine S., "Conductive polymer-carbon black composites-based sensor arrays for use in an electronic nose," Sensor Review, vol. 19, pp. 300-305, 1999.

Neuhaus W., "Uber die Riechscharfe des Hundes fur Fettsauren," Zeitschrift Fur Vergleichende Physiologie, vol. 35, p. 527, 1953.

Nimal A. T., Mittal U., Singh M., Khaneja M., Kannan G. K., Kapoor J. C., Dubey V., Gutch P. K., Lal G., Vyas K. D. and Gupta D. C., "Development of handheld SAW vapor sensors for explosives and CW agents," Sensors and Actuators B, vol. 135, pp. 399-410, 2009.

Osan T. M., Cerioni L. M., Forguez J. and Olle J. M., "NQR: From imaging to explosives and drugs detection," Physica B: Condensed Matter, vol. 389, pp. 45-50, 2007.

Oxley J. C., Smith J. L. and Chen H., "Decomposition of a multi-peroxidic compound: triacetone triperoxide (TATP)," Propellants, Explosives, Pyrotechnics, vol. 27, pp. 209-216, 2002.

Oxley J. C., Smith J. L., Shinde K. and Moran J., "Determination of the vapor density of triacetone triperoxide (TATP) using a gas chromatography headspace technique," Propellants, Explosives, Pyrotechnics, vol. 30, pp. 127-130, 2005.

Parajuli S. and Miao W., "Sensitive Determination of Hexamethylene Triperoxide Diamine Explosives, Using Electrogenerated Chemiluminescence

Enhanced by Silver Nitrate," Analytical Chemistry, vol. 81, pp. 5267-5272, 2009.

Park M., Cella L. N., Chen W., Myung N. V. and Mulchandani A., "Carbon nanotubes-based chemiresistive immunosensor for small molecules: Detection of nitroaromatic explosives," Biosensors and Bioelectronics, vol. 26, p. 1297–1301, 2010.

Pearce C. I., Pattrick R. A., Vaughan D. J., Henderson C. M. and van der Laan G., "Copper oxidation state in chalcopyrite: Mixed Cu d^9 and d^{10} characteristics," Geochimica, vol. 70, pp. 4635-4642, 2006.

Pella P. A., "Measurement of the Vapor Pressure of TNT, 2,4-DNT, 2,6-DNT and EGDN," Journal of Chemical Thermodynamics, 1977, 9(4), 301, vol. 9, p. 301, 1977.

Perr J. M., Furton K. G. and Almirall J. R., "Gas chromatography positive chemical ionization and tandem mass spectrometry fot the analysis of organic high explosives," Talanta, vol. 67, pp. 430-436, 2005.

Pinnaduwage L. A., Boiadjiev V., Hawk J. E. and Thundat T., "Sensitive detection of plastic explosives with self-assembled monolayer-coated microcantilevers," Applied Physics Letters, vol. 83, pp. 1471-1473, 2003.

Primera-Pedrozo O. M., Soto-Feliciano Y. M. and Pacheco-Londo L. C., "Detection of high explosives using reflection absorption infrared spectroscopy with fiber coupled grazing angle probe/FTIR," Sensing and Imaging, vol. 10, pp.

1-13, 2009.

Rabenecker P. and Pinkwart K., "A Look Behind Electrochemical Detection of Explosives," Propellants, Explosives, Pyrotechnics, vol. 34, p. 274–279, 2009.

Ras M. R., Borrull F. and Marce R. M., "Sampling and preconcentration techniques for determination of volatile organic compounds in air samples," TrAC Trends in Analytical Chemistry, vol. 28, pp. 347-361, 2009.

Rasanen R., Nousiainen M., Parakorpi K., Sillanripaa M., Polari L., Anttalainen O. and Utriainen M., "Determination of gas phase triacetone triperoxide with aspiration ion mobility spectrometry and gas chromatography–mass spectrometry," Analytica Chimica Acta, vol. 623, p. 59–65, 2008.

Ray M. D., Sedlacek A. J. and Wu M., "Ultraviolet mini-Raman lidar for stand-off, in situ identification of chemical surface contaminants," Review of Scientific Instruments, vol. 71, pp. 3485-3489, 2000.

Riva J., Marelli S. P., Redaelli V., Sforzini E., Luzi F. and Bondio G. P., "Effect of training on behavioral reactivity and neurotransmitter levels in drug detection dogs," Journal of Veterinary Behavior: Clinical Applications and Research, vol. 5, pp. 38-39, 2010.

Romain A. C. and Nicolas J., "Long term stability of metal oxide-based gas sensors for E-nose environmental applications: an overview," Sensors and

Actuators B, vol. 146, pp. 502-506, 2010.

Rowell F., Seviour J., Lim A. Y., Elumbaring-Salazar C. G., Loke J. and Ma J., "Detection of nitro-organic and peroxide explosives in latent fingermarks by DART- and SALDI-TOF-mass spectrometry," Forensic Science International, vol. 221, pp. 84-91, 2012.

Sato K., Shikida M., Matsushima Y., Yamashiro T., Asaumi K., Iriye Y. and Yamamoto M., "Characterization of orientation-dependent etching properties of single-crystal silicon: effects of KOH concentration," *Sensors and Actuators A*, vol. 64, pp. 87-93, 1998.

Sauer K. L., Suits B. H., Garroway A. N. and Miller J. B., "Three-frequency nuclear quadrupole resonance of spin-1 nuclei," Chemical physics Letters, vol. 342, pp. 362-368, 2001.

Sayago I., Gutierrez J., Ares L., Robla J. I., Horrilo M. C., Getino J., Rino J. and Agapito J. A., "Long-term reliability of sensors for detection of nitrogen oxides," Sensors and Actuators B, vol. 26, pp. 56-58, 1995.

Schaller E., Bosset J. O. and Escher F., "Electronic noses and their application to food," LebensmittelWissenschaft und-Jechnologie, vol. 31, pp. 305-316, 1998.

Schierbaum K., Weimar U. and Gopel W., "Conductance, work function and catalytic activity of SnO2-based gas sensors," Sensors and Actuators B, vol. 3, pp. 205-214, 1991.

Seiyama T., Kato A., Fujishi K. and Nagatani M., "A New detector for gaseous components using semiconductive thin films," Analytical Chemistry, vol. 34, pp. 1502-1503, 1962.

Sharma S. K., Misra A. K., Lucey P. G., Angel S. M. and McKay C. P., "Remote Pulsed Raman Spectroscopy of Inorganic and Organic Materials to a Radial Distance of 100 Meters," Applied Spectroscopy, vol. 60, pp. 871-876, 2006.

Shankaran D. R., Gobi K. V., Sakai T., Matsumoto K., Toko K. and Miura N., "Surface plasmon resonance immunosensor for highly sensitive detection of 2,4,6-trinitrotoluene," Biosensors and Bioelectronics, vol. 20, p. 1750–1756, 2005.

Sharma S. K., Misra A. K. and Sharma B., "Portable remote Raman system for monitoring hydrocarbon, gas hydrates and explosives in the environment," Spectrochimica Acta A, vol. 61, pp. 2404-2412, 2005.

Shen C., Li J., Han H., Wang H., Jiang H. and Chu Y., "Triacetone triperoxide using low reduced-field proton transfer reaction mass spectrometer," International Journal of Mass Spectrometry, vol. 285, pp. 100-103, 2009.

Shen Y., Yamazaki T., Liu Z., Meng D., Kikuta T., Nakatani N., Saito M. and Mori M., "Microstructure and H2 gas sensing properties of undoped and Pd-doped SnO2 nanowires," Sensors and Actuators B, vol. 135, pp. 524-529, 2009.

Shriver-Lake L. C., Patterson C. H. and Van Bergen S. K., "New Horizons: explosive detection in soil extracts with a fiber-optic biosensor," Field Analytical Chemistry and Technology, vol. 4, pp. 239-245, 2000.

Silversmit G., Depla D., Poelman H., Marin G. B. and Gryse R., "Determination of the V^{2p} XPS binding energies for different vanadium oxide oxidation states (V^{5+} to V^{0+})," Journal of Electron Spectroscopy and Related Phenomena, vol. 135, p. 167–175, 2004.

Skala T., Veltruska K., Moroseac M., Matolinova I., Cirera A. and Matolin V., "Redox process of Pd-SnO_2 system," Surface Science, Vols. 566-568, pp. 1217-1221, 2004.

Smith J. A., Blanz M., Rayner T. J., Rowe M. D., Bedford S. and Althoefer K., "^{14}N quadrupole resonance and ^{1}H T1 dispersion in the explosive RDX," Journal of Magnetic Resonance, vol. 213, pp. 98-106, 2011.

Smith J. A., Rayner T. J., Rowe M. D., Barras J., Peirson N. F., Stevens A. D. and Althoefer K., "Magnetic field-cycling NMR and ^{14}N, ^{17}O quadrupole resonance in the explosive pentaerythritol tetranitrate (PETN)," Journal of Megnetic Resonance, vol. 204, pp. 139-144, 2010.

Singh S., "Sensors-An effective approach for the detection of explosives," Journal of Harzardous Materials, vol. 144, pp. 15-28, 2007.

Spangler G. E., Carrico J. P. and Campbel D. N., "Recent advances in ion mobility spectrometry for explosives vapor detection," Journal of Testing

and Evaluation, vol. 13, pp. 234-240, 1985.

Spangler G. E. and Lawless P. A., "Ionization of nitrotoluene compounds in Negative ion plasma chromatography," Analytical Chemistry, vol. 50, pp. 884-892, 1978.

Stambouli A., Bouri A. E., Bouayoun T. and Bellimam M. A., "Headspace GC/MS detection of TATP traces in post-explosion debris," Forensic Science International , vol. 146S, pp. 191-194, 2004.

Symanski S. S. and Bruckenstein S., "Conductometric sensor for parts per billion sulfur dioxide determination," Analytical Chemistry, vol. 58, pp. 1771-1777, 1986.

Takats Z., Cotte-Rodriguez I., Talaty N., Chen H. and Cooks R. G., "Direct, trace level detection of explosives on ambient surfaces by desorption electrospray ionization mass spectrometry," Chemical Communications, vol. 41, pp. 1950-1952, 2005.

Tan R., Guo Y., Zhao J., Li Y., Xu T. and Song W., "Synthesis, characterization and gas-sensing properties of Pd-doped SnO_2 nano particles," Transactions of Nonferrous Metals Society of China, vol. 21, pp. 1568-1573, 2011.

Thammakhet C., Thavarungkul P., Brukh R., Mitra S. and Kanatharana P., "Microtrap modulated flame ionization detector for on-line monitoring of methane," Journal of Chromatography A, vol. 2005, pp. 243-248, 1072.

Todd M. W., Provencal R. A., Owano T. G., Paldus B. A., Kachanov A.,

Vodopyanov K. L., Hunter M., Coy S. L., Steinfeld J. I. and Arnold J. T., "Application of mid-infrared cavity-ringdown spectroscopy to trace explosives vapor detection using a broadly tunable (6-8 μm) optical parametric oscillator," Applied Physics B, vol. 75, pp. 367-376, 2002.

Tournier G., Pijolat C., Lalauze R. and Patissier B., "Selective detection of CO and CH_4 with gas sensors using SnO_2 doped with palladium," Sensors and Actuators B, Vols. 26-27, pp. 24-28, 1995.

Tribe W. R., Newnham D. A., Taday P. F. and Kemp M. C., "Hidden object detection: security applications of terahertz technology," Proceedings of SPIE, vol. 5354, pp. 168-176, 2004.

Tsud N., Johanek V., Stara I., Veltruska K. and Matolin V., "XPS, ISS and TPD of Pd-Sn interactions on Pd-SnOx systems," Thin Solid Films, vol. 391, pp. 204-208, 2001.

Urbanski T., Chemistry and Technology of Explosives, London: Pergamon Press, 1964.

Uthanna S., Subramanyam T. K., Naidu B. S. and Rao G. M., "Structure–composition–property dependence of reactive magnetron sputtered ZnO thin films," Optical Materials, vol. 19, p. 461–469, 2002.

Vereshchaginam E., Wolters R. A. and Gardeniers J. G., "Measurement of reaction heats using a polysilicon based microcalorimetric sensor," Sensors and Actuators A, vol. 169, p. 308–316, 2001.

Waggoner L. P., "Chapter 3 – Detection of Explosives by Dogs," in Aspects of Explosives Detection, Oxford, UK, Elsevier, 2009, pp. 27-40.

Wakelin D., Isotopic ratio analysis of explosives traces – a new type of evidence, UK: United Kingdom Defence Evaluation and Research Agency report, 2000.

Wang J., "Electrochemical Sensing of Explosives," Electroanalysis, vol. 19, p. 415–423, 2007.

Wang B. and Lin Q., "Temperature-modulated differential scanning calorimetry in a MEMS device," Sensors and Actuators B, vol. 180, pp. 60-65, 2013.

Whelan D. J., Spear R. J. and Read R. W., "The thermal decomposition of some primary explosives as studied by differential scanning calorimetry," Thermochimica Acta, vol. 80, p. 149–163, 1984.

Wilkinson J., Konek C. T., Moran J. S., Witko E. M. and Korter T. M., "Terahertz absorp spectrum of triacetone triperoxide (TATP)," Chemical Physics Letters, vol. 478, pp. 172-174, 2009.

Williams D. E., "Semiconducting oxides as gas-sensitive resistors," Sensors and Actuators B, vol. 57, pp. 1-16, 1999.

Williams M. and Johnston J. M., "Training and maintaining the performance of dogs (Canis familiaris) on an increasing number of odor discriminations in a controlled setting," Applied Animal Behaviour Science, vol. 78, pp. 55-65, 2002.

Wilson R., Clavering C. and Hutchinson A., "Paramagnetic bead based enzyme electrochemiluminescence immunoassay for TNT," Journal of Electroanalytical Chemistry, vol. 557, pp. 109-118, 2003.

Wu M., Ray M., Fung K. H., Ruckman M. W., Harder D. and Sedlacek A. J., "Stand-off Detection of Chemicals by UV Raman Spectroscopy," Applied Spectroscopy, vol. 54, pp. 196-220, 2000.

Xu J., Liu H., Yuan T., Kersting R. and Zhang X. C., "Advanced terahertz time-domain spectroscopy for remote detection and tracing," Proceedings of SPIE, vol. 5070, pp. 17-27, 2003.

Yamazoe N., Kurokawa K. and Seiyama T., "Effects of additives on semiconductor gas sensor," Sensors and Actuators, vol. 4, pp. 283-289, 1983.

Yang W. Y., Kim W. G. and Rhee S. W., "Radio frequency sputter deposition of single phase cuprous oxide using Cu_2O as a target material and its resistive switching properties," Thin Solid Films, vol. 517, pp. 967-971, 2008.

Yinon J., "Detection of explosives by electronic noses," Analytical Chemistry, vol. 75, pp. 99-105, 2003.

Yinon J., "Analysis and detection of explosives by mass spectrometry," in Aspects of Explosives Detection, Oxford, UK, Elsevier, 2009, pp. 147-169.

Yuan T., Liu H., Xu J., Al-Douseri F., Hu Y. and Zhang X. C., "Terahertz time-

domain spectroscopy of atmosphere with different humidity," Proceedings of SPIE, vol. 5070, pp. 28-37, 2003.

Yuasa M., Masaki T., Kida T., Shimanoe K. and Yamazoe N., "Nano-sized PdO loaded SnO_2 nanoparticles by reverse micelle method for highly sensitive CO gas sensor," Sensors and Actuators B, vol. 136, pp. 99-104, 2009.

Zalewska A., Pawlowski W.and Tomaszewski W., "Limits of detection of explosives as determined with IMS and field asymmetric IMS vapour detectors," Forensic Science International, vol. 226, pp. 168-172, 2013.

Zang J., Guo C., Hu F., Yu L. and Li C., "Electrochemical detection of ultratrace nitroaromatic explosives using ordered mesoporous carbon," Analytica Chimica Acta, vol. 683, p. 187–191, 2011.

Zark A., Kaplan D. and Kendler S., "A MEMS-based microthermal analysis of explosive materials," Sensors and Actuators A, vol. 199, pp. 129-135, 2013.

Zhang T., Liu L., Qi Q., Li S. and Lu G., "Development of microstructure In/Pd-doped SnO_2 sensor for low level CO detection," Sensors and Actuators B, vol. 139, pp. 287-291, 2009.

Zhang W. H., Zhang W. D. and Chen L. Y., "Highly sensitive detection of explosive triacetone triperoxide by an In_2O_3 sensor," Nanotechnology, vol. 21, p. 315502, 2010.

Zhang Y., Ma X., Zhang S., Yang C., Zheng O. and Zhang X., "Direct detection of

explosives on solid surfaces by low temperature plasma desorption mass spectrometry," Analyst, vol. 134, pp. 176-181, 2009.

Zhang Y., Xiang Q., Xu J., Xu P., Pan Q.and Li F., "Self-assemblies of Pd nanoparticles on the surfaces of single crystal ZnO nanowires for chemical sensors with enhanced performances," Journal of Material Chemistry, vol. 19, pp. 4701-4706, 2009.

Zimmermann S., Abel N., Baether W. and Barth S., "An ion-focusing aspiration condenser as an ion mobility spectrometer," Sensors and Actuators B, vol. 125, pp. 428-434, 2007.

Zubel I., Barycka I., Kotowska K. and Kramkowska M., "Silicon anisotropic etching in alkaline solutions IV: The effect of organic and inorganic agents on silicon anisotropic etching process," *Sensors and Actuators A*, vol. 87, pp. 163-171, 2001.